

https://dspace.org/

An improved ribozyme processing system that generates active RNA interference effector molecules from Pol II expression cassettes

Hean, Justin

2009-05-28T08:19:10Z
http://hdl.handle.net/10539/6986

Downloaded from a DSpace repository. https://dspace.org/

AN IMPROVED RIBOZYME PROCESSING SYSTEM THAT GENERATES ACTIVE RNA INTERFERENCE EFFECTOR MOLECULES FROM POL II EXPRESSION CASSETTES

Justin Hean

A dissertation submitted to the Faculty of Science, University of the Witwatersrand, in fulfilment of the requirements for the degree of Master of Science

Johannesburg, 2008

Declaration

I, Justin Hean, declare that this dissertation is my own, unaided work. It is being submitted for the Degree of Master of Science in the University of the Witwatersrand, Johannesburg. It has not been submitted before for any degree or examination in any other University.

_____
(Signature of Candidate)

_____day of_____ 200__

Presentations and Patents

Conference Proceedings

1. Hean, J., Ely, A., Weinberg, M.S. and Arbuthnot P.B. A ribozyme processing system that generates active RNAi effector molecules from Pol II expression cassettes. Keystone Symposia on Molecular and Cellular Biology; 2007 Jan 28 – Feb 2; Keystone, Colorado

Patents

1. Arbuthnot PB, Weinberg MS, inventors. Interference and inhibition of viral gene expression using expression cassettes that comprise a combination of ribozymes with either siRNA or miRNA. Patent Number PCT/IB2004/002816. PCT application filed 1 September 2004.

Abstract

RNA interference (RNAi) has been shown to be highly effective in targeted gene knockdown and has the potential to be applied for therapy by silencing pathology-causing genes. However, there remain several undesired properties associated with the utilisation of RNAi for therapeutic purposes. These include: innate immunostimulation, “off-target” cellular sequences and the possibility of saturating the endogenous RNAi pathway, which is required for microRNA biogenesis. RNA Polymerase III (Pol III) promoters have been used predominantly to generate exogenous expressed RNAi precursors. Pol III promoters possess constitutive activity in most tissue types and their transcripts can be easily tailored into microRNA-like cellular precursor structures. Regulation of Pol III promoters is however difficult to achieve, and their lack of tissue specificity and high activity are responsible for the toxic saturating effects on the RNAi pathway. In contrast, RNA polymerase II promoters express mRNAs which can be regulated and are differentially expressed in specific tissues. However, Pol II-transcripts have additional sequences such as the 5’ 7-methyl guanosine cap and 3’ polyadenylation sequence which make them unsuitable for the generation of important RNAi precursors such as short hairpin RNAs (shRNAs). This study aimed to produce a series of cytomegalovirus (CMV) promoter-controlled expression cassettes that would generate shRNAs lacking unwanted flanking sequences. The precise hairpin RNA strand was processed post-transcriptionally through the action of chimaeric *cis*-cleaving hammerhead ribozymes that are incorporated up- and down-stream of the

shRNA. The hammerhead ribozymes were restored from a minimal state by inserting additional extra-core elements allowing for intracellular activity. This design for producing active RNAi effector sequences was termed a Ribozyme Processing System (RyPS). To evaluate the inhibitory efficacy of RyPS, a previously characterised shRNA targeted against the *X* open reading frame of the hepatitis B virus was inserted into a RyPS expression cassette. *In vitro* co-transcription and cleavage experiments demonstrated the processing potential of RyPS. This resulted in the formation of 3 products; the upstream and downstream ribozymes and the shRNA. Northern blot analysis of *in vitro* transcription products revealed the shRNA and downstream ribozyme were smaller than anticipated. Using primer extension analysis the precise ribozyme cleavage sites of the up- and downstream ribozymes were mapped. The upstream ribozyme mapped the predicted site, however multiple cleavage sites were mapped for the downstream ribozyme. The aberrant cleavage of the downstream ribozyme resulted in an shRNA cleaved within the antisense region, a sequence which dictates the targeting and inhibitory potential of the shRNA. Intracellular transfection of RyPS resulted in little to no inhibition of both live virus and targeted reporter genes. It was noted however that the ribozymes maintained intracellular activity according to a luciferase-based knockdown assay, in which ribozyme activity resulted in luciferase mRNA destruction. By applying these results to RNA folding algorithms, a model can be developed where atypical cleavage by the flanking ribozymes is avoided, and further allow for the design of more stable RyPS and individual ribozyme. Although the current design of the RyPS cassette was shown to be ineffective at producing active shRNAs, possible optimisation would

involve the substitution of the shRNA, or replacing the chimaeric hammerhead ribozyme species with a naturally occurring species. With these changes further developments of this post-transcriptional processing system may soon result in effective Pol II-generated sequences for therapeutic RNAi.

Acknowledgements

1. My sincere thanks to my supervisor, Patrick Arbuthnot, whose guidance and patience is much appreciated. I would also like to thank my supervisor for providing the opportunity to attend an international conference.

2. Thanks to my colleagues, Dr. Marc Weinberg and Abdullah Ely for assistance on various practical aspects of my research.

3. To my colleagues of the Antiviral Gene Therapy Unit, who often provided support and ideas in time of need.

4. To the funding bodies from which I have received financial assistance for the duration of my Degree, the University of the Witwatersrand Postgraduate Merit Award, the Poliomyelitis Research Foundation and the Antiviral Gene Therapy Unit.

Table of Contents

DECLARATION ..... **II**

PRESENTATIONS AND PATENTS ..... **III**

CONFERENCE PROCEEDINGS III
PATENTS III

ABSTRACT ..... **IV**

ACKNOWLEDGEMENTS ..... **VII**

TABLE OF CONTENTS ..... **VIII**

LIST OF FIGURES ..... **X**

LIST OF TABLES ..... **XII**

NOMENCLATURE AND ABBREVIATIONS ..... **XIII**

LIST OF SYMBOLS ..... **XV**

INTRODUCTION **1**

RNA INTERFERENCE: THE POWER OF SILENCE 2
MicroRNAs are generated with the nucleus *3*
Cytoplasmic processing and RISC assembly *8*
Silencing the enemy: RNAi and Therapeutics *10*
Resistance development *15*
HAMMERHEAD RIBOZYME MECHANISM AND USES IN THERAPY 17
History of discovery *17*
Mechanism of cleavage: Past theories and current models *18*
Ribozymes as therapeutic molecules *29*
THE RIBOZYME PROCESSING SYSTEM 31

MATERIALS AND METHODS **40**

GENERATION OF RYPS CLONES 42
PCR *44*
Plasmid construction and cloning *45*
GENERATION OF THE LUCIFERASE-RYPS REPORTER SYSTEM 52
DNA PREPARATION FOR GENERAL USE AND TRANSFECTION 58
IN VITRO TRANSCRIPTIONS 58
Template Generation *58*
In vitro transcription *60*
TISSUE CULTURE, TRANSFECTIONS AND RNA COLLECTION 61
CELL CULTURE 61
Transfections *64*
ELISA against HBsAg *64*
Dual luciferase based assay *65*
NORTHERN BLOTS AND ASSOCIATED PROCEDURES 66
RNA extractions *66*

Electrophoresis *67*
Blotting *68*
Hybridisation and oligonucleotide preparation *68*
Oligonucleotide probe preparation *68*
Hybridisation *68*
CLEAVAGE SITE DETERMINATION BY PRIMER EXTENSION REACTIONS 69
Primer extension *71*
Sequencing-size determination reaction *71*

RESULTS AND DISCUSSION 73

IN VITRO TRANSCRIPTIONS 73
NORTHERN BLOT ANALYSIS OF RNA GENERATED BY IN VITRO TRANSCRIPTIONS 94
CELLULAR ASSESSMENT AND HBV KNOCKDOWN 102
ASSESSMENT OF INTRACELLULAR RIBOZYME ACTIVITY 110
PREDICTIVE MODELLING OF RYPS SECONDARY STRUCTURE 114
DETERMINATION OF RYPS CLEAVAGE SITES: PRIMER EXTENSION REACTIONS 119

APPENDICES 131

APPENDIX 1 131
APPENDIX 2 132
APPENDIX 3 134

REFERENCES 135

List of Figures

Figure 1. 1: Generation of Precursor microRNA 7
Figure 1. 2: Schematic representation of the RNAi pathway within mammalian cells. 14
Figure 1. 3: Nucleotides within the highly conserved catalytic core of a hammerhead ribozyme. 19
Figure 1. 4: Three different states in which the minimal hammerhead ribozyme have been artificially constructed. 20
Figure 1. 5: The various transitions states of the catalytic region of the hammerhead ribozyme, applying the two possible cleavage theories. 24
Figure 1. 6: Difference between the secondary and tertiary structure of a fast-acting hammerhead ribozyme. 26
Figure 1. 7: Penta-coordinated state of a hammerhead ribozyme, proposed by Martick and Scott, 2006. 28
Figure 1. 8: The theoretical secondary structure of RyPS. 33
Figure 1. 9: Illustration of the possible cleavage products by RyPS. 35
Figure 1. 10: A representation of the HBV genome. 38

Figure 2. 1: General overview of the experimental procedures followed over the duration of experimentation. 40
Figure 2. 2: A diagrammatic representation of the steps taken to generate vectors capable of expressing RyPS within a mammalian cell. 43
Figure 2. 3: A plasmid map of pTZ57R, used for T/A cloning experiments. 46
Figure 2. 4: A plasmid map of pCI-neo. 49
Figure 2. 5: Overview of methodologies to generate the luciferase-RyPS reporter system. 52
Figure 2. 6: Representative figures of the outcomes when the RyPS constructs were cloned behind *Renilla* luciferase. 54
Figure 2. 7: Plasmid map of psiCheck2.2. 57

Figure 2. 8: Schematic representation of the DNA templates used in the *in vitro* transcription reactions. 59
Figure 2. 9: Basic overview of the experiments involved in the cellular assessment of RyPS. 63
Figure 2. 10: Overview of the primer extension reaction used to determine the cleavage sites of each of the ribozymes in RyPS. 70

Figure 3. 1: Illustration of the possible products formed by the faster RyPS during *in vitro* transcriptions. 74
Figure 3. 2: Diagrammatic comparison of the various hammerhead ribozymes included within the RyPS species. 79
Figure 3. 3: An autoradiograph of *in vitro* transcription products subjected to electrophoresis in a 10% denaturing polyacrylamide gel. 84
Figure 3. 4: Templates used for *in vitro* transcriptions. 86
Figure 3. 5: Schematic representation of the RyPS products generated during *in vitro* transcription, separated by electrophoresis. 88
Figure 3. 6: An autoradiograph of the RyPS *in vitro* transcription products, using PCR generated templates. 92
Figure 3. 7: An ethidium bromide stain of RNA generated by *in vitro* transcription prior to transfer onto a nitrocellulose membrane. 97
Figure 3. 8: Comparison of the three northern blots for the 5’ and 3’ ribozymes and the shRNA of RyPS. 100
Figure 3. 9: A schematic representation of the region within psiCheck2.2-HBx containing the luciferase genes, *Renilla* luciferase (hRLuc) and Firefly luciferase (HFLuc). 103
Figure 3. 10: Normalised ratio of *Renilla*:Firefly luciferase assay, using the dual luciferase reporter system. 105
Figure 3. 11: A normalized ELISA against HBsAg of RyPS against live HBV. 108
Figure 3. 12: A normalized ratio of *Renilla*:Firefly dual luciferase assay, in detection of RyPS ribozyme intracellular activity. 112

Figure 3. 13: Intended and predicted structures of RyPS.....117
Figure 3. 14: Primer extension reactions together with sequencing data indicate the region of cleavage caused by each of the ribozymes. 123

Figure 3. 15: A schematic representation of the possible adaptation to the currently used ribozymes in RyPS. 129

List of Tables

Table 2. 1: Definitions for abbreviations used in materials and methods.....41
Table 2. 2: Primers used to generate required RyPS fragments (and knockout clones) by PCR 44
Table 2. 3: Clone screening primers which bind the flanking regions of the MCS in pTZ57R 47
Table 2. 4: Adapted T7 and T3 primers used in the PCR screening of positive RyPS clones inserted into pCI-neo.....50
Table 2. 5: Primers used to generate RyPS fragments from PCR containing the correct restriction sites for cloning into psi-Check2.2 55

Table 3. 1: Potential RyPS products and their predicted sizes to be generated by *cis*-cleavage after an *in vitro* transcription reaction using template generated by restriction digest.....76
Table 3. 2: Size predictions of the RyPS products produced by *cis*-cleavage after an *in vitro* transcription using PCR products as template.....87

Nomenclature and Abbreviations

Ago – Argonaute protein

AmpR – ampicillin resistance gene

CCR5 – chemokine (C-C) receptor 5

dATP – deoxyadenosine triphosphate

dCTP – deoxycytosine triphosphate

Del – deleted (refers to a non-functional mutant)

dGTP – deoxyguanosine triphosphate

DNA – deoxyribonucleic acid

dNTP – deoxynucleoside triphosphate

ds – double stranded

dTTP – deoxythymidine triphosphate

ELISA – enzyme-linked immunosorbent assay

g - gravitational force

GTP – guanosine triphosphate

HBV – Hepatitis B virus

HDV – Hepatitis D virus

Hek293 – Human embryonic kidney cell line

HIV – Human immunodeficiency virus

Huh7 – Human hepatoma cell line

LB – Luria Bertani

mA – milliAmperes

MCS – multiple cloning site

miRNA – microRNA

mRNA – messenger RNA

nt – nucleotide

ORF – open reading frame

p - plasmid

PAZ – piwi/argonaute/Zwille

p-bodies – processing bodies

PCR – polymerase chain reaction

PLMV – Peach latent mosaic virus

Pol II and Pol III – Polymerase II and Polymerase III respectively

Pre-miRNA – precursor miRNA

Pri-miRNA – primary miRNA

PTGS – Post Transcriptional Gene Silencing

Ran-GTP – GTP-bound ran

RISC – RNA induced silencing complex

RNA – ribonucleic acid

RNase - ribonuclease

RNAi – RNA interference

RSV – respiratory syncytial virus

RyPS – Ribozyme Processing System

Rz – ribozyme

shRNA – short hairpin RNA

siRNA – small interfering RNA

SV40 – simian vacuolating virus 40

TRBP – TAR RNA-binding protein

Trunc – truncated

u - unit

UV – ultra violet

V - volts

VS – Varkud satellite

List of Symbols

α – alpha-

β – beta-

Δ - delta

f – femto- (x 10^{-15})

γ – gamma-

μ – micro- (x 10^{-6})

m – milli- (x 10^{-3})

n – nano- (x 10^{-9})

p – pico- (x 10^{-12})

Introduction

Unique new therapeutics against various diseases are often required to be developed, particularly when the disease-causing agent develops resistance to the existing drugs, or when administration of the drug becomes non-feasible. Drug administration to patients is a difficulty in developing countries such as sub-Saharan Africa, since travel, storage and patient compliance are many tasks that require attention. Ideally potential therapeutic drugs used in these environments would require a large degree of stability, relatively easy drug administration and minimal patient compliance. One particular therapeutic interest, known as RNA interference (RNAi), has gained momentum in the past few years, revealing a system with elaborate cellular pathways. RNAi utilizes innate (small processed RNA strands produced specifically for RNAi) or exogenous sources of RNA (such as viral RNA) to induce the targeted degradation or suppression of a specific RNA strand. From a therapeutic perspective these exogenous RNA species can be introduced into a living system encoded within various DNA templates such plasmids. This provides cost effective and stable therapeutic particles which may provide a solution to drug management within developing countries.

RNA Interference: The Power of Silence

This highly conserved and homologous pathway within eukaryotes has been noted as far back as twenty years ago (Izant and Weintraub 1984; Fire et al. 1991; Fire et al. 1998). The molecular mechanism was far from being understood, however it was noted that by adding anti-sense RNA to a cell knockdown of a particular homologous target was induced. Fourteen years later, Fire and Mello established the first basic requirements for the RNAi pathway, and received the Nobel Prize for physiology or medicine in 2006 for their contribution and initial elucidation of the pathways in RNAi. Their discovery showed that double stranded RNA was far more powerful in inducing knockdown than the single anti-sense counterpart within *Caenorhabditis elegans* (Fire et al. 1998). Little did Fire and Mello know, but their discovery would lead to the rapid elucidation of multiple RNA processing pathways within the cell. Prior to their discovery, anti-sense RNA was thought to induce generalized knockdown of all cellular RNA, placing the cell within a "lockdown" state, in which little to no transcription takes place (Proud 1995). It was also believed that double-stranded RNA is stable enough not to unwind within a cellular environment, remaining as a double helix. Fire and Mello's discovery suggested that certain cellular species and pathways are involved in the unwinding of nucleic acids, and furthermore, involved in target and effector molecule recognition and binding (Mello and Conte Jr 2004). It was shown soon thereafter that if *C. elegans* was placed in an environment containing dsRNA, knockdown would occur of mRNA sequences that shared homology with the dsRNA (Tabara et al. 1998). Furthermore, if *C.*

elegans was fed a diet of bacteria were made to express dsRNA targeting a particular gene, knockdown effects were witnessed on that particular homologous target (Timmons and Fire 1998; Timmons et al. 2001). So powerful was this effect it was seen to be carried over into the progeny of *C. elegans* within the germ line (Grishok et al. 2000). Knockdown studies were soon found to be highly successful in plants (post-transcriptional gene silencing, or PTGS), fungi (quelling) and *Drosophila* (RNAi) (Romano and Macino 1992; Fagard et al. 2000; Aravin et al. 2001) .

MicroRNAs are generated with the nucleus

Innate RNAi plays a vital role in cellular development and maintenance, assisting in the regulation of protein and RNA species production within the cell. These regulatory events are initiated by small 21-22nt RNA species known as microRNAs (miRNAs), which are ubiquitous within cells and over one hundred have been classified within the human genome (Lee et al. 2002). MicroRNAs exist in unprocessed forms initially and require processing before inducing target knockdown, these are termed primary microRNAs or pri-miRNAs (Lee et al. 2002; Bartel 2004). Their biogenesis starts in the nucleus, initiated either by a Polymerase II or III promoter (Pol II and Pol III respectively). Typically Pol III promoters are highly active and induce expression within most cell types, furthermore these promoters are involved in the expression of smaller RNA species such as tRNAs, 5S ribosomal RNA and U6 snRNA (Bartel 2004). Polymerase II promoters cause the transcription of mRNA and certain small RNAs, including the small nucleolar RNAs (snoRNAs) and small nuclear RNAs (snRNAs) (Bartel 2004). Several data indicate that Pol II

promoters are responsible for generating many of the miRNA species, owing to some pri-miRNA species being larger than 1kb and that Pol III is unable to generate such large RNA fragments; some pri-miRNAs have been shown to have uridine repeats, which would cause transcription termination by Pol III; pri-miRNAs require differential expression during development, a feature provided by Pol II, and not by Pol III (Bartel 2004; Cai et al. 2004). Other species of miRNAs are found within introns of pre-mRNA and are known as mirtrons. These particular species of pri-miRNAs undergo normal RNA splicing during intron excision and remain as mitron lariats before they are debranched and folded into precursor microRNA or pre-miRNA (Ruby et al. 2007). This form of pre-miRNA generation bypasses any form on nuclear endonuclease III processing.

The pri-miRNA transcript is initially processed by a member of the RNase III endonuclease super-family known as Drosha, into a ~60-70nt stem-loop product known as precursor-microRNA or pre-microRNA (Lee et al. 2002; Basyuk et al. 2003; Lee et al. 2003; Bartel 2004). Drosha does not act alone within the nucleus, and forms a complex with several other proteins such as Pasha (partner of Drosha), collectively known as the Microprocessor (Denli et al. 2004; Gregory et al. 2004). Pasha (known as DGCR8 in mammals) plays and important and interesting role, as it is responsible for the stabilisation of Drosha as well binding of the pri-microRNA. This occurs because DGCR8 contains two dsRNA binding domains in the C-terminal region, both equally responsible for anchoring pri-miRNAs within the Microprocessor (Han et al. 2006; Yeom et al. 2006). Also within the C-terminal of DGCR8 is the binding and stabilizing domain which interacts with the middle domain

of Drosha. The N-terminal domain of DGCR8 contains a nuclear localization signal, responsible for the transport of DGCR8 into the nucleus and potentially retaining it there (Yeom et al. 2006).

Drosha cleaves its target pri-miRNA, leaving a phosphorylated 5' and a 2 nucleotide 3' overhang end (Basyuk et al. 2003), producing a pre-miRNA which is transported into the cytoplasm. Pre-miRNA transport occurs via the nuclear protein Exportin-5, a dsRNA binding protein which is Ran-GTP dependent (Yi et al. 2003; Bartel 2004; Bohnsack et al. 2004). The above processes are schematically described in Figure 1.1. RNA interference is unable to induce knockdown within the nucleus, as multiple protein species and complexes involved in the RNAi pathway are solely located within the cytoplasm. This has particular importance as certain viruses replicate within the nucleus, thus leaving them unaffected by the RNAi machinery. It is required for the target mRNA molecule to enter the cytoplasm, in which it can be identified and processed by the RNAi machinery. Use of RNAi against nuclear replicating viruses would require combinatorial approaches, in which various therapeutic agents are employed, one of which may be ribozymes (catalytic RNA molecules) which are able to remain active within the nucleus, cleaving their targets.

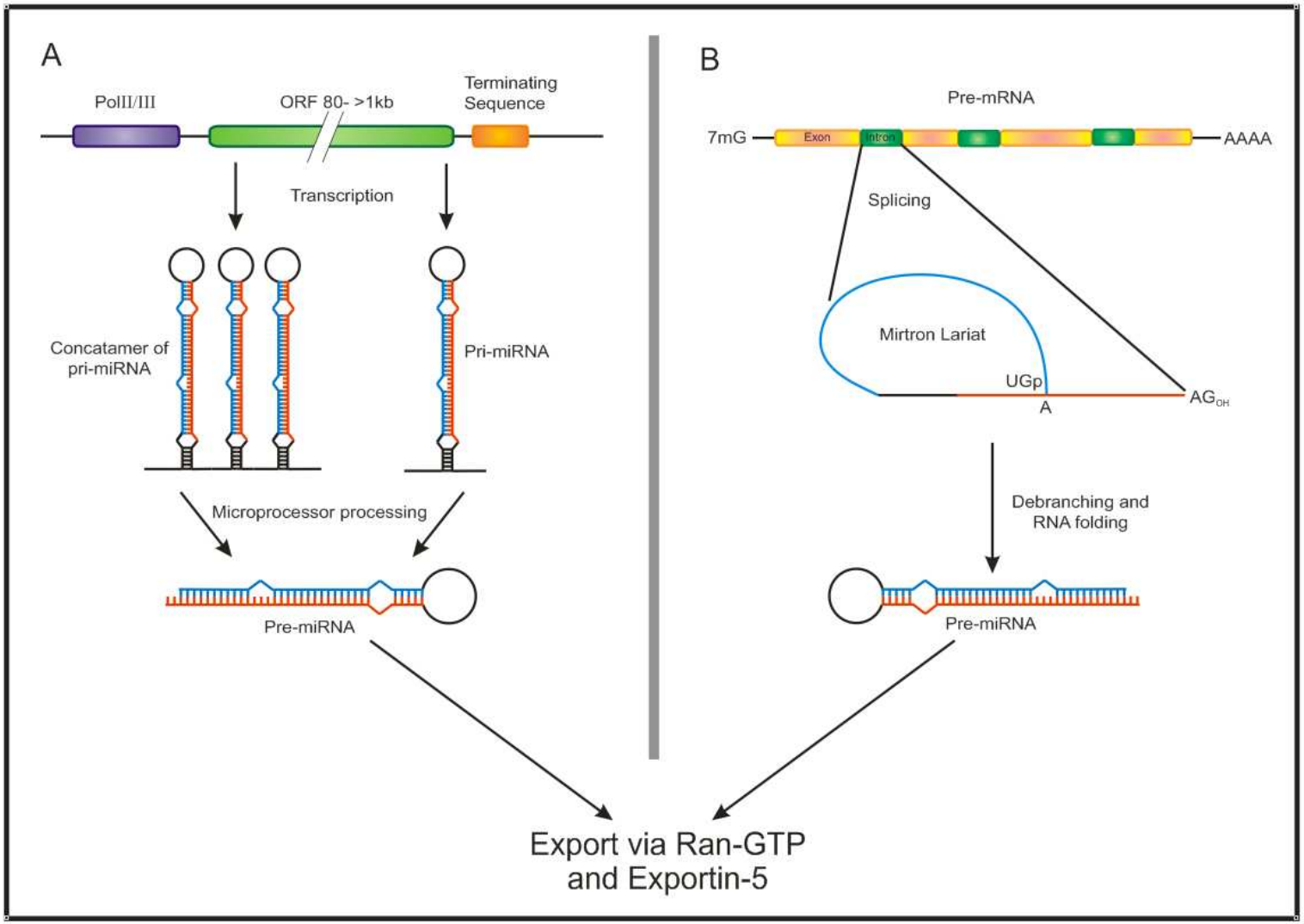
A
PolII/III
ORF 80- >1kb
Terminating Sequence
Transcription
Concatamer of pri-miRNA
Pri-miRNA
Microprocessor processing
Pre-miRNA
B
Pre-mRNA
7mG
Exon
Intron
AAAA
Splicing
Mirtron Lariat
UGp
A
AG$_{OH}$
Debranching and RNA folding
Pre-miRNA
Export via Ran-GTP and Exportin-5

Figure 1. 1: Generation of Precursor microRNA

Precursor microRNAs (pre-miRNA) can be generated by two methods, depending on their source. **A,** pre-miRNAs are transcribed from either a Pol II or Pol III promoter, to produce either a single pri-miRNA (>80 nucleotides) or a polycistronic pri-miRNAs containing multiple pri-miRNAs (can be over 1kb). Both forms of pri-miRNAs are processed by Drosha, within the Microprocessor resulting in a pre-miRNA product. In the second method, **B**, pre-miRNAs are derived from spliced introns. The intron-pre-miRNAs are known as mirtrons, and require no processing by the Microprocessor, but rather debranching to release the conserved adenine from the guanine typical of intron lariats, allowing for the pre-miRNA formation. Once either pathway has generated a pre-miRNA, it is exported into the cytoplasm via the Ran-GTP dependent Exportin-5 pathway.

Cytoplasmic processing and RISC assembly

The Drosha processed pre-miRNA is exported to the cytoplasm via Exportin-5, then recognised and bound by Dicer, a cytoplasmic RNase III endonuclease (Grishok et al. 2001; Hutvagner et al. 2001). The PAZ (piwi/argonaute/Zwille) domain within Dicer contains a binding pocket for the 2 nucleotide 3' overhang of the pre-miRNA and facilitates the binding of the remainder of the pre-miRNA into the RNase portion of Dicer (MacRae et al. 2006). Dicer contains two RNase domains, each responsible for cleaving one strand of the double helix exactly 25 nucleotides from the binding pocket of the PAZ domain. Starting from the 5'end and two helical turns towards the loop of the pre-miRNA, Dicer cleaves the dsRNA in a similar manner to Drosha producing a 5' phosphate and a 2 nucleotide 3' overhang. This 25 nucleotide distance is facilitated by the connector helix between the RNase and PAZ domain, allowing for the exact measurement (MacRae et al. 2006).

Invasive RNAs, such as those of viral origin, enter the RNAi path at this point. Presence of dsRNA is typical of many viral infections. This is also processed by Dicer into 21-23 nucleotide fragments, known as small interfering RNAs (siRNAs). However without Microprocessor processing, viral RNAs are not as efficiently processed as a result of the initial interaction between the 2 nucleotide 3' overhang of the pre-miRNA and the PAZ domain of Dicer (MacRae et al. 2006).

The final process of the RNAi pathway results in either translational suppression or degradation of the target RNA within the cytoplasm. After Dicer has cleaved its target, be it innate or exogenously sourced, several proteins are recruited to

aid the transfer of the miRNA/siRNA to the RNA induced silencing complex (RISC). Two of the important proteins recruited are Argonaute (Ago2 in particular) and TRBP (HIV-1 TAR RNA-binding protein) (Lee et al. 2006; Kok et al. 2007; MacRae et al. 2008). Helicase is also required, as it plays two roles in the process; firstly to unwind the double stranded miRNA into its sense and antisense components; and secondly to recognize self and non-self RNAs by the presence of the 2 nucleotide 3' overhang (Marques et al. 2006). Both the sense and antisense stands have the potential to be incorporated into RISC, however their selection is dependent on the stability of the 5' region. The less stable and easier to unwind strand from the 5' region is selected and incorporated into RISC (Khvorova et al. 2003a; Schwarz et al. 2003; Patzel et al. 2005).

The argonaute proteins are a large family of proteins, and at least one is present per RISC assembly (Bartel 2004). Like many of the defined proteins involved in the RNAi pathway, Ago proteins have domains involved in RNA binding, in particular a PAZ domain and a PIWI domain. Both these domains are highly conserved, and the PIWI domain containing a fold that resembles RNase-H like fold involved in cleavage (Faehnle and Joshua-Tor 2007), however not all species of Ago are known to cleave their target. The only Ago species defined thus far to cleave its target is Ago2 (Liu et al. 2004). Target RNA cleavage within RISC is dependent on features within the guide antisense sequence, and how it associates with the target mRNA sequence. Complete and near complementarity between guide and target results in mRNA destruction, cleavage occurring ten nucleotides up from the 5' start of the antisense strand. During cleavage the guide strand remains

unaffected (Khvorova et al. 2003a; Schwarz et al. 2003; Bartel 2004). Predominately, foreign RNA has perfect complementarity, resulting in its destruction. Poor complementarity results in translational suppression, in which RISC remains bound to the target mRNA strand (Khvorova et al. 2003a; Schwarz et al. 2003; Bartel 2004). Translational suppression, amongst other RNAi processes, would seem to occur within P-bodies of the cytoplasm, in which no translational machinery are present (Liu et al. 2005b; Liu et al. 2005a; Lian et al. 2007).

Silencing the enemy: RNAi and Therapeutics

RNA interference has the ability to induce almost complete knock down of its target, making it an extremely potent and specific therapeutic tool. Any disease reliant on RNA as an intermediate can be targeted, which ranges from viral infections such as Hepatitis B virus and human immunodeficiency virus (HIV), to cancers and autosomal genetic diseases. One of the first reported successful treatments against disease was shown in 2003, using a mouse model (Song et al. 2003). Since then, clinical trials have passed phase 2 against respiratory syncytial virus (RSV) and age-related macular degeneration (Dykxhoorn and Lieberman 2006).

Therapeutic molecules can enter the RNAi pathway at multiple stages, by either being expressed within the nucleus from an exogenously sourced DNA template, or introduced as synthesized RNA, directly into the cytoplasm. It is possible to enter the RNAi pathway at multiple stages, in the form of pri-miRNAs, short hairpin RNAs or pre-miRNAs, and miRNAs or siRNAs. Other studies have utilized

long hairpins, containing multiple siRNAs which rely on Dicer processing (Barichievy et al. 2007). Ultimately using synthetic siRNAs to induce target knockdown would avoid competition between exogenous and innate pre-miRNAs within the nucleus. This study has chosen to utilize Dicer as the initial stage of processing of the RNAi molecules introduced. The main reasons for this are that by only using Dicer, nuclear processing can be bypassed, and as Grimm et al. 2006 have suggested one can perhaps avoid saturating the nuclear processing component of the RNAi pathway. Furthermore, by using the catalytic activities of certain RNA species (such as ribozymes) it may be possible to generate a shRNA independent of Pol III promoter expression. Currently Pol III promoters are used to generate pre-miRNAs, shRNAs and siRNAs owing to their ability to transcribe small RNAs without the requirement of large transcription termination sequences; however some of these promoters have undesired properties such as high levels of transcription and are transcriptionally active in most cell types. Pol II promoters cannot easily be used for the generation of siRNAs due to the extra elements produced with mRNA, such as 5' 7-methyl guanosine caps and polyadenylated 3' ends. Should one be able to couple tissue specific inducible transcription of a therapeutic molecule, as well as generating an exact RNAi effector molecule independent of Microprocessor processing, this therapeutically offers a considerable amount of benefit. Benefits include avoidance of possible cytotoxic effects produced when saturating the RNAi processing system within the nucleus; tissue specific inducible expression, which is energy cost effective in cells that do not require treatment. This project aims to utilise the catalytic processing power of ribozymes to generate an active RNAi molecule that

requires minimal processing, while having tissue specific activity from the Pol II promoters.

Even though one is able to generate an active and effective RNAi therapeutic, one field of therapeutics remains challenging and requires a large degree of development. The hurdle within this field is delivery of the effector systems, whether it be template DNA or synthetic RNA. Current delivery strategies include binding moieties such as simple sugars to the RNA molecule, which are exclusively recognized by specific tissue type; using an antibody complex with bound RNAs to target specific tissue types; encasing the RNA or DNA templates within liposome vesicles; using lenti- and adenoviral vectors to convey DNA template to specific cell types (Dykxhoorn and Lieberman 2006).

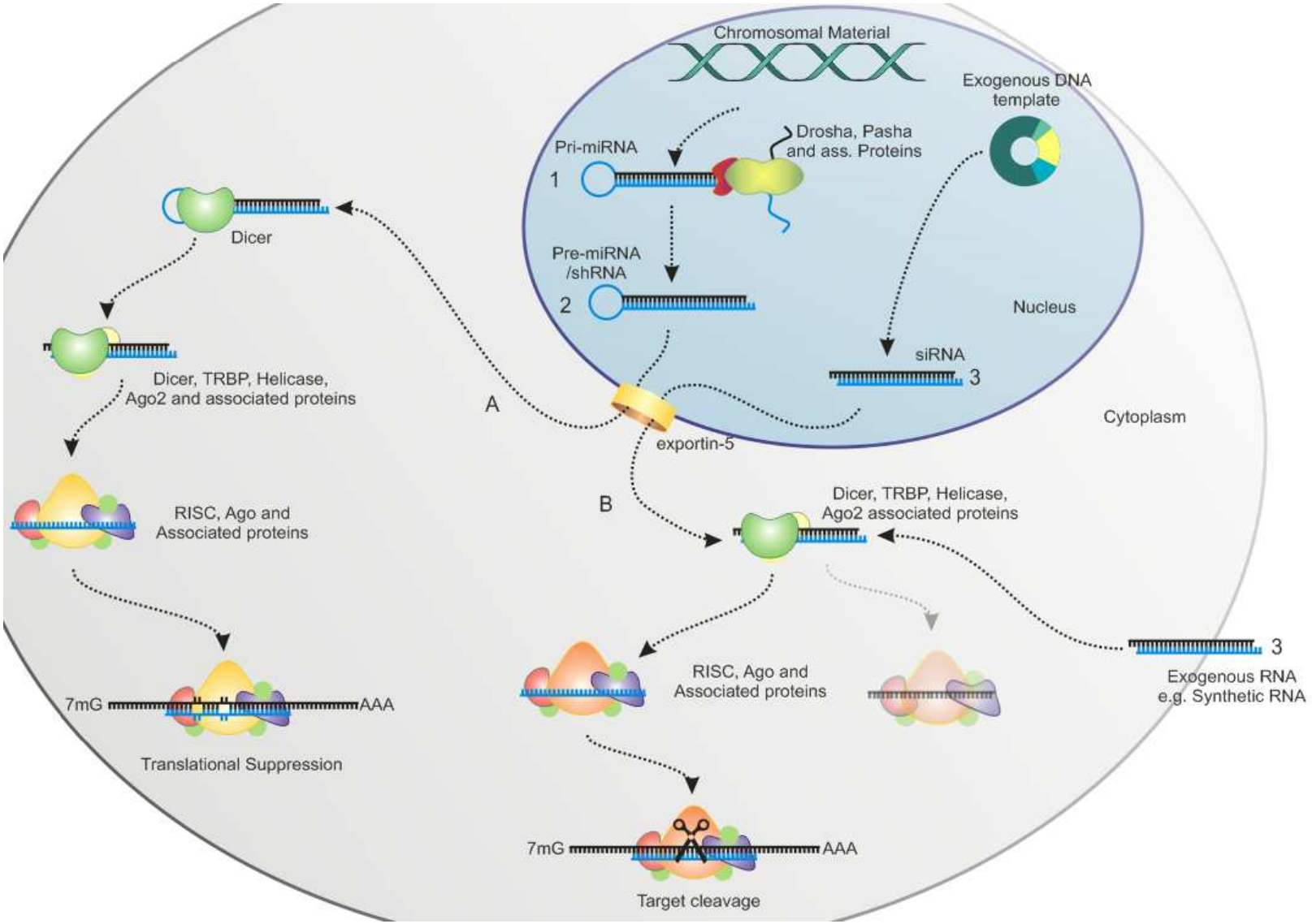
Chromosomal Material
Exogenous DNA template
Drosha, Pasha and ass. Proteins
Pri-miRNA
1
Pre-miRNA /shRNA
2
Nucleus
siRNA
3
Dicer
Dicer, TRBP, Helicase, Ago2 and associated proteins
A
exportin-5
Cytoplasm
B
RISC, Ago and Associated proteins
Dicer, TRBP, Helicase, Ago2 associated proteins
7mG
AAA
Translational Suppression
RISC, Ago and Associated proteins
3
Exogenous RNA e.g. Synthetic RNA
7mG
AAA
Target cleavage

Figure 1. 2: Schematic representation of the RNAi pathway within mammalian cells.

Effector RNA sequences are transcribed from the host chromosomal material as pri-miRNAs, processed and exported via exportin-5 into the nucleus, or alternatively off a DNA template as miRNAs, siRNAs or shRNAs. Once in the cytoplasm, the RNA duplex is processed by Dicer into ~21-23nt duplex as in path A. The RNA duplex is then incorporated into RISC, and induces translational suppression owing to mismatches between effector and target sequences. Path B typically involves siRNA duplexes inducing target mRNA cleavage once incorporated into RISC. One can introduce therapeutic nucleic acids into the RNAi pathway at 3 major points: **1)**, as a pri-miRNA, (transcribed from exogenous sources of DNA such as plasmids) which requires processing by the Microprocessor activity; **2)** as a shRNA or pre-miRNA that only requires nuclear export and Dicer processing and **3)** as siRNAs, produced individually as sense and anti-sense strands, and forming a duplex within the nucleus. Synthetic RNA can also be used to generate siRNAs, which can be introduced into the cell via transfection.

Resistance development

Like most biological systems, resistance will evolve against drugs and therapeutic molecules used to treat disease. Certain viruses have potential to mutate easily and become escape mutants, immune to the effects of the therapeutic molecule. In particular, in the RNA viruses (single and double stranded) RNA replication relies on the RNA-dependent RNA polymerase, which is inherently a poor copier, inserting on average 1 mistake every ten thousand bases (Zheng et al. 2005). This would theoretically result in escape mutants forming rapidly, depending on viral replication rate and mutation rate. Studies done on polio and La Crosse Virus have shown that escape mutants can be generated in as little as 72 hours post treatment (Gitlin et al. 2002; Soldan et al. 2005; Zheng et al. 2005).

To overcome the chances of creating escape mutants, multi-targeting strategies have been employed, often targeting several different sites. Long hairpins (Barichievy et al. 2007; Weinberg et al. 2007), interfering multimers (Wilson and Richardson 2006) and combinatorial approaches (Li et al. 2006) have been used. An interesting combination used by Li et al. 2006, incorporated the use of a siRNA, a decoy tat sequestering molecule and a ribozyme. The siRNA was targeted against the tat/rev region of HIV mRNA, forming the first form of knockdown. The tat decoy, was able to translocate to the nucleus, and bind to Tat proteins, which are required for HIV replication, and lastly a ribozyme that targets and cleaves the CCR5 mRNA, used by HIV to gain access into host cells (Li et al. 2006). These ribozymes are a small species known as hammerhead ribozymes which are catalytically active RNA

molecules, naturally involved in *cis*-cleavage in a multitude of small plant pathogens, or as of late involved in therapeutic strategies when cleaving in *trans*-. This study incorporates the *cis*- cleaving activity of hammerhead ribozymes to generate a shRNA molecule. This strategy would be effective, as the ribozymes are independent of any processing systems found within the cellular environment, functioning within a cellular environment unaided. The following section will elaborate on the mechanism of hammerhead ribozyme cleavage, its versatility, diversity and simplicity and explaining why these small catalytic molecules are effective and independent within a cellular environment, making them ideal therapeutic tools.

Hammerhead Ribozyme Mechanism and uses in Therapy

History of discovery

The initial discovery that RNA is both an information carrying molecule as well as a catalytic agent was made in the early 1980s by Cech and colleagues, and later by Alteman and colleagues (Kruger et al. 1982; Guerrier-Takada et al. 1983). The hammerhead ribozyme is one of the smallest known ribozymes, catalyzing the nucleolytic transesterification of the phosphodiester backbone, yielding a 2'3'-cyclic phosphate and a 5' hydroxyl terminus (Prody et al. 1986). Other small species of ribozyme include the hairpin ribozyme (Buzayan et al. 1986; Dange et al. 1990), hepatitis delta virus (HDV) ribozyme (Wu et al. 1989) and the *Neurospora* mitochondrial Varkud satellite (VS) ribozyme (Saville and Collins 1990). Larger species of ribozymes are often involved as part of cellular processes, such as the RNA subunit of RNase P (Guerrier-Takada et al. 1983) and introns I and II (Brody and Abelson 1985; Sharp 1987).

The hammerhead ribozyme is the best characterized of the small ribozymes. The initial discovery of *cis*-cleavage by hammerhead ribozymes was within both positive and negative strands of viroids and viroid-like satellite sequences (Hutchins et al. 1986; Forster and Symons 1987; Daros and Flores 1995). Hammerhead ribozymes were also later discovered in caudate amphibians (Epstein and Gall 1987), *Dolichopoda* cave crickets (Rojas et al. 2000), shistosomes (Ferbeyre et al. 1998),

and *Arabidopsis thaliana* (Przybilski et al. 2005). Hammerhead ribozymes derived from small plant pathogens have active roles in viral replication, as they are involved in separating multimeric genomic concatemers into precursors used in transcription as well as replicating the viral genome (Bratty et al. 1993; Symons 1997). Interestingly it is suggested that hammerhead ribozymes do not share a common ancestry, and that their origins are independent of each other (Salehi-Ashtiani and Szostak 2001).

Mechanism of cleavage: Past theories and current models

The core of the hammerhead ribozyme consists of eleven highly conserved nucleotides, created by the junction of three helices, seen in Figure 1.3 (Hertel et al. 1992) . In several studies the minimal hammerhead ribozyme has been generated in various forms as a single strand. Each of the hammerhead species generated differs, being defined by the point at which they are connected by their stems and loops. Three known variations can occur; by opening stem II and I (Clouet-D'Orval and Uhlenbeck 1996); by opening stem II and III (Jeffries and Symons 1989); and by opening stem I and III (Haseloff and Gerlach 1989). These are schematically shown in Figure 1.4.

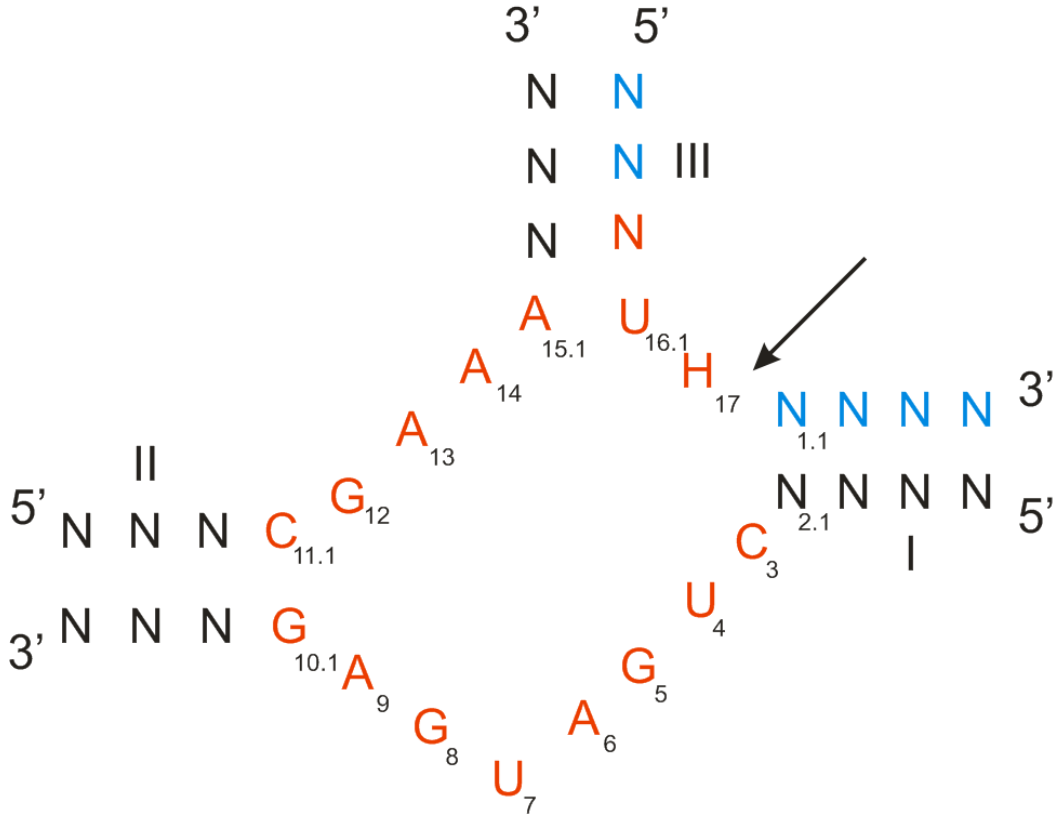

Figure 1. 3: Nucleotides within the highly conserved catalytic core of a hammerhead ribozyme.

The numbers accompanying the bases are the international nomenclature used when referring to nucleotides within the catalytic core. Stems I, II and III can be made of any stable Watson-Crick base pair. The nucleotides in red indicate those involved in the conserved catalytic core. The blue nucleotides indicate a target strand, should the ribozyme be acting in *trans*. Within the target sequence is the cleavage triplet NUH, where N is any nucleotide and H is any nucleotide but G. The numbering system was developed by Hertel et al. 1992, to standardise the data generated from various laboratories. The core was labelled in a clockwise manner, and decimal numbers indicate the first number of a helix.

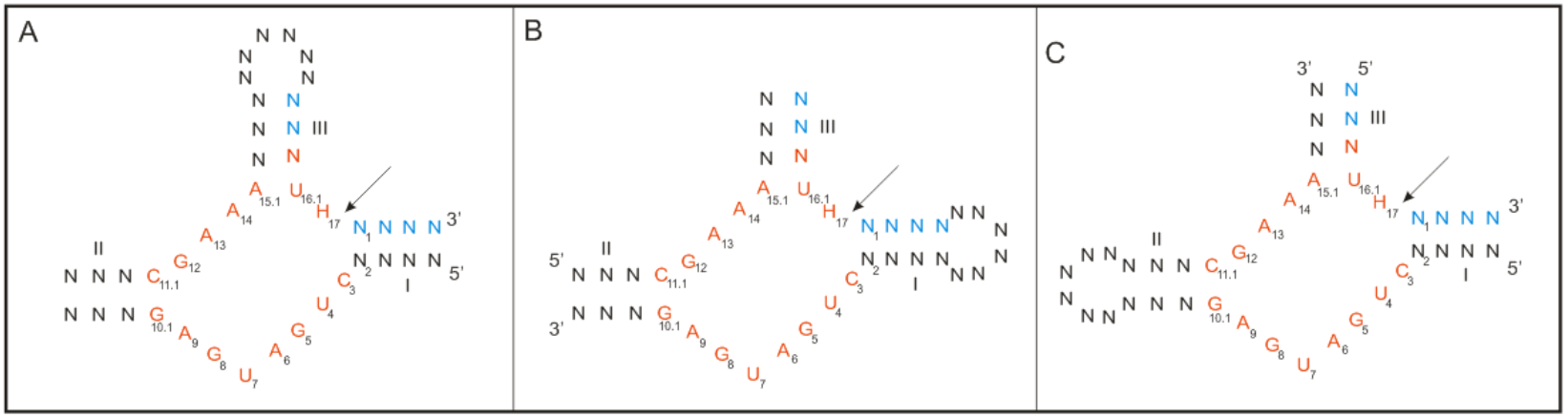

Figure 1. 4: Three different states in which the minimal hammerhead ribozyme have been artificially constructed.

In **A**, helix I and II were left open, and helix III looped. Similarly in **B** and **C**, various ends were left open or looped. Therapeutically, open helix I and III is the most viable, as most of the catalytic core is contained when the ribozyme is looped at helix II.

The hammerhead ribozyme undergoes extensive secondary and tertiary structure changes to allow for the correct positioning within the catalytic core to allow for cleavage (Martick and Scott 2006). Some of these changes involve the formation of a three-dimensional γ or 'wishbone' structure causing stem II and III to co-axially align, and stem I and II to lie adjacent to one another, depicted in Figure 1.6.

The core of the hammerhead ribozyme consists of two domains, the first comprising of 5'-$C_3U_4G_5A_6$-3', as well as the H_{17} residue, typically seen as C_{17} owing to it inducing enhanced cleavage rates. The second domain comprises of 5'-$G_{12}A_{13}A_{14}A_{15}$-3' as well as 5'-G_8A_9-3'. Although not seen as a domain, the motif 5'-$NU_{16}H_{17}$-3' is of high importance as it makes up the cleavage triplet at which the trans-esterification reaction takes place. The 5'-$NU_{16}H_{17}$-3' motif can withstand large sequence variation, making it ideal for a trans-cleaving therapeutic, cleaving the target strand after H_{17} (Haseloff and Gerlach 1989).

One flaw in the studies performed on hammerhead ribozymes was the removal of extra-core elements, which are often not highly conserved sequences, and were overlooked for over 15 years (Uhlenbeck 2003). Removal of these elements generated ribozymes known as minimal ribozymes and were considered to have an optimal cleavage rate of 1 min^{-1}, under conditions of 10 mM divalent magnesium ions, concentrations far higher than in the mammalian cell (Hertel et al. 1994). This would seem an ineffective cleavage strategy for plant viruses, as hammerhead

ribozymes are known to cleave within cellular environments, and such high magnesium concentrations are not found in those particular environments.

Furthermore, the cleavage mechanism was proving to be elusive as a result of the lack of consistent crystallographic data. Two predominating theories were accepted as the mechanism of cleavage of the minimal hammerhead ribozyme, both incorporating the usage of magnesium ions within the core, effectively creating a metalloenzyme. The first theory, known as the single ion theory, proposed that a hydroxyl group of a hydrated single divalent metal ion acted as a general base toward the 2' hydroxyl group of the N_{17} ribose sugar. This caused the 2' oxygen of the hydroxyl group to become a greater nucleophile, resulting in the nucleophilic attack on the adjacent phosphate and the generation of a cyclic 2',3' phosphate and a 5' hydroxyl group. This process occurs in the presence of a proton as an electron acceptor near the 5' oxygen (Torres and Bruice 1998; Takagi et al. 2001). The second theory, known as the double ion theory, requires that the 2' hydroxyl of the ribose sugar and the 5' leaving oxygen of $N_{1.1}$ are both stabilised by a divalent metal ion (behaving like Lewis acids), typically magnesium. The stabilisation in turn caused the phosphate group to become prone to nucleophilic attack, facilitated by the 2' hydroxyl group. This process occurs without any protons being terminal electron acceptors, unlike the first theory. Eventually the divalent metal ions are replaced by protons to form hydroxyl groups post cleavage (Lott et al. 1998; Takagi et al. 2001). Several other mechanistic theories were generated at the time, however the predominantly accepted theories were the single and double divalent metal ion mechanism, described in Figure 1.5.

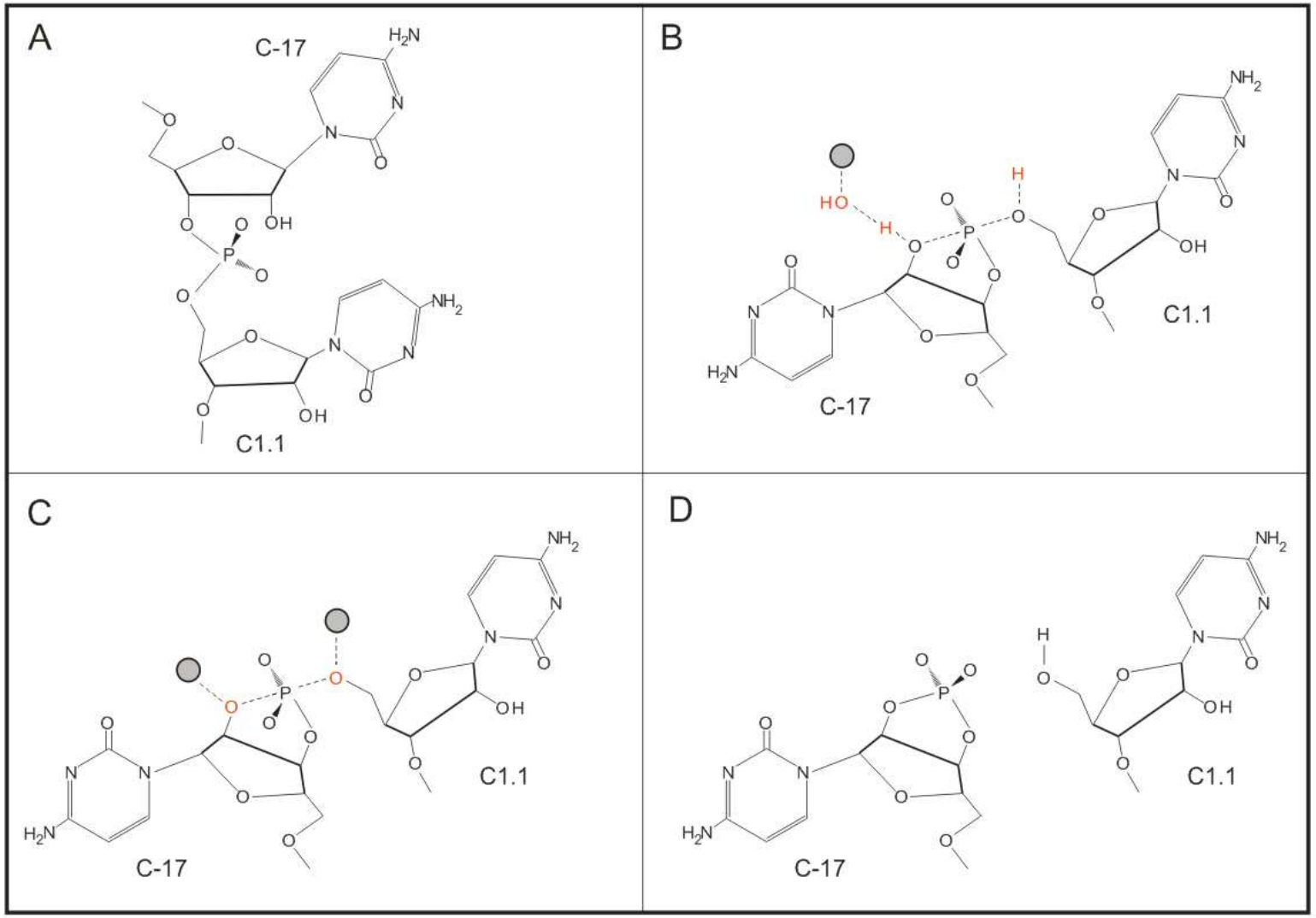
A
C-17
C1.1
B
C-17
C1.1
C
C-17
C1.1
D
C-17
C1.1

Figure 1. 5: The various transitions states of the catalytic region of the hammerhead ribozyme, applying the two possible cleavage theories.

In **A**, the ribozyme is in a state prior to cleavage initiation. H_{17} (C_{17}) contains the 2' hydroxyl group which initiates the nucleophilic attack on the scissile phosphate of C_1. **B**, demonstrates the single ion mechanism, whereby a hydroxyl group bound to the magnesium ion (grey ball) abstracts the hydrogen present on the 2' hydroxyl group of H_{17}. This in turn causes increased instability on the 2' oxygen and in turn attacks the scissile phosphate, resulting in a penta-coordinated state. **C** demonstrates the double ion mechanism, in which similar to the single ion theory, the 2' oxygen is directly abstracted by the magnesium ion, and the 5' oxygen is treated in a similar fashion. This makes the leaving group oxygen of $C_{1.1}$ more stable, and the nucleophilic attack occurs on the scissile phosphate. Panel **D** shows the ribozyme post-cleavage products, a 2'3' cyclic phosphate and a 5'-OH group.

Hammerhead ribozymes were recently re-examined to reassess the cleavage kinetics, and it was established that the cleavage rate of “restored” hammerhead ribozymes was far greater compared to the minimal species, when the extra-core elements were present (De la PenÄ et al. 2003; Khvorova et al. 2003b). The loops of stem I and II of *cis*-cleaving ribozymes were found to undergo non-canonical base pairing, resulting in a phenomenon known as a “kissing loop”, which influenced the cleavage rate (De la PenÄ et al. 2003; Khvorova et al. 2003b). With these extra-core elements present, the reverse ligation reaction is also possible albeit occurring far less than the cleavage reaction (Canny et al. 2007). Figure 1.6 demonstrates a potential kissing loop interaction within a hammerhead ribozyme, causing the coaxial alignment of stems II and III, and the parallel alignment of stems I and II.

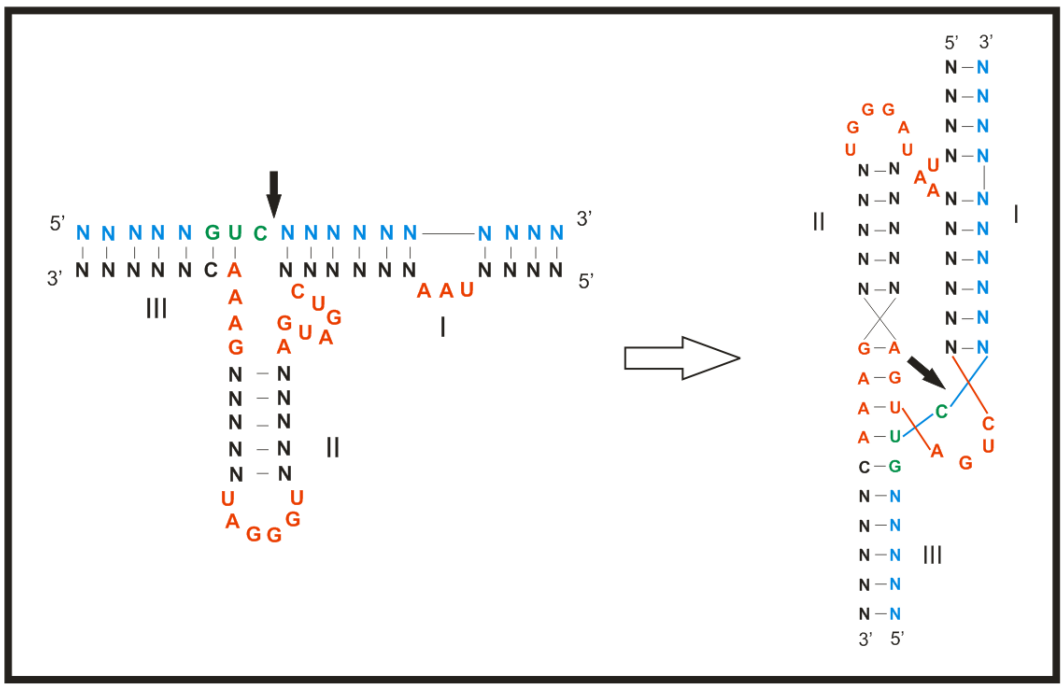

Figure 1. 6: Difference between the secondary and tertiary structure of a fast-acting hammerhead ribozyme.

On the left is the representation of the secondary structure of a hammerhead ribozyme. For cleavage to occur a complex tertiary conformation is required, stabilised by the kissing loop interaction of the extra core elements (5'-UGGGAU-3' and 5'-UAA-3') on helix I and II. Helix II and III have aligned co-axially, and helix I and II undergoing parallel alignment.

In 2006, Martick and Scott produced crystallographic data of the hammerhead ribozyme that would change the outlook on the cleavage mechanism. Their data showed that the extra-core elements were vital to the formation of the tertiary structure required for hammerhead ribozyme cleavage. The "kissing loop" was shown to be strong enough to induce partial unwinding of stem I, ultimately leading to an intricate set of events within the catalytic core never witnessed before (Blount and Uhlenbeck 2005). Some of these events include catalytic core stabilisation by the canonical base-pairing of nucleotides G_8 and C_3; bases such as G_{12}, A_{13} and A_{14} promote conformational locking within the pocket; G_5 and A_6 wedge themselves between C_{17} and $N_{1.1}$, forcing catalytic sites closer to each other (Martick and Scott 2006). This model explains what the minimal model could not, how core bases interacted without being over 20 Å apart. Possibly the most important aspect taken from this work is that divalent metal ions are not crucial for catalysis, and instead play a supportive role in charge neutralization of the phosphate backbone and possibly within the catalytic core (Martick and Scott 2006). Thus instead of metal ions, G_{12} behaves as a general base, abstracting the hydrogen of the 2' hydroxyl group, allowing for the penta-coordinated state to form (Han and Burke 2005; Lambert et al. 2006; Martick and Scott 2006). In order to stabilize the 5'-oxygen leaving group, G_8 behaves as a general acid (Martick and Scott 2006). This reaction is depicted in Figure 1.7. These findings make natural hammerhead ribozymes suitable therapeutic candidates within an intracellular environment. Their functionality within a cellular environment allows for the targeting and cleavage of a particular RNA strand, allowing hammerhead ribozymes to be directly involved in cleavage of a

target strand, or part of a processing system with aims to release effector therapeutic molecules.

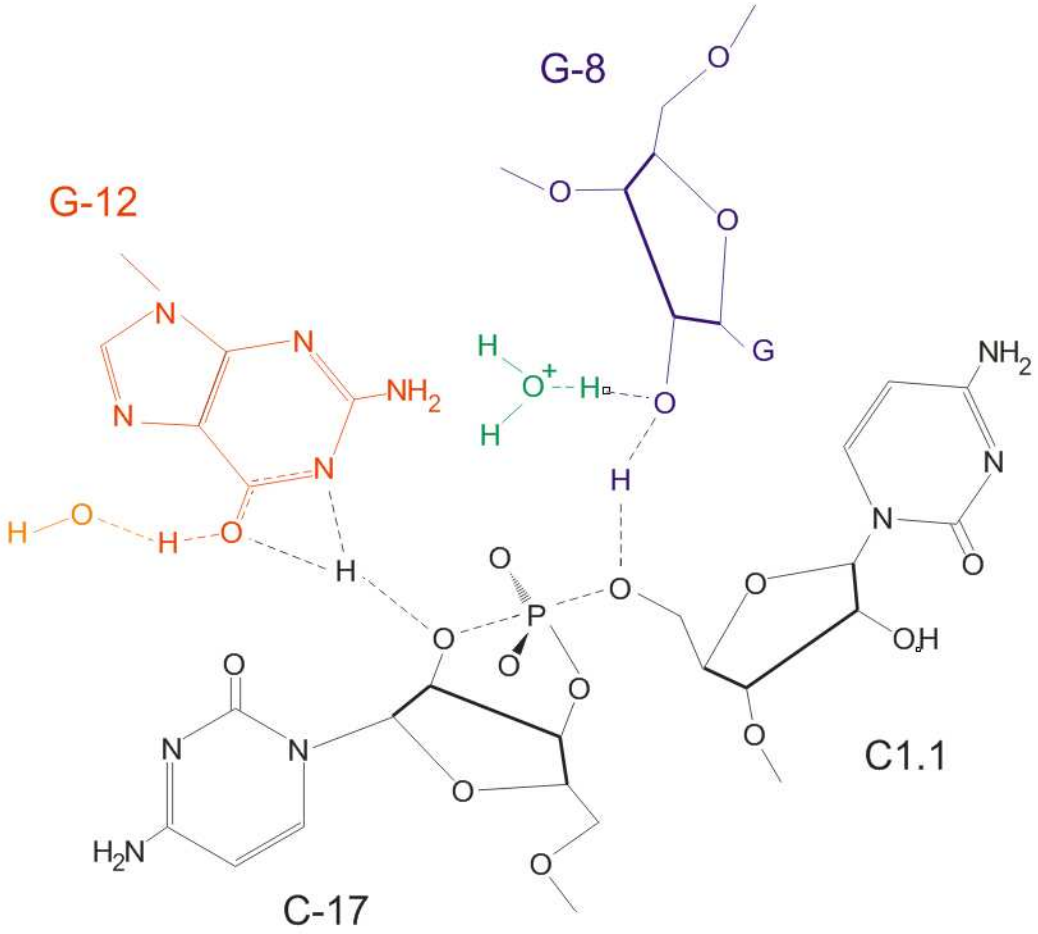

Figure 1. 7: Penta-coordinated state of a hammerhead ribozyme, proposed by Martick and Scott, 2006.

G_{12} behaves as a general base, abstracting the hydrogen from the 2' hydroxyl group. G_8 behaves like a general acid, stabilizing the 5' oxygen in the penta-coordinated state. These events provide greater stability for the cleavage reaction to occur, in which the phosphate will release the 5' oxygen and produce a 2'3' cyclic phosphate.

One could question whether these extra-core elements are so necessary, since minimal hammerhead ribozymes were able to undergo cleavage *in vitro*. One theory is that the very nature of the hammerhead ribozyme is structurally dynamic, and a momentary conformation required for cleavage may occur. Another idea is that the divalent metal ions are able to play a role in the catalytic reaction, as previously proposed (Uhlenbeck 2003; Kisseleva et al. 2005).

Ribozymes as therapeutic molecules

Minimal *trans*-cleaving hammerhead ribozymes had low efficacy against their targets owing to the poor cleavage ability within a cellular environment. The advent of RNAi for therapeutic purposes caused majority of the interest in RNA based therapy to be shifted from ribozyme therapeutics. However, since the restoration of the natural hammerhead ribozyme, and increased understanding of the cleavage mechanism, hammerhead ribozymes have several advantages over RNAi as therapeutic molecules. Hammerhead ribozymes are more specific than siRNAs, owing to the exact complementarity that is required by the ribozyme catalytic site, thus no off targeting can occur (Jackson et al. 2003; Akashi et al. 2005). A side effect of using RNAi effector molecules is the risk of inducing immunostimulation pathways, such as the interferon pathway, which ribozyme do not (Sledz et al. 2003; Judge et al. 2005; Karpala et al. 2005). Furthermore, the innate RNAi pathway is not affected by hammerhead ribozymes, avoiding possible toxic side effects seen by Grimm et al. 2006. Another advantage is that ribozymes function independently

within the cell, and are able to function within the nucleus, an area inaccessible to RISC.

This study did not use the *trans*-cleaving abilities of the hammerhead ribozyme, instead kept it as the more naturally occurring *cis*-cleavage. Hammerhead ribozymes were incorporated into a cleavage-processing system to generate a shRNA that does not rely on Drosha and associated proteins for processing. These hammerhead ribozymes have the ability to function within a cellular environment at physiological concentrations of magnesium, making them ideal processors. Furthermore by having these ribozymes in place, it is possible to use tissue specific inducible promoters such as the Pol II promoters, which therapeutically is a very appealing feature.

The Ribozyme Processing System

A ribozyme processing system (RyPS) was constructed in order to generate precise Dicer-compatible molecules, driven by tissue specific Pol II promoters. This system is unique in its approach, as it allows for several unique features as an RNAi therapeutic: RyPS is able to generate a precise Dicer substrate, void of Drosha processing. This decreased bio-processing is advantageous as there is a decreased chance of creating competition for processing with innate RNAs Grimm et al. 2006; The exact Dicer substrate does not require the conventional Pol III promoter expression, allowing for inducible, tissue specific, and lower levels of expression. Furthermore the RyPS has the potential to be used as a concatemer, generating multiple shRNA sequences from a single promoter, preventing promoter exclusion.

RyPS is composed of one shRNA and two hammerhead ribozymes. The hammerhead ribozymes flank either side of the shRNA, their cleavage sites defining the start and end of the shRNA. In theory, the hammerhead ribozymes would be stable enough to form a cleavage-capable molecule, despite the presence of a strong hairpin structure. This system is an improvement of its predecessor, in which minimal/slow hammerhead ribozymes were used (Ely, A. 2005 MSc dissertation, University of the Witwatersrand). It is now known that these minimal constructs, although useful in primary hammerhead structure-function studies, have no functioning in mammalian cells owing to the metal ion concentration required for cleavage being inadequate. The hammerhead ribozymes currently used in RyPS have

the extra-core elements restored within the stems allowing for tertiary structure conformational change and increased cleavage rates. This species of hammerhead ribozyme does not naturally occur, rather it is a derivative of peach latent mosaic virus (PLMV) ribozyme. One change in particular is the addition of the 5'-UAA-3' bulge on stem I. The bulge (5'-UAA-3') present on stem I originates from a loop structure capping the PLMV RNA sequence. This newly incorporated and adapted bulge facilitates the interaction of loop II and stem I, allowing for the formation the kissing-loop structure.

Theoretically, the kissing-loop interaction will allow for the RyPS to achieve the correct conformation to cleave at the designated sites, releasing the shRNA into the nucleus to be translocated by Exportin-5. A theoretical schematic of the secondary structure of RyPS is shown in Figure 1.8. In this diagram one can depict the three elements of RyPS, namely the two flanking ribozymes and the shRNA

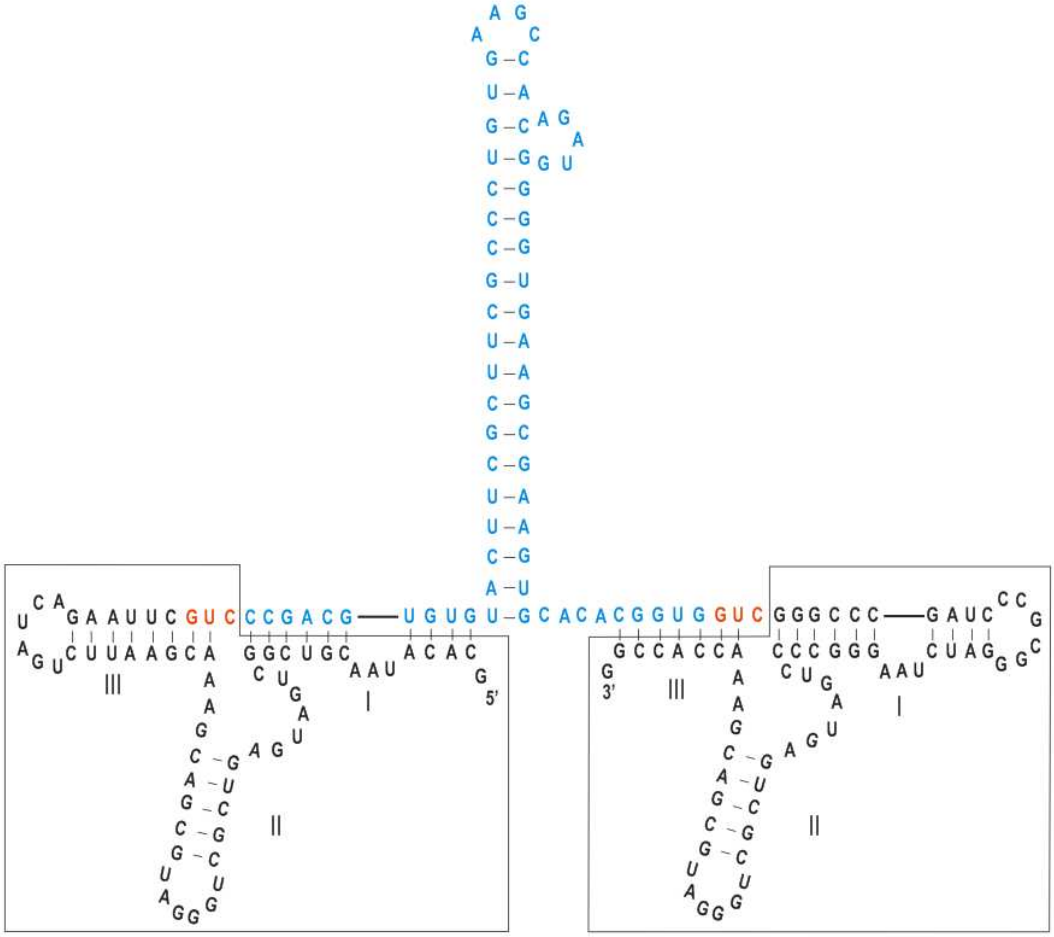

Figure 1. 8: The theoretical secondary structure of RyPS.

Within the boxes are the PLMV-derived flanking hammerhead ribozymes shown in black. The left flanking ribozyme has the stem II and III looped structure, whereas the right flanking ribozyme has stem I and II looped. The ribozyme cleavage site of each flanking ribozyme is shown in red, and it should be noted that the left flanking ribozyme retains the cleavage triplet 5'-GUC-3', whereas the right flanking ribozyme releases the triplet to be included as part of the 2 nucleotide 3' overhang of the shRNA. Letters shown in blue indicate the bulk of the shRNA.

The cleavage products generated may not always be perfect, like any cellular species of RNA and protein, mis-folding does occur. The products of an unprocessed RyPS cannot enter the RNAi machinery, and will most likely be degraded. There are 6 possible species that can result after RyPS processing, the first three and most common species will be the released 5' ribozyme, 3' ribozyme and shRNA. Other minor species present would be a result of mis-folding and include the entire RyPS, a conjugated 5' ribozyme- shRNA and a conjugated 3' ribozyme-shRNA.

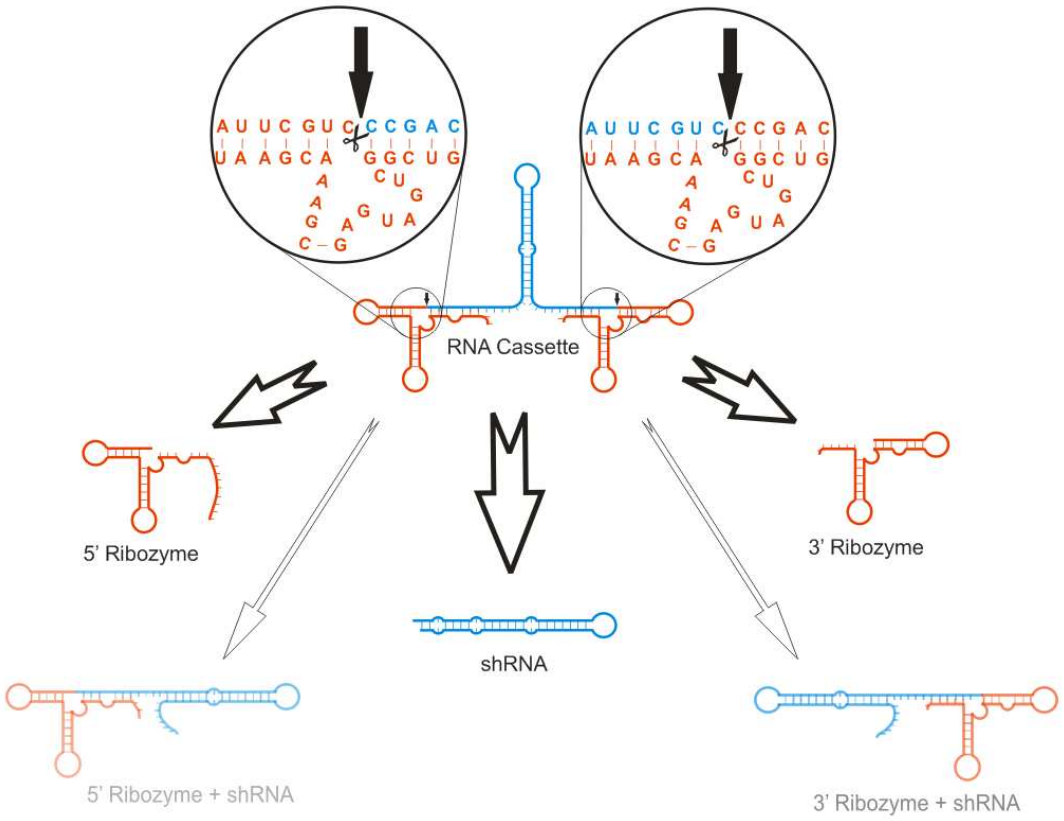

Figure 1. 9: Illustration of the possible cleavage products by RyPS.

The three predominant products are the 5' ribozyme, shRNA and the 3' ribozyme indicated by the bold arrows. The other three products are an uncleaved RNA cassette, a 5' ribozyme shRNA conjugate and a shRNA 3' ribozyme conjugate, indicated by the faint arrows.

As RyPS is intended to act as a therapeutic molecule, testing of it will be done in two sections. The first section will deal with the functionality of the hammerhead ribozymes, their ability to cleave and produce products *in vitro* and intracellularly. The second section will deal with the ability of the released shRNA to knockdown its target effectively. For this a hairpin was chosen that targets a region within the hepatitis B virus (HBV) genome that was previously designed by colleagues, and is known to be highly effective in inducing knockdown (Carmona et al. 2006).

The shRNA within RyPS contains an anti-sense sequence targeted against the X open reading frame (ORF) of HBV. The X ORF overlaps with two other major HBV mRNA sequences, namely the polymerase protein and the surface protein (the surface protein composes of three variants) which makes these sequences ideal as targets for therapeutic purposes, as not only is the mRNA for the X-protein targeted but the mRNA for the polymerase and all 3 surfaces proteins as well. Furthermore, this restricts the virus' ability to mutate easily against the RNAi effector molecule, as a single nucleotide change results in over 3 changes in separate viral strands. Figure 1.10 gives an outline for the genome of the HBV genome, indicating overlapping ORFs as well as the target site of the anti-sense sequence of the shRNA.

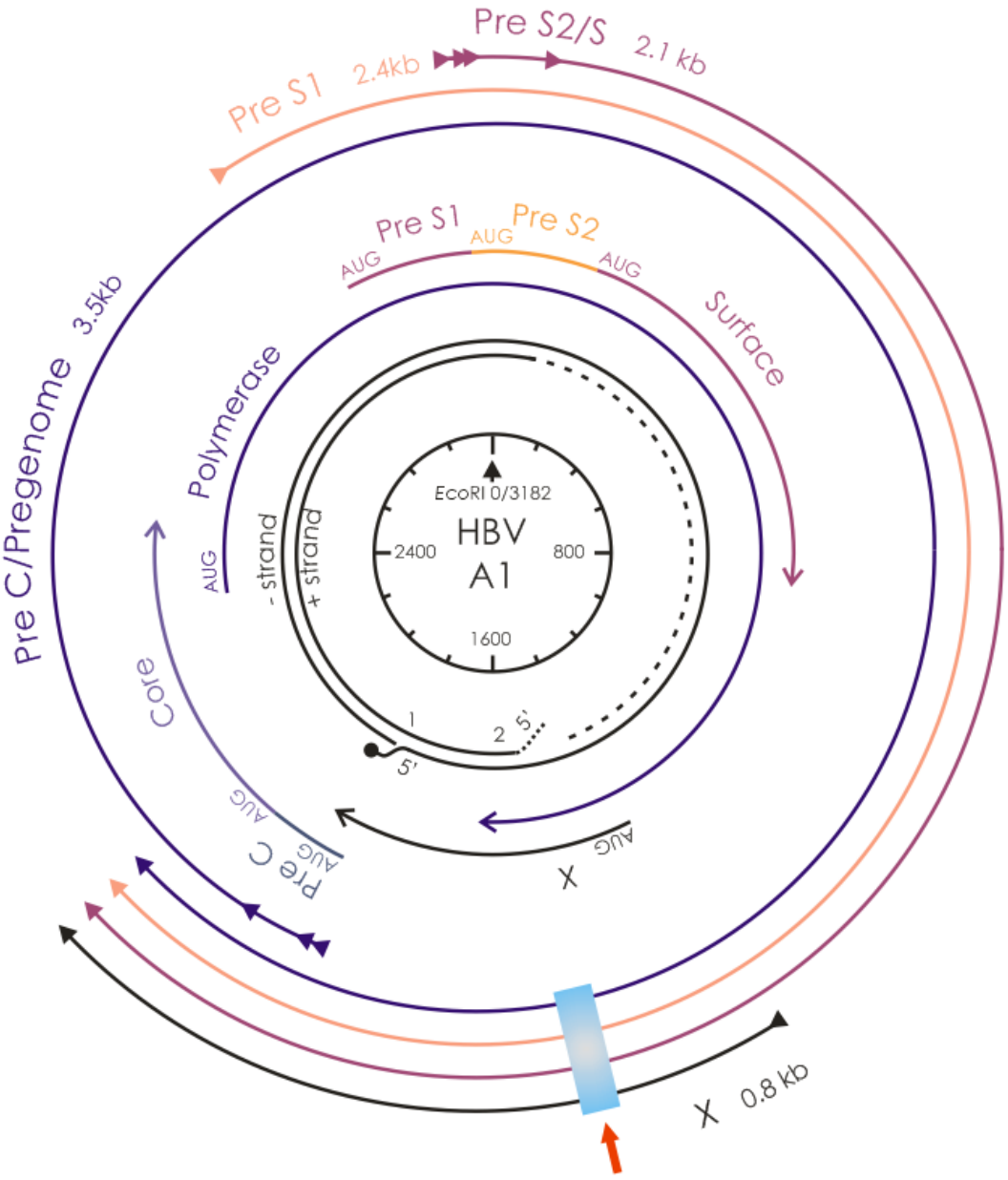
Pre S2/S
2.1 kb
Pre S1
2.4kb
Pre S1
AUG
Pre S2
AUG
AUG
Surface
Pre C/Pregenome
3.5kb
Polymerase
AUG
- strand
+ strand
EcoRI 0/3182
HBV
A1
2400
800
1600
1
2
5'
5'
Core
Pre C
AUG
AUG
X
AUG
X
0.8 kb

Figure 1. 10: A representation of the HBV genome.

The centre of the diagram represents the DNA genome, associated. Radiating outwards are the core, polymerase, pre S1, pre S2, surface and X ORFs, their start indicated by an AUG. The outer shell represents the RNA sequences responsible as the transcripts for translation. The Pre C/Pregenome encodes the various core proteins, the polymerase protein, and also functions as a template for viral replication. The pre S1 encodes one of the S1 protein, involved in the surface of viral particles. Similarly, S2 and S encodes for the S2 and surface proteins, involved in the surface of the viral particles. The X RNA strand is the smallest of the RNA strands generated, and shares sequence homology with all the previously mentioned HBV RNA species. The X protein has been allocated a multitude of roles, some of which are not clearly defined, however it is known that the X protein plays an important role in viral replication. In targeting the X mRNA, viral replication is severely affected, furthermore by targeting this region all other viral mRNAs are targeted. The pre C/core and S proteins may not be as severely affected by the X-targeting shRNA as their ORF lies further upstream. However, the polymerase ORF falls within the targeted region and it may also be effectively knockdown. The blue bar across all mRNA species indicates the region the shRNA targets against.

This study aimed to produce an RNA processing system, capable of generating a molecule involved in the knockdown of HBV. Unique in its design and function the RyPS provides several advantages over currently used RNAi based therapeutics which include: minimal bioprocessing required by the shRNA, which avoids disruption of the innate cellular pathways; sensitive, tissue specific and inducible expression is possible using Pol II promoters; this product can be encoded within a DNA vector, offering several benefits such as stability and the ease of packaging into lenti- and adenoviral particles. Although not included in this study, ribozymes could be designed to target regions on the HBV genome, providing a 3 way attack on the target as opposed to one. A single promoter can be used to transcribe a battery of RyPS, each encoding a shRNA which targets an individual site, helping to curb the generation of escape mutants. RyPS template (DNA) is a stable molecule, is easily transported and easily mass produced at source. This is an ideal feature for developing countries which cannot support cold-chains for particular sensitive drugs with limited shelf lives.

Materials and Methods

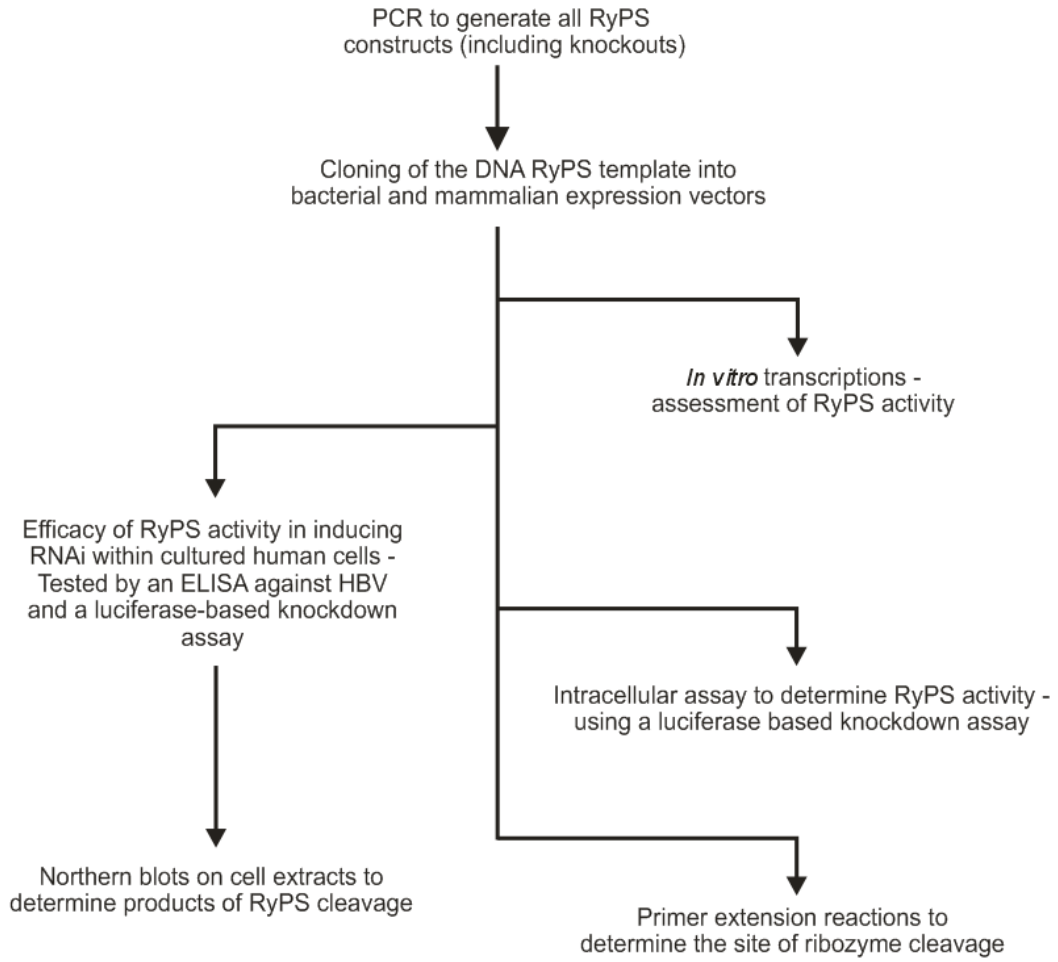

Figure 2. 1: General overview of the experimental procedures followed over the duration of experimentation.

Table 2. 1: Definitions for abbreviations used in materials and methods

Abbreviation	Definition
RyPS	Ribozyme Processing System
5'Rz	Refers to the hammerhead ribozyme upstream the shRNA of RyPS
3'Rz	Refers to the hammerhead ribozyme downstream the shRNA of RyPS
Δ	Prefix to a ribozyme, indicating a mutational change of that particular ribozyme
Del	Deletion within a ribozyme causing its loss of activity
Trunc	Truncation of the ribozyme, decreasing cleavage ability
pCI-	Refers to the CMV promoter-based mammalian expression plasmid pCI-neo
pTZ-	Refers to a bacterial expression plasmid, pTZ57R, a T/A cloning vector
psi-Check2.2	Refers to the plasmid containing two independently expressed luciferase genes, used in knockdown studies
Rz	An abbreviation for ribozyme used in figures.

Generation of RyPS clones

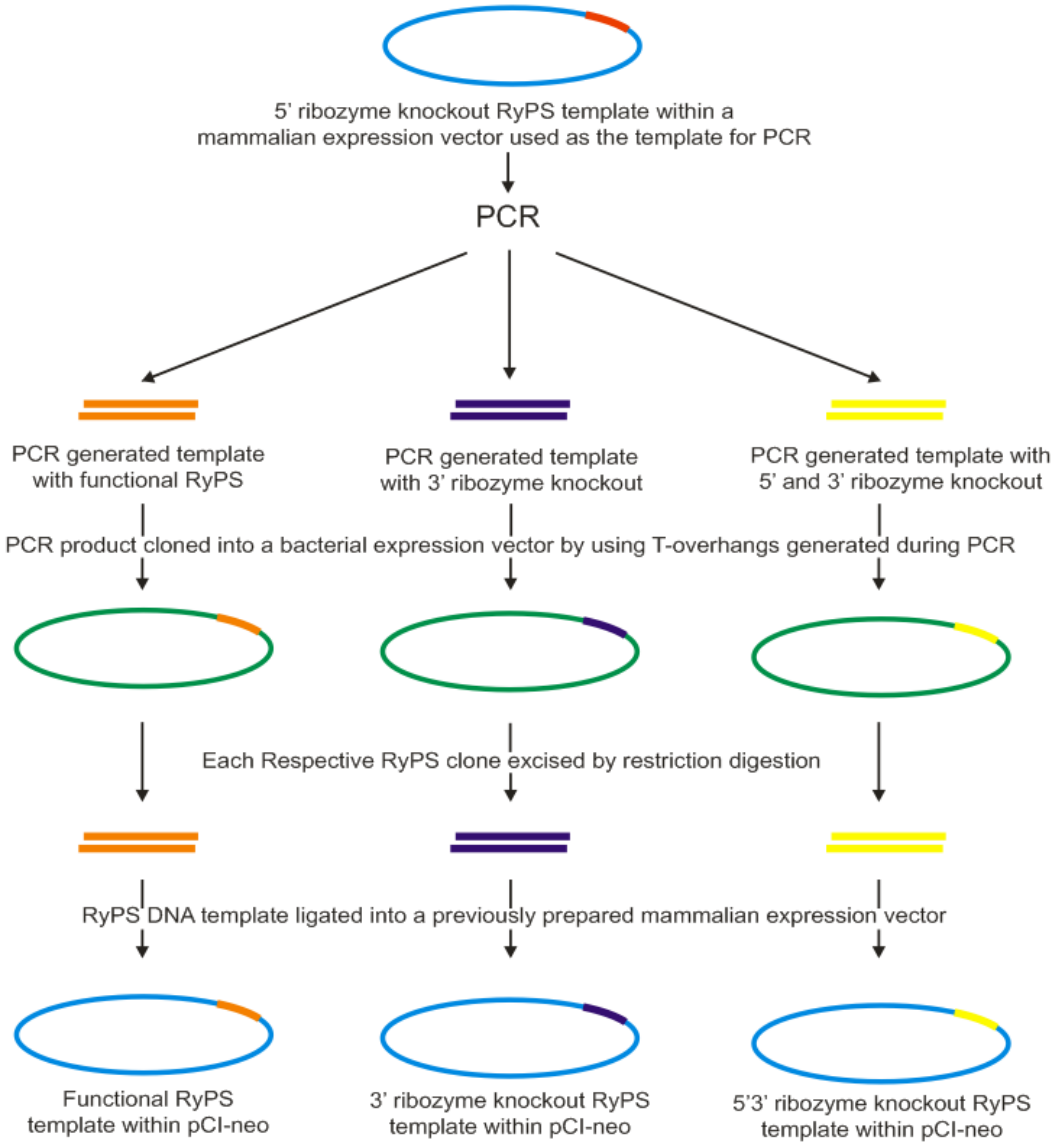

Figure 2. 2: A diagrammatic representation of the steps taken to generate vectors capable of expressing RyPS within a mammalian cell.

PCR was used to generate the faster and mutant knockout RyPS clones. Previously, a RyPS clone was generated in which a deleterious deletion was present within the catalytic pocket of the 5' ribozyme, rendering it unable to cleave. This 5' ribozyme knockout clone was used as a template in PCR, allowing for the generation of the other RyPS species. This was achieved by using primers that would introduce new mutations, or reinstate missing bases to restore activity. All required RyPS species were generated in this manner, Fast RyPS, 5' ribozyme knockout mutant, 3' ribozyme knockout mutant and the 5'3' ribozyme knockout mutant. PCR was followed by T/A cloning, in which a single T overhang on the 3' ends of the PCR products are ligated into plasmid vectors (pTZ57R) with single A overhangs. This vector has a multiple cloning site which contains several unique restriction sites, making the excision of the PCR fragment for further cloning easier. The DNA encoding RyPS was excised from pTZ57R and cloned into the mammalian expression vector pCI-neo.

PCR

pCI-Δ5'$_{del}$RyPS, a mutant RyPS which has lost 5' ribozyme activity, was previously generated and used as a template in PCR reactions to generate RyPS (fully functional cassette), Δ3'$_{del}$RyPS (a non-functional 3' ribozyme within RyPS), and Δ5'3'$_{del}$RyPS (both ribozymes within RyPS were non-functional) fragments.

Table 2. 2: Primers used to generate required RyPS fragments (and knockout clones) by PCR

Sequence	Function
A) 5'-GATCGCTAGCCACATAACGTC-3'	Generic forward primer
B) 5'-GATCCTCGAGCACATAACGTCGG TGATGA-3'*	Forward primer to restore 5' ribozyme activity
C) 5'-GATCGTCGACCGGTGGTTTCGTCGCATC-3'	Reverse primer
D) 5'-GATCGTCGACCGGTGGTTTCGTCGCA TCCCAGC GACTCATC_GGGG-3'#	Reverse primer to generate non-functional deletion

* Insertion of T restores 5' ribozyme activity

Deletion of A results in the inhibition of 3' ribozyme activity

One hundred nanograms of template was used in each PCR reaction containing 1 mM $MgCl_2$, 0.2 mM dATP, dCTP, dGTP and dTTP, 20 pmol forward primer, 20 pmol reverse primer, 10 µl 5x GoTaq Flexi Buffer and 1.25 u GoTaq DNA polymerase (Promega, Wisconson USA) in a final volume of 50 µl. Samples were initially denatured for 2 minutes at 95°C and then subjected to 30 cycles of 15

seconds denaturation at 95°C, 15 seconds of annealing 55°C and 30 seconds elongation at 72°C. The final elongation step was 10 minutes at 72°C, ensuring the addition of A-overhangs to the fragments.

The appropriate volume of loading dye was added to each PCR sample and subjected to electrophoresis in a boric acid 1.5% agarose gel. The agarose gel contained 0.6 μg ethidium bromide per 1 ml of gel, to allow for DNA viewing under UV trans-illumination. Correctly sized DNA fragments (~216 bp) were purified from the agarose using the MinElute Gel Extraction Kit as per instruction provided (Qiagen, California USA).

Plasmid construction and cloning

The purified PCR fragments were ligated into a bacterial expression system, pTZ57R/T (Fermentas, Ontario Canada) which contains a multiple cloning site (MCS) for simplified cloning. The MCS contains a large variety of single cutting restriction sites, providing a fair selection of restriction sites should it be required to transfer/clone the fragment into other expression systems. Often for the purposes of these experiments, pTZ57R is used as an intermediate, allowing for the transfer of the PCR fragment into a mammalian expression system, such as pCI-neo and psiCheck2.2.

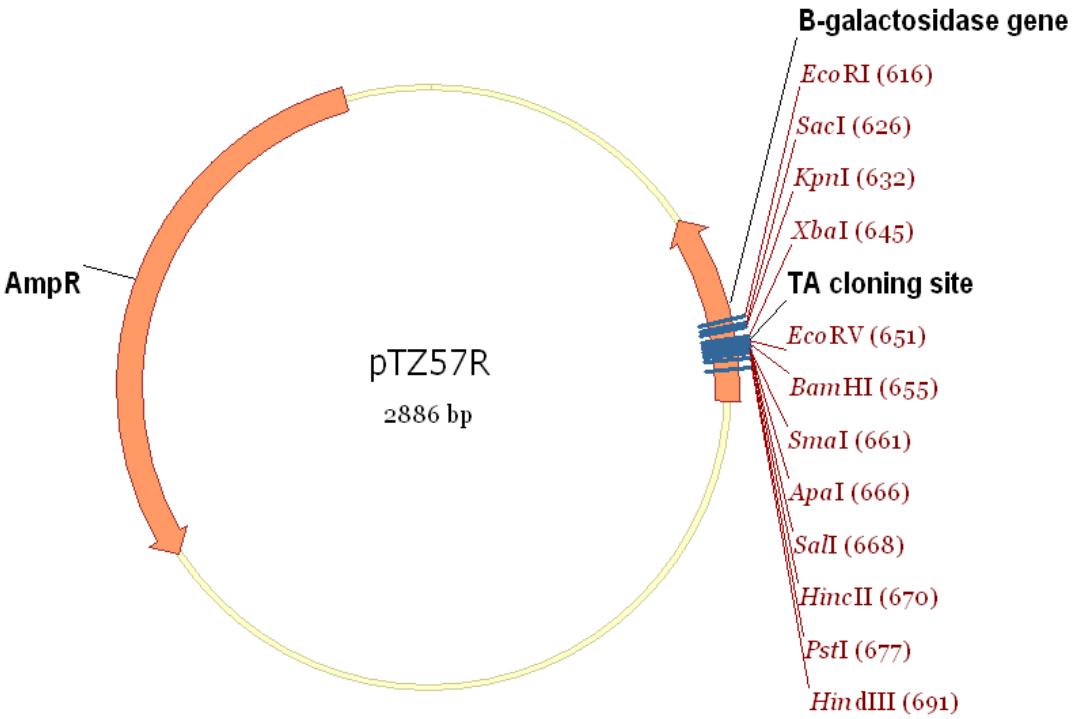

Figure 2. 3: A plasmid map of pTZ57R, used for T/A cloning experiments.

Some of the unique restriction sites found within the multiple cloning site are shown in red. The multiple cloning site (T/A cloning site) is located within the β-galactosidase gene, and insertion of a fragment into the cloning site would disrupt β-galactosidase functioning, and if transformed into a β-galactosidase negative bacterial strain, prevents the metabolism of X-Gal. Bacterial colonies with the intact β-galactosidase gene metabolise X-Gal to a blue product, visible to the unaided eye, while bacterial colonies containing the DNA sequence of interest remain white. pTZ57R also contains an ampicillin resistance gene for selective purposes.

The ligation reaction contained 0.054 pmol PCR fragment, 0.18 pmol backbone plasmid (with T-overhangs), 3 µl 10x ligation buffer and 5 u T4 DNA ligase in a final volume of 30 µl. The ligation was incubated at 16°C for 1 hour with agitation every 20 minutes.

Chemically competent *Escherichia coli*, strain DH5α, were transformed according to the method in Appendix 3 and spread onto Luria Bertani (LB) agar plates supplemented with ampicillin, 1.6 mg isopropyl-β-D-thiogalactopyranoside (IPTG) and 0.8 mg 5-bromo-4-chloro-3-indolyl-β-D-galactopyranoside (X-Gal) and incubated at 37°C overnight. Single white colonies were picked the following day and screened by PCR for insert using the M13 forward and M13 reverse primers, which flank the MCS of pTZ57R.

Table 2. 3: Clone screening primers which bind the flanking regions of the MCS in pTZ57R

Sequence	Function
5'-GTAAAACGACGGCCAGTG-3'	Binds the M13F site
5'-CAGGAAACAGCTATGACC-3'	Binds the M13R site

Bacterial colonies served as template in each PCR reaction containing 1 mM $MgCl_2$, 0.2 mM dATP, dCTP, dGTP and dTTP, 10 pmol forward primer, 10 pmol reverse primer, 4 µl 5x GoTaq Flexi Buffer and 0.625 u GoTaq DNA polymerase (Promega, Wisconsin USA) in a final volume of 20 µl. Samples were initially lysed

and denatured for 2 minutes at 95°C and then subjected to 30 cycles of 15 seconds denaturation at 95°C, 15 seconds of annealing 55°C and 30 seconds elongation at 72°C. The reaction proceeded over 25 cycles. The M13 sites flank the multiple cloning site in pTZ57R, M13F 36 bases upstream of the T/A site, and M13R lies 84 bases downstream of the T/A site. A diagrammatic representation of the MCS of pTZ57R can be found in Appendix 1.

DNA products generated from PCR were subjected to gel electrophoresis and viewed under UV trans-illumination. A positive result yielded fragments 377bp in size.

Positive bacterial colonies were inoculated into 10 ml of LB broth, and incubated at 37°C overnight. The following day bacterial cells were harvested by centrifugation, and plasmids extracted by the alkaline lysis method using the High Pure Plasmid Isolation Kit (Roche, Switzerland). The insert was restricted from the bacterial expression plasmid (total of 500ng DNA) using 10 u of each *Xho*I and *Xba*I, Buffer O (50 mM Tris-HCl, 10 mM $MgCl_2$, 100 mM NaCl and 0.1 mg/ml BSA, pH 7.5) (Fermentas, Ontario Canada) in a total volume of 50 µl for 2 hours at 37°C. The restriction digest reaction was subjected to electrophoresis, and DNA fragments viewed by UV transillumination once stained with ethidium bromide. The DNA fragment was purified from the agarose gel using the MinElute Gel Extraction Kit (Qiagen, California, USA). The mammalian expression plasmid, pCI-neo, was restricted and purified in a similar manner. This allowed for the generation of compatible ends when the plasmid was cleaved with *Xho*I and *Xba*I.

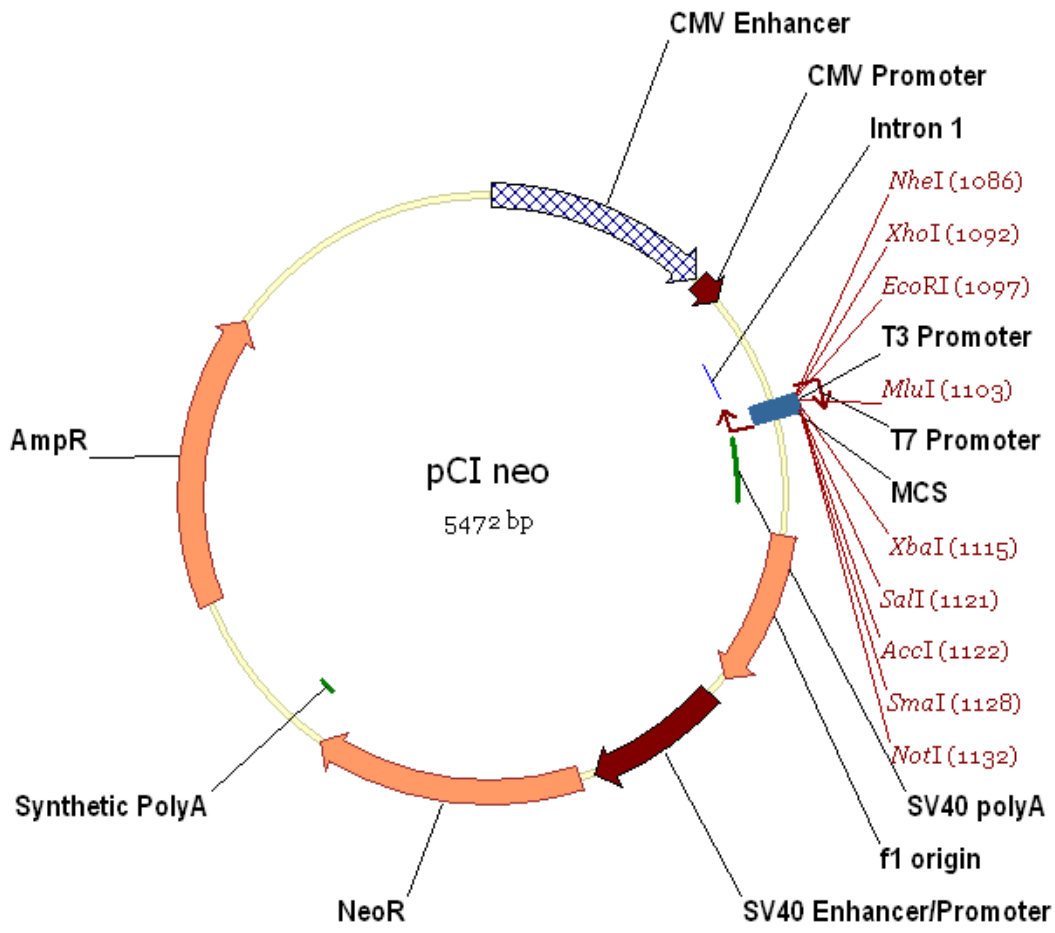

Figure 2. 4: A plasmid map of pCI-neo.

The mammalian expression vector, pCI-neo, contains various elements that allow for its prokaryotic replication as well as eukaryotic expression. The cytomegalovirus (CMV) promoter is used for the expression of products cloned within the multiple cloning site of the vector. The vector also contains an intron, expressed by the CMV promoter as well as various elements taken from the Simian vacuolating virus 40 (SV40) such as a polyadenylation signal and a promoter. The vector contains 2 selectable markers, namely neomycin and ampicillin resistance. Neomycin resistance is used in eukaryotic, while ampicillin in prokaryotic cells. The T7 and T3 sites can be used for sequencing analyses as well as start sites for *in vitro* transcriptions.

The fragment isolated from the pTZ57R clones was ligated into the previously prepared pCI-neo backbone (*XbaI* and *XhoI* restriction). Ligation of the restricted insert involved 0.054 pmol fragment, 0.18 pmol backbone plasmid, 10 u T4 DNA ligase and the respective buffer (Fermentas, Ontario Canada). The reaction proceeded at 18°C overnight. The following day DH5α bacteria were transformed with the ligation reaction, plated onto ampicillin supplemented LB agar plates and grown at 37°C overnight. Often it was found that incubation of the bacterial colonies required longer than 14-15 hours of incubation, and often 20 hour incubation produced more visible colonies. Thus, overnight incubation on plates often refers to 20 hour incubations.

Bacterial colonies were screened by PCR using adapted T7 and T3 primers which are larger than the conventional providing greater specificity during screening. This method is similar to that used to screen pTZ57R colonies with M13F/R primers. The T7 promoter site is 7 bases upstream of the inserted product, and the T3 23 bases downstream, producing a positive result in the form of ~280 bases.

Table 2. 4: Adapted T7 and T3 primers used in the PCR screening of positive RyPS clones inserted into pCI-neo

Sequence	Function
5'-GTACTTAATACGACTCACTATAGG-3'	T7 Primer
5'-AGCATTAACCCTCACTAAAGGG-3'	T3 Primer

Bacterial colonies were resuspended as template in each PCR reaction containing 1 mM $MgCl_2$, 0.2 mM dATP, dCTP, dGTP and dTTP, 20 pmol forward primer, 20 pmol reverse primer, 4 µl 5x GoTaq Flexi Buffer and 1.25 u GoTaq DNA polymerase (Promega, Wisconsin USA) in a final volume of 20 µl. Samples were initially denatured and lysed for 2 minutes at 95°C and then subjected to 25 cycles of 15 seconds denaturation at 95°C, 15 seconds of annealing 60°C and 30 seconds elongation at 72°C. PCR products were subjected to agarose gel (2%) electrophoresis, and DNA fragments viewed by UV trans-illumination. Positive clones were sequenced by dye termination sequencing (Inqaba Biotechnologies, South Africa)

Generation of the luciferase-RyPS reporter system.

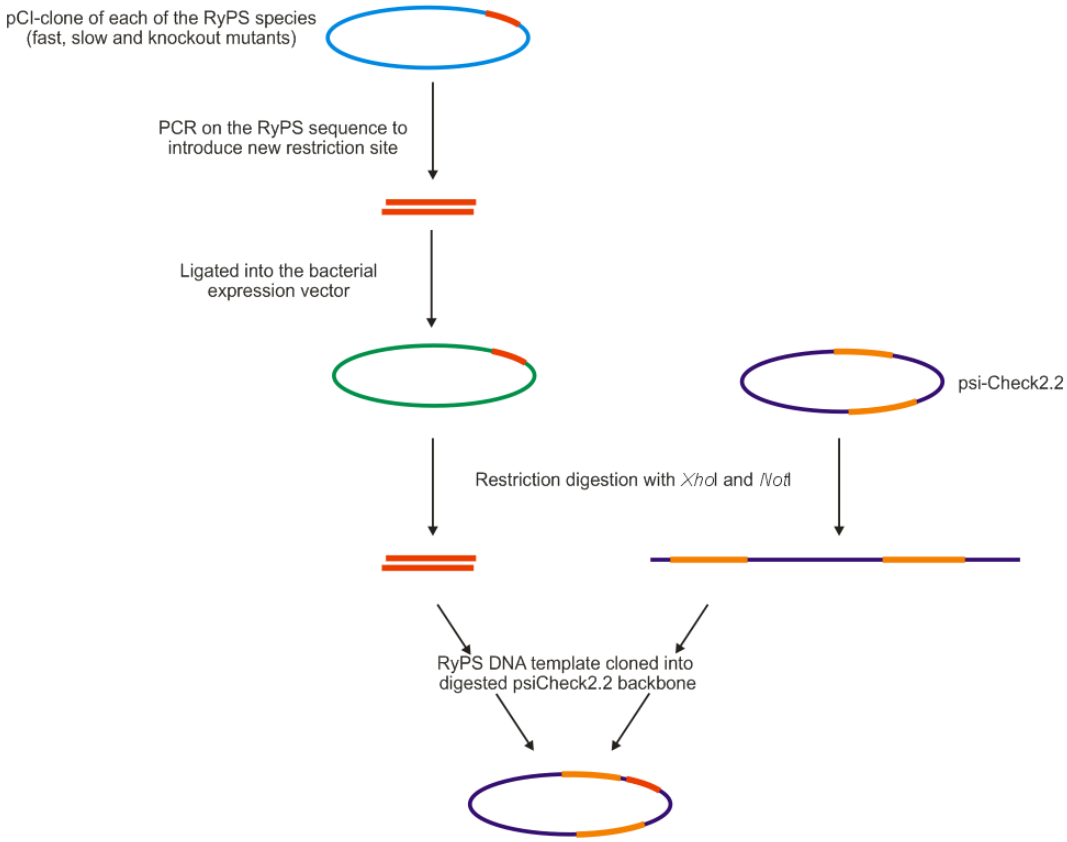

Figure 2. 5: Overview of methodologies to generate the luciferase-RyPS reporter system.

The pCI-neo clones containing the correct respective RyPS clones were used as template in a PCR reaction in which new restriction sites were introduced. The PCR fragment was inserted into the MCS of pTZ57R by T/A cloning. Screened colonies with positive insert were restriction digested with *Xho*I and *Not*I and the DNA RyPS fragment was ligated into the MCS site psiCheck2.2, which similarly was pre-treated with *Nhe*I and *Xho*I. RyPS-encoding DNA indicated by red, luciferase genes indicated in orange.

Individual functioning of each of the ribozymes with RyPS was tested. It was required to have the ribozymes function within RyPS, and not as single entities, as a change in surrounding sequences of the ribozymes may have an effect on the cleavage activity of each of the ribozymes. The RyPS system was cloned into a dual luciferase reporter system. The dual luciferase reporter system contains Firefly and *Renilla* luciferase, each transcribed from individual promoters. In doing so, one can target either of the luciferases, inducing their knockdown, while the other expresses for background control levels. Both luciferases are encoded within a single plasmid, thus providing a very sensitive accurate reporter system. Each of the RyPS clones (functional on knockout mutants) were cloned downstream of the coding region of *Renilla* luciferase, thus any ribozyme activity would lead to the disruption of the mRNA strand and hence its degradation. By testing each of the knockout mutants, activity of the functioning respective ribozyme could be determined. Figure 2.6 gives an overall representation of the general mechanism of the Luciferase-RyPS cassettes.

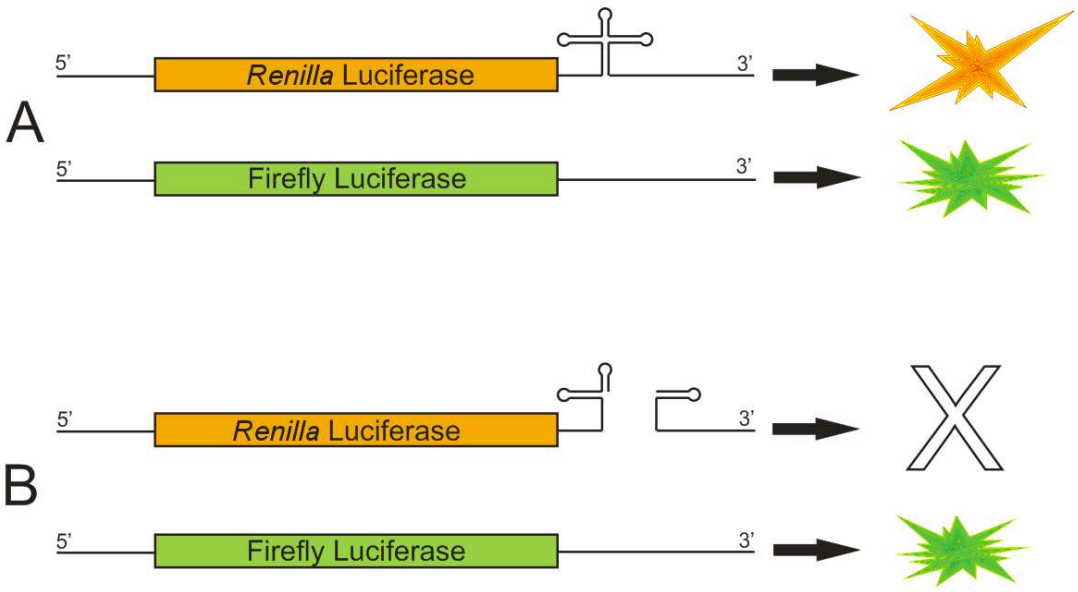

Figure 2. 6: Representative figures of the outcomes when the RyPS constructs were cloned behind *Renilla* luciferase.

Within a cellular environment a non-active cassette, such as the Δ5'Δ3'Rz RyPS or slow RyPS, would result in functional *Renilla* luciferase detectable in an assay (**A**). If the ribozyme(s) was active (RyPS, Δ5' ribozyme knockout or Δ3' ribozyme knockout RyPS), little luciferase activity would be seen (**B**). In both experiments, Firefly luciferase served as a background control.

RyPS encoded sequences within pCI-neo were used as template in the following PCR reaction: 100 pg template, 1 mM $MgCl_2$, 0.2 mM dATP, dCTP, dGTP and dTTP, 20 pmol forward primer, 20 pmol reverse primer, 4 µl 5x GoTaq Flexi Buffer and 1.25 u GoTaq DNA polymerase (Promega, Wisconsin USA) in a final volume of 20 µl. PCR samples were initially denatured for 2 minutes at 95°C and then subjected to 30 cycles of 15 seconds denaturation at 95°C, 15 seconds of

annealing 55°C and 30 seconds elongation at 72°C. The final elongation step was 10 minutes at 72°C.

Table 2. 5: Primers used to generate RyPS fragments from PCR containing the correct restriction sites for cloning into psi-Check2.2

Sequence	Function
A) 5'-GATCCTCGAGCACATAACGTCG-3'	Forward primer to generate "faster" RyPS
B) 5'-GATCGCGGCCGCCGGTGGTTTCGTCGCATC-3'	Reverse primer to generate "faster" RyPS
C) 5'-GATCCTCGAGTCTAGACGCCTGATGAGTC-3'	Forward primer to generate original/ slow RyPS
D) 5'-GATCGCGGCCGCACTAGTTGCTTTGAGGCACT-3'	Reverse primer to generate original/ slow RyPS

PCR products were subjected to electrophoresis and stained with ethidium bromide. Fragments were purified from the agarose gel and ligated into pTZ57R, transformed into DH5α cells and screened by M13F/R PCR, as previously performed.

The positive RyPS clones, now containing modified restriction sites for insertion into psiCheck2.2, were treated with *Xho*I and *Not*I (Fermentas, Ontario Canada) in the following reaction: 1 μg template DNA, 5 μl buffer O, 10u of each restriction enzyme in a total volume of 50 μl, incubated at 37°C for 2 hours. Similarly, linearised psiCheck2.2 backbone was prepared this way. Ligation of the restricted insert involved 0.054 pmol fragment, 0.18 pmol backbone plasmid, 10 u T4 DNA ligase and the respective buffer. The reaction proceeded at 18°C overnight. The following day DH5α cells were transformed with the ligation reaction, plated onto ampicillin supplemented LB agar plates and grown at 37°C overnight.

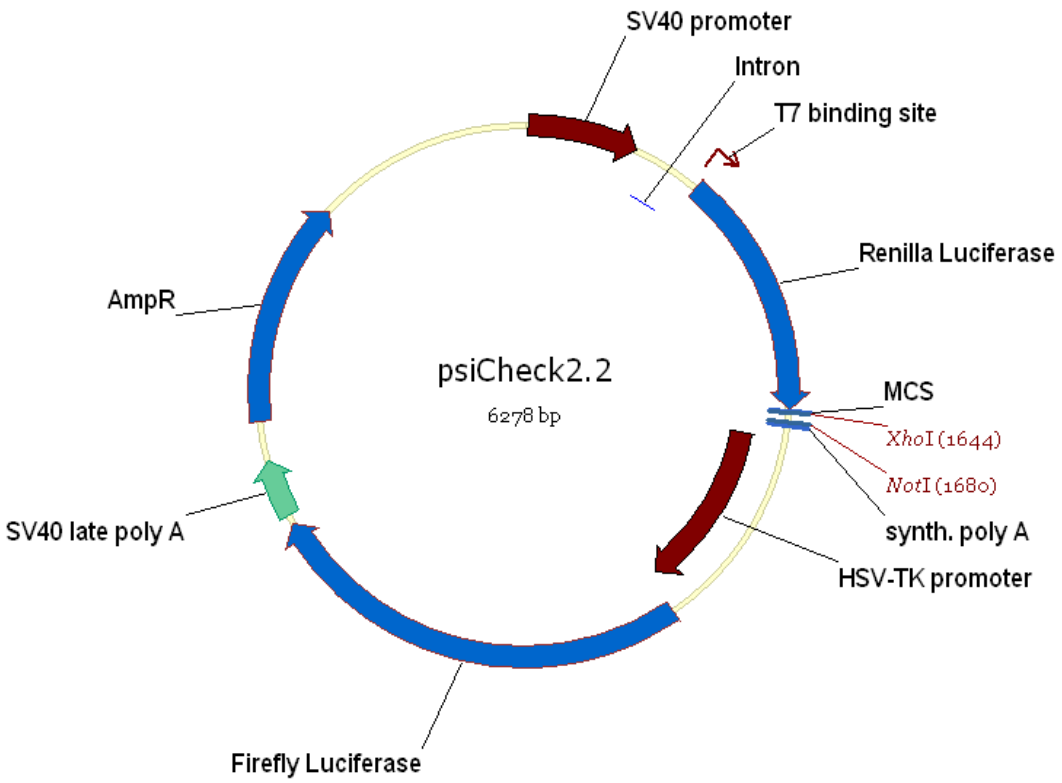

Figure 2. 7: Plasmid map of psiCheck2.2.

Renilla luciferase expression is transcribed by a SV40 promoter. Downstream of the *Renilla* gene is the multiple cloning site, often used for insertion of target sequence in knockdown studies. Firefly luciferase is used as a background control when *Renilla* is knocked down, and is transcribed by a Herpes Simplex Virus (HSV) promoter. The plasmid also contains an ampicillin resistance gene (AmpR), used for bacterial selection and culture.

DNA preparation for general use and transfection.

Clones were picked and grown in 3 ml LB broth at 37°C with shaking for 8 hours. This culture was used to inoculate 50 ml LB broth for DNA used in cloning experiments or 200ml LB broth for transfections. Both were grown at 37°C overnight with shaking. Bacterial cells were harvested by centrifugation, at 4000xg for 20 and 35 minutes for the 50 ml and 200 ml cultures respectively. Supernatant was discarded and the bacterial pellets were treated with the Hispeed plasmid midi kit or EndoFree plasmid maxi kit supplied by Qiagen according to manufacturer's instructions. This preparation relies on the alkaline lysis of bacterial cells in which a sudden pH change causes the precipitation of the non-plasmid bacterial components such as chromosomal DNA and cellular proteins.

In vitro transcriptions

Template Generation

PCR was used to generate template for *in vitro* transcription. The T7 (forward) primer and a respective reverse primer was used in the following PCR reaction containing 100 ng of template, 1 mM $MgCl_2$, 0.2 mM dATP, dCTP, dGTP and dTTP, 20 pmol forward primer, 20 pmol reverse primer, 10 µl 5x GoTaq Flexi Buffer and 1.25 u GoTaq DNA polymerase (Promega) in a final volume of 50 µl. Initially samples were denatured for 2 minutes at 95°C, and then subjected to 30 cycles of: 95°C for 30 seconds, 55°C for 15 seconds and 72°C for 15 seconds. DNA fragments were purified from an agarose gel post electrophoresis as mentioned

previously. Alternatively, template was generated by restriction digest. Each respective (pCI-neo clone) clone was treated for 2 hours by *Bgl*II and *Xba*I in 2x Buffer Tango (66 mM Tris-acetate, 20 mM Mg-acetate, 132 mM K-acetate and 0,2 mg/ml BSA, pH 7.9) at 37°C. This generates a fragment that contains the upstream T7 promoter site as well as an extended 3'Rz. Restriction fragments were purified by electrophoresis and gel elution, as mentioned previously.

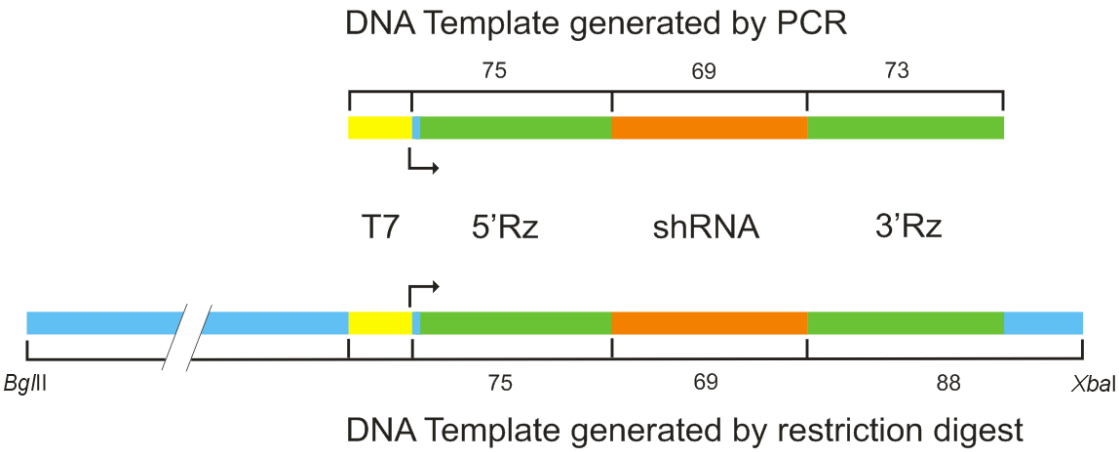

Figure 2. 8: Schematic representation of the DNA templates used in the *in vitro* transcription reactions.

Shown in green are the DNA templates of the flanking ribozymes, in orange the shRNA. The T7 promoter binding site is shown in yellow, and the arrow denotes the transcription start site. Light blue regions indicate DNA belonging to the backbone of pCI-neo.

Having these two templates allowed for various factors to be incorporated. PCR generated template provides the exact template for RyPS to be produced which includes the T7 binding site. This method causes the 5' and 3' ribozyme RyPS products to be similarly sized, which may cause difficulty in identification of bands species in further analysis. However the advantage to this is that an exactly RyPS system is produced without flanking sequences which may interfere with processing or folding. Generating template by restriction digest results in a larger 3' ribozyme, which is easier to distinguish from the 5'.

In vitro transcription

The *in vitro* transcription reaction comprised of 350 ng DNA template, 20 μCi [α-^{32}P]ATP and the required components from MEGAshortscript™ high yield transcription kit (Ambion, California USA). The reaction was performed at 37°C for 2 hours. An equal volume of loading dye was added to the transcription reaction and samples placed on ice. Two microlitres were loaded on a 41 cm denaturing polyacrylamide gel (Appendix 1). Electrophoresis was performed at 1500 V and 30 mA for 5 hours in 1x TBE buffer. An X-ray film was exposed to the gel for 15 minutes in a cassette at -70°C and developed.

Tissue culture, transfections and RNA collection

Two cell lines were involved in the experiments performed, namely Human embryonic kidney cells (Hek293) and Human hepatocytes (Huh7). Hek293 were found to grow in culture more easily and consequently were used in experiments which did not require any hepatitis B virus products.

Cell culture

Cells lines were cultured in Dulbecco/Vogt Modified Eagle's Minimal Essential Medium (DMEM) containing 10% foetal calf serum (FCS), and kept at 37°C and 5% CO_2. Once cells reached 90-100% confluency they were split to 30% confluency, by removing any media with a phosphate-buffered saline (PBS) wash, and then adding an equal volume (as the media) of PBS to the cells and incubating at 37°C for 5 minutes. The PBS was then removed and one tenth of that volume replaced with DMEM. Hek293 cells at this point were easily removed off the surface of the dish. Huh7 cells however, are treated with 3.5 mg trypsin per 10 cm^2 dish for 5 minutes at 37°C in place of the second PBS wash used for Hek293 cells, and then removed from the culture dish surface in a similar fashion. Cells were counted using a haemocytometer where necessary.

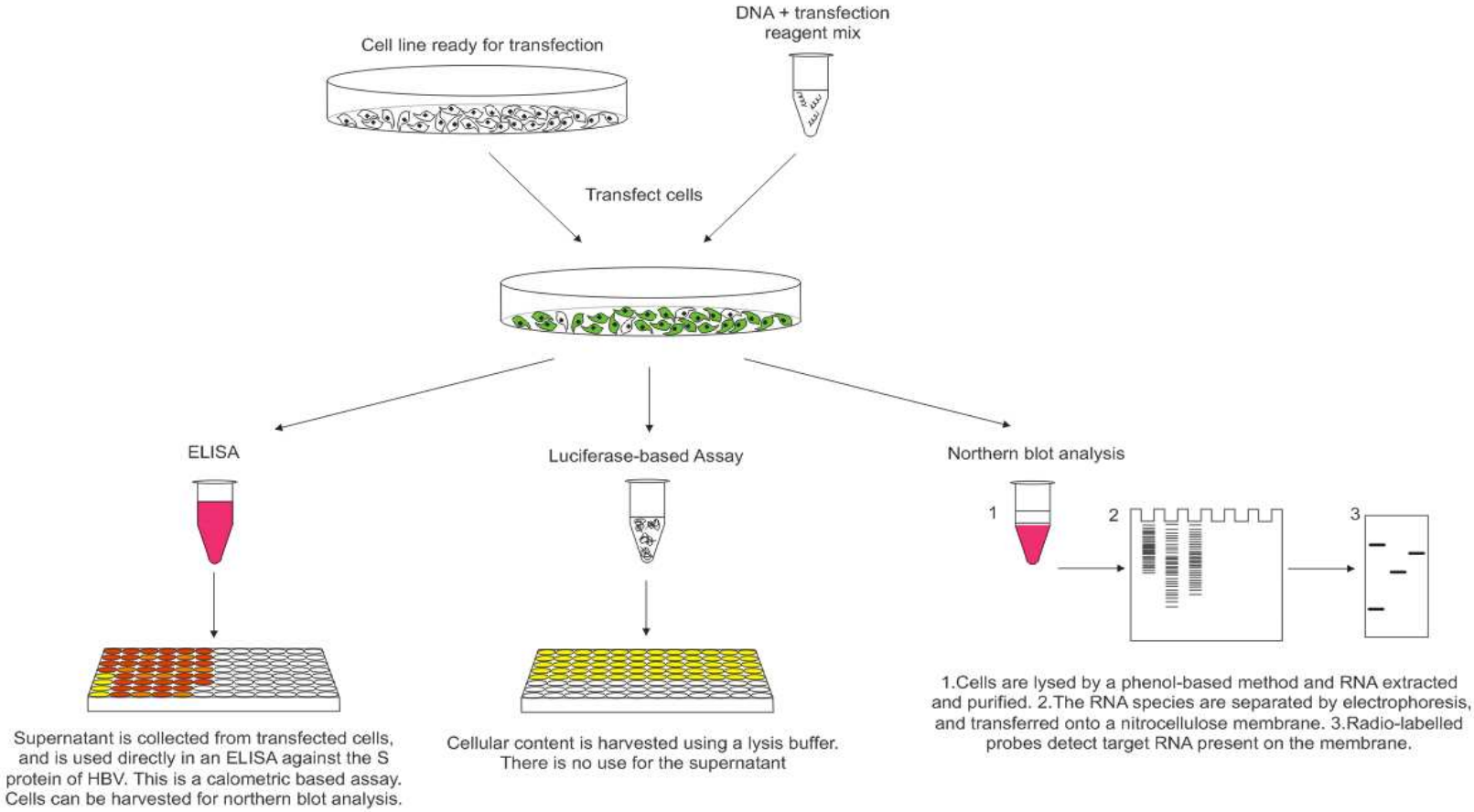
Cell line ready for transfection
DNA + transfection reagent mix
Transfect cells
ELISA
Luciferase-based Assay
Northern blot analysis
1
2
3
Supernatant is collected from transfected cells, and is used directly in an ELISA against the S protein of HBV. This is a calometric based assay. Cells can be harvested for northern blot analysis.
Cellular content is harvested using a lysis buffer. There is no use for the supernatant
1.Cells are lysed by a phenol-based method and RNA extracted and purified. 2.The RNA species are separated by electrophoresis, and transferred onto a nitrocellulose membrane. 3.Radio-labelled probes detect target RNA present on the membrane.

Figure 2. 9: Basic overview of the experiments involved in the cellular assessment of RyPS.

Each experiment was separately performed, post transfection. Cells turn green owing to GFP being present within the transfection mix, a control step to ensure transfection was effective.

Transfections

All transfections were carried out in wells with a 2cm diameter (typically a 24 well dish), unless otherwise stated. Per well, 1 μg of DNA was added to 50 μl of optiMEM (Invitrogen, California USA), and incubated for 5 minutes as well as 1 μl of lipofectamine (Invitrogen, California USA) was added to 50 μl of optiMEM and incubated for 5 minutes. Both DNA and lipofectamine mixes were combined, thoroughly mixed and incubated for a further 20 minutes in the dark. This was then added to the cells and incubated at $37^{o}C$, 5% CO_2 for 5 hours, after which the medium was removed and replaced with fresh DMEM supplemented with 10% FCS. Cells were left for 48 hours post transfection without a change of media, and necessary components harvested.

ELISA against HBsAg

An ELISA was performed against the HBsAg of hepatitis B virus. This assay allows for the detection the viral production within a cell, as the S proteins are shed from the cells into the media, or sera. To measure viral replication, an ELISA against the E antigen would be more fitting, as this protein appears when viral transcripts are produced. It is necessary to use Huh7 cells for this experiment, as HBV does not replicate in Hek293 cells.

Forty eight hours post transfection, supernatant was removed from Huh7 cells (stored at $-20^{o}C$ if necessary) for an antiHBsAg ELISA, using the Monolisa Ag HBs Plus kit (Bio-Rad, California USA). The assay relies on a “sandwich” based

approach, whereby the detection monoclonal antibodies are bound to a peroxidase. This assay is colorimetric in nature, and final results are measured at 450 and 650 nm. For a full protocol, refer to Bio-Rad Monolisa Ag HBs Plus kit protocol.

Dual luciferase based assay

The luciferase assay is a more sensitive assay compared to the ELISA. This increased sensitivity is for several reasons, including that data do not rely on the uniformity of cells per dish, usage of a background control encoded on the same plasmid as the target molecule and optical sensitivity of the system is greater. A region downstream of *Renilla* luciferase mRNA is targeted, resulting in its knockdown, while Firefly luciferase provides a comparable background.

The supernatant was removed from Hek293 cells and discarded. No washing was done to remove the minor amount of supernatant left, as cells may lift from the plate surface. Cells were then incubated with 100 µl 1x Passive lysis buffer (Promega, Wisconsin USA) for 20 minutes at 37°C, with no shaking. Cell lysate was thoroughly mixed until homogeneous. Ten microlitres of each sample was aliquotted into a plate specifically designed for fluorescence-based optical readings (Promega, Wisconsin USA). In sequential order, 50 µl of luciferase assay reagent II (LARII) was added (contains Firefly luciferase substrate), and a fluorescence measured with a green trace, 50 µl of Stop and Glo (which contains *Renilla* luciferase substrate and Firefly luciferase quenching agents) was added and fluorescence measured with a blue trace (This protocol has been modified from the original Dual-Luciferase

Reported Assay System from Promega, California USA). In this experiment, *Renilla* luciferase mRNA was knocked down, thus the Firefly luciferase served as a background control. It is also possible to knockdown Firefly luciferase mRNA, however *Renilla* would then have to serve as a background control.

Northern blots and associated procedures

The northern blot is a sensitive assay in which RNA can be detected using either a DNA or RNA probe. Sensitivity can be controlled by the stringency steps used to remove incorrectly bound probe. Furthermore, radioactively labelled probes provide a large degree of sensitivity in the detection of minuscule amount of RNA.

RNA extractions

Huh7 cells were cultured using methods mentioned previously under cell culture, however, a 10 cm culture dish was used. (Transfections were based on the same ratio of cells:DNA. Thus the amount of DNA used per transfection scales with the amount of cells present per dish.) Forty eight hours post transfection, supernatant was removed and cellular content was harvested by adding 1 ml Tri-Reagent (Sigma), incubating for 5 minutes at room temperature. Cell lysate was collected and 200 µl chloroform added, which was gently vortexed briefly and left to stand at room temperature for 15 minutes. Samples were subjected to centrifugation at 12,000xg for 15 minutes at 4°C. The upper clear phase contained RNA, and was separated from the sample and to this 500 µl isopropanol was added. Samples were left at room

temperature for 15 minutes and then subjected to centrifugation at 12,000xg for 10 minutes at 4°C. Supernatant was discarded and the RNA pellet washed in 1ml 75% ethanol and centrifuged for 10 minutes at 7,500xg 4°C. RNA pellets were air dried for 10 minutes and resuspended in 100 µl TE buffer (10 mM Tris, 1 mM EDTA pH 8). RNA samples were immediately stored at -20°C. It is important to note that all reagents used as well as procedures performed should be as RNase-free as possible. It can be achieved by treating instruments such as spatulas with 1% SDS solution, and then autoclaving afterward. DEPC treated water (Appendix 2) was used to make all solutions such as buffers. Reagents used were certified to be of analytical grade, and were kept separate from those used in general lab usage.

Electrophoresis

A 20 cm 12% denaturing polyacrylamide gel was loaded with 30 µg of each respective RNA sample (RNA was premixed with a DNA/RNA loading dye). Electrophoresis was performed in 0.5x TBE buffer at 350 V and 30 mA for 5 hours, or until the bromophenol blue band reaches the bottom of the gel. The gel, filter paper and nylon membrane (Hybond N) were all cut to the size of the area in which the RNA had migrated within the gel. A sandwich setup was created where by the gel was placed on moistened membrane, and then three layers of moistened filter paper were placed on both sides (0.5x TBE was used to moisten).

Blotting

Semi-dry electrophoresis was carried out at 300 mA (3.3 mA/cm^2) for 30 minutes. The membrane was removed and dried at room temperature, after which the RNA was UV cross-linked for 1000 μJ over a period of 1 minute and then baked at 80°C for 30 minutes.

Hybridisation and oligonucleotide preparation

Oligonucleotide probe preparation

End-labelled DNA probe was prepared by using 10 u T4 polynucleotide kinase (Fermentas, Ontario Canada), 1 μl 10x T4 polynucleotide kinase buffer, 20 μCi [γ-^{32}P]ATP (3000 Ci/mmol), 10 pmol DNA oligonucleotide in a final volume of 10 ml, incubated for 30 minutes at 37°C. Probe oligonucleotides were purified in a Sephadex G-25 column.

Hybridisation

Membranes were prehybridised with 25 ml Rapid-Hyb buffer (Amersham, New Jersey USA) for 30 minutes at 42°C (0.25 ml/cm^2). Labelled probe was added to the hybridisation buffer after the prehybrisation step.

Hybridisation was then allowed to proceed for one hour at 42°C. The hybridisation buffer was discarded, and the blot washed with the non-stringent 5x SSC 0.1% SDS solution for 20 minutes at room temperature. Wash solutions were

discarded and blot dried at room temperature. X-ray film was exposed to the blot overnight at -70°C.

Cleavage site determination by primer extension reactions

Primer extension reactions provide information to determine where the template (target) starts (from the 5' end). This is accomplished by having a primer bound downstream undergo a polymerase reaction (either by reverse transcriptase for RNA or Taq polymerase for DNA). In this case, reverse transcriptase and a DNA probe were used to determine at what point the products produced by RyPS cleavage start. The 3' ribozyme (thus the 3' ribozyme cleavage site) was probed and the shRNA (thus where the 5' ribozyme cleaves). If used in conjunction with a marker ladder size increases can easily be distinguished. This experiment utilized a sequencing reaction as a ladder, using similar probes as in the primer extension. In doing this, not only can the size difference be noted, exact site of cleavage can also be mapped.

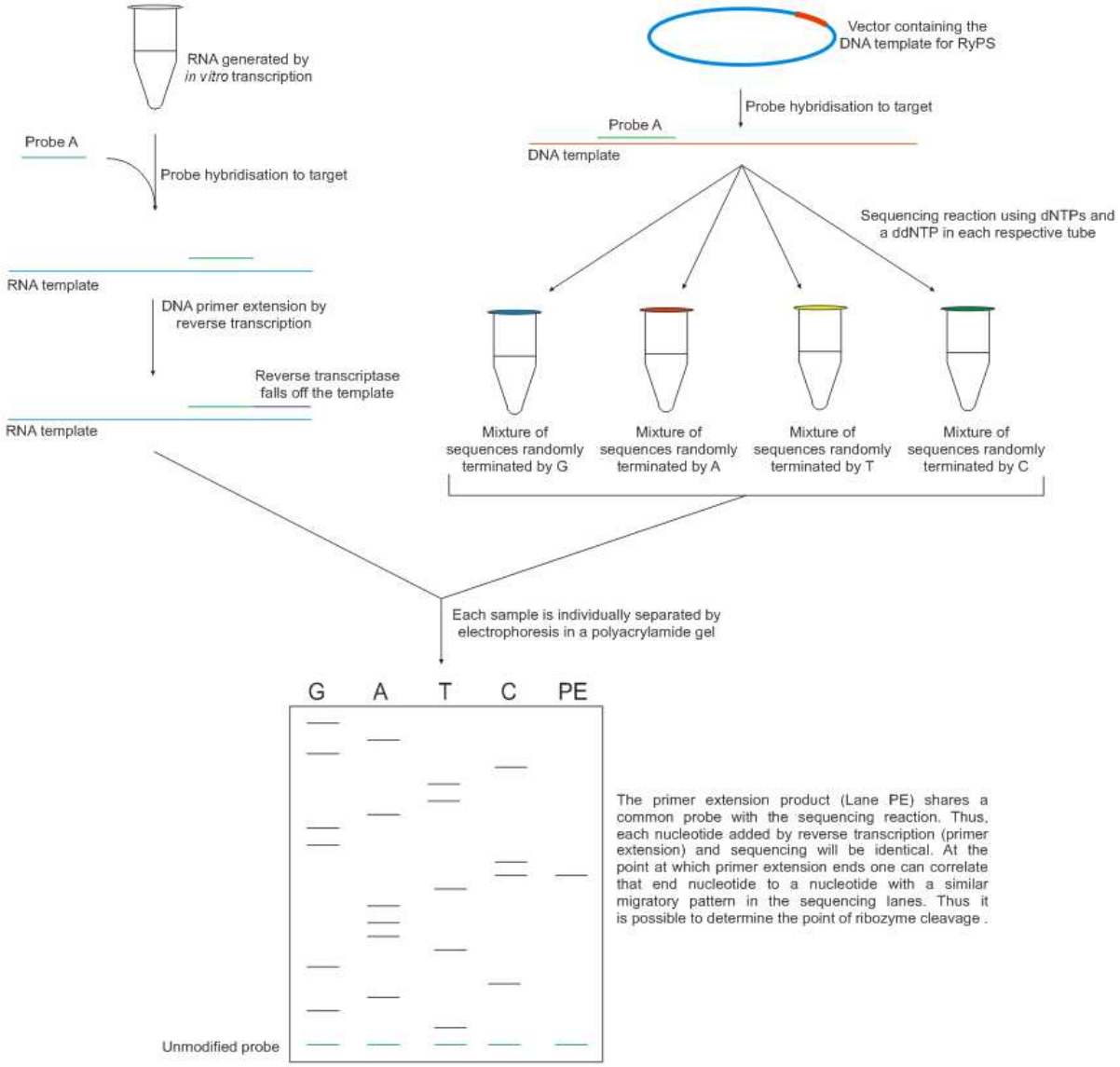

Figure 2. 10: Overview of the primer extension reaction used to determine the cleavage sites of each of the ribozymes in RyPS.

Primer extension

The adapted T7 primer and a reverse primer were used in the following PCR reaction containing 100 ng of template, 1 mM $MgCl_2$, 0.2 mM dATP, dCTP, dGTP and dTTP, 20 pmol forward primer, 20 pmol reverse primer, 10 µl 5x GoTaq Flexi Buffer and 1.25 u GoTaq DNA polymerase (Promega) in a final volume of 50 µl. PCR conditions as follows; 2 minutes at 95°C, 30 cycles of: 95°C for 30 seconds, 55°C for 15 seconds and 72°C for 15 seconds. DNA fragments were purified from an agarose gel post electrophoresis as mentioned previously.

The MEGAshortscript™ high yield transcription kit was used for the *in vitro* transcription reaction and contained 350 ng DNA template. The reaction was carried out at 37°C for 1 hour. Samples were stored at -20°C directly after incubation until use.

End labelled probe used in the reverse transcription reaction was generated in a similar manner used for the northern blots.

RNA template generated from the in vitro transcription was used in a reverse transcription reaction. The protocol followed was as per stipulation in the Sensiscript® Reverse Transcription Handbook from Qiagen.

Sequencing-size determination reaction

Sequencing was performed using the same oligoprobes in the reverse transcription kit. This would allow for a direct correlation between the size of the

primer extended product and relevant positioning in the sequencing reaction, thus one would be able to determine exact position of ribozyme cleavage. The CycleReader^{TM} DNA sequencing kit from Fermentas was used and 150 fmol of DNA template in the form of whole plasmid (pCI-neo clones) used in the reaction. Both reactions were stopped by the addition of an equal volume of DNA/RNA loading dye.

Five microlitres of each reaction (primer extension and sequencing) was loaded into a 41cm denaturing 10% polyacrylamide gel and was subjected to electrophoresis at 1500 V 30 mA. An X-ray film was exposed to the migrated products overnight at -70°C and autoradiography performed.

Results and Discussion

In vitro Transcriptions

Initially it was necessary to determine whether RyPS was able to function in an environment optimal for ribozyme activity. The RyPS predecessor showed some activity within the *in vitro* environment, using minimal hammerhead ribozymes. Thus it was assumed that a greater rate of cleavage was obtainable by the faster hammerhead ribozymes. This activity is thought to be due to concentration of divalent cations, which within the *in vitro* environment is often far higher than is required by hammerhead ribozymes for cleavage, thus within this environment results obtained represent products from RyPS cleavage, and not whether RyPS is viable in cellular environments. The surplus of magnesium ions present within the buffers (6 mM) allows for cleavage to take place, irrespective of the hammerhead ribozyme being minimal form. Ideally 3 major cleavage products would result from RyPS cleavage, namely the 5' and 3' ribozymes, and the shRNA. The other products that would be expected are caused by malformation of any structures within RyPS, preventing cleavage, however these species would be present in far smaller amounts compared to the main cleavage products. Figure 3.1 demonstrates the possible products generated by RyPS.

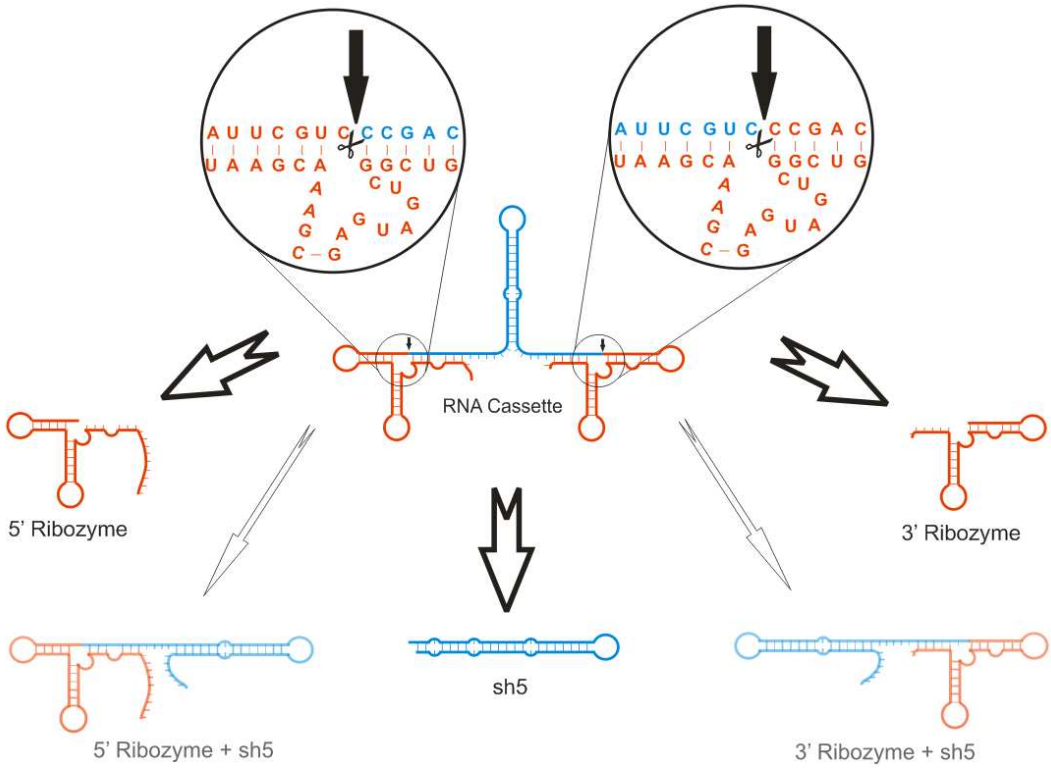

Figure 3. 1: Illustration of the possible products formed by the faster RyPS during *in vitro* transcriptions.

The RyPS products indicated by the bold arrows are the major products, whereas those by the thin arrows are the minor products. Any of the knockout RyPS species, would produce products indicated by the thin arrows, and would be a predominant species in that particular reaction.

Producing the RyPS within an *in vitro* environment would be the first step in visualizing the potential cleavage products. The environment of the reaction (which is dependent on the conditions which would suit the bacteriophage T7 polymerase for peak activity) has a high concentration of magnesium ions, far higher that would be found in any cellular environment. Using this environment, the rate limiting factor is

not the presence of divalent magnesium, and both minimal and fast ribozymes will function fully.

Initially DNA template for the *in vitro* transcription was generated by restriction digests of the respective plasmids. Depending on the restriction enzyme used, one could control the length of template downstream of RyPS, thus the larger the end length, the larger the 3' ribozyme would be after cleavage. It is assumed that owing to the degree of secondary structure present within the ribozyme, the extra downstream sequence generated from downstream restriction sites will not interfere with the 3' ribozyme cleavage reaction. *Sal*I was used to cleave downstream of the 3' ribozyme. However it was speculated that because it is not a blunt cutting enzyme may give rise to additional products of different sizes in the transcription reaction owing to premature release of the polymerase from the template, which may vary from 1-2 bases in size. This size variation of the 3' ribozyme was found to occur (data not shown), and template was therefore generated by the blunt-cutting *Sma*I digest. This caused the 3' ribozyme to be slightly larger (7 bases) however predictive RNA folding analysis showed that the secondary structure of the hammerhead was not affected (data not shown). Tabulated in Table 3.1 are the sizes of expected RyPS products from template generated by a *Bgl*II and *Sma*I digest.

Table 3. 1: Potential RyPS products and their predicted sizes to be generated by *cis*-cleavage after an *in vitro* transcription reaction using template generated by restriction digest

Product	5'Rz (nt)	3'Rz (nt)	Hairpin (nt)	5'Rz-hairpin (nt)	Hairpin-3'Rz (nt)	RyPS (nt)
Minimal System	71	62	69	140	131	202
Fast System	75	88	69	144	157	232
Δ5'Rz Knockout	Absent	88	Absent	144	157	231
Δ3'Rz Knockout	75	Absent	Absent	144	157	231
Δ5'Δ3' Knockout	Absent	Absent	Absent	Absent	Absent	230

The RNA produced from the *in vitro* transcriptions was radio-labelled, and separated in an acrylamide based gel by electrophoresis. The gel was exposed to X-ray film, and the RNA products from RyPS cleavage was visualized as bands. It was found that irrespective of the nature of the 3' end of the template (overhanging or blunt) multiple bands would still form from the 3' ribozyme ranging in 1-2 bases.

Cloning generated a truncated 5’ ribozyme and served as a useful control element in size determination and comparison to other RyPS RNA species present. The truncated 5’ ribozyme is 11 bases smaller than the normal, thus making it 64 bases pairs in size. This truncation results in the removal of the bulge (5’-UAA-3’) from stem I, essentially rendering the fast hammerhead to a structure similar to that of a minimal hammerhead ribozyme, unable to form sustained tertiary structures during cleavage. Without the presence of either loop II or bulge on stem I, the tertiary structure required for cleavage would only occur when there is a correct momentary conformational change. The structural differences of the three 5’ ribozymes (fast, minimal and truncated), are compared Figure 3.2.

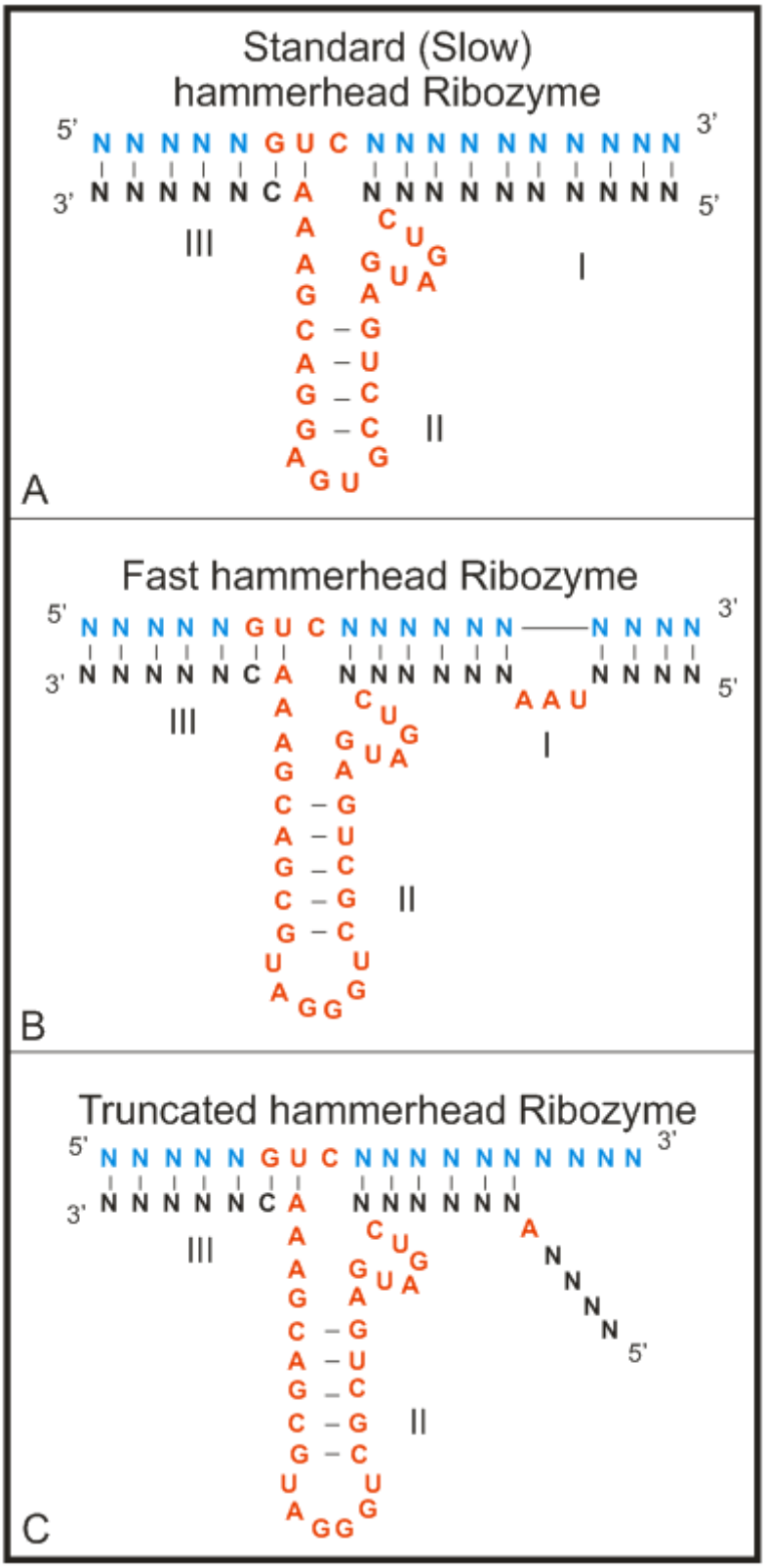
Standard (Slow)
hammerhead Ribozyme
5'
3'
3'
5'
III
I
II
A
Fast hammerhead Ribozyme
5'
3'
3'
5'
III
I
II
B
Truncated hammerhead Ribozyme
5'
3'
3'
5'
III
II
C

Figure 3. 2: Diagrammatic comparison of the various hammerhead ribozymes included within the RyPS species.

The catalytic core of the hammerhead ribozyme does not change, and is constant in each of the ribozyme species. In **A**, the minimal ribozyme is smaller than the faster counterpart, these differences accounted for the decreased size of stem I (5'-UAA-3' bulge), stem II as well as loop II. **B** includes the bulge and loop structures involved in tertiary stabilization. The truncated ribozyme **C**, only has one adenosine from the stem I bulge remaining and cannot participate in tertiary structure formation.

An *in vitro* transcription of 4 of the clones, slow RyPS, fast RyPS, Δ5'Rz RyPS and truncated 5'Rz RyPS, showed that the RyPS was highly efficient in its *cis*-cleavage, producing almost all product and very little initial substrate. The three predominant products can be seen in Figure 3.3, in descending order of 3' ribozyme, 5' ribozyme and then shRNA. The slow RyPS underwent poor cleavage of the 3' ribozyme, as most of the shRNA and the 3' ribozyme remain bound together which is postulated to occur because of the different cleavage triplet (5'-CUC-3') encoded within the 3' slow ribozyme. It is known that the triplet NUH is a universal cleavage triplet for hammerhead ribozymes, however certain triplets have shown improved cleavage.

Δ5'Rz RyPS clone does not allow for any cleavage activity within the 5' ribozyme, owing to the deletion of the highly conserved uracil group within the ribozyme catalytic pocket. The uracil is part of the motif 5'-$C_3U_4G_5A_6$-3' which plays a pivotal role in the formation of the tertiary structure of the hammerhead ribozyme. This motif undergoes an 180° internal rotation to facilitate the tertiary structure formation, and consequently removal of any of the four nucleotides would result in a loss of ribozyme flexibility, hence loss of activity. Interestingly it has been found, that when that particular uracil in the 5'-$C_3U_4G_5A_6$-3' motif is substituted with a cytosine to 5'-$C_3C_4G_5A_6$-3', the ribozyme still maintains activity (data not shown). This activity is expected because of the presence of the pyrimidine base found within both cytosine and uracil.

Δ5'Rz RyPS has an inactive 5' ribozyme thus only the 3' ribozyme and the conjugated 5' ribozyme-shRNA will be present as cleavage products after *in vitro* transcription. This allowed for the deductive identification of the band species present on the X-ray film produced by *in vitro* transcription. Furthermore, this data was supported by the positioning by the truncated 5' ribozyme, confirming the identities of all the band species. In Figure 3.3, all the band species can be identified, clearly showing the potential of ribozyme cleavage activity within an *in vitro* environment.

RyPS functions well within an *in vitro* environment, as shown in previous studies using the minimal hammerhead ribozymes (unpublished data), and is postulated to occur because of the magnesium ion content. However, if the postulated cleavage and conformation mechanism by Martick and Scott 2006 is valid, then the high magnesium ion concentration will have little to do with the outcome of the cleavage reaction. Instead, the metal ions function to bind to the negatively charged phosphodiester backbone of RNA, causing an overall decrease in the negative charge of the backbone, and thus increased overall stability of secondary and tertiary structures. Previously it was thought that the magnesium ions play a direct role in cleavage reaction, and depending on their role would act as general acids or bases, similar to the functional groups found within the catalytic pocket of a hammerhead ribozyme. The minimal hammerhead ribozyme system had no other means to initiate cleavage other than using metal ions as catalysts and randomly instantaneous cleavage conformation, owing to the lack of extra-core elements. It would not be impossible for the metal ion-initiated cleavage theories to apply to the fast acting

hammerhead ribozymes in which magnesium ions enter the catalytic pocket and become involved in the cleavage reaction. This would seem to be the case for the slow RyPS, even though it is unable to sustain a tertiary structure responsible for cleavage, as it is still able to cleave within an *in vitro* environment. It is possible that ribozyme cleavage could occur via both mechanisms, by which metal ions as well as core elements help facilitate the cleavage reaction while extra-core elements provide stability for tertiary structure and align required groups for cleavage. The cleavage reaction of the slow RyPS (Figure 3.3 in results) during *in vitro* transcription shows that the 3' ribozyme undergoes very poor cleavage and is thought to occur because of the cleavage triplet used. It has been shown that NUH is the best general formula for the cleavage triplet, and has been extended to NHH which is far more accommodating for target cleavage sites or triplets however is known to be less effective for cleavage, resulting in slower cleavage. The best rate of hammerhead ribozyme cleavage has been found using the 5'-GUC-3' cleavage triplet, and the slow minimal RyPS used the triplet code is 5'-CUC-3' in the 3' ribozyme, which most likely accounts for the poor cleavage seen from *in vitro* transcriptions. One may attribute the decrease in cleavage to the change from a purine to a pyrimidine base, and as Martick and Scott 2006 indicate, special arrangement within the catalytic pocket of the ribozyme plays an important role in cleavage. It would appear that even though not highly conserved, the cleavage triplet sequences play an important role in rate of cleavage, and I suspect that it is owing to overall stem III stability in keeping the tertiary structure more stable during cleavage.

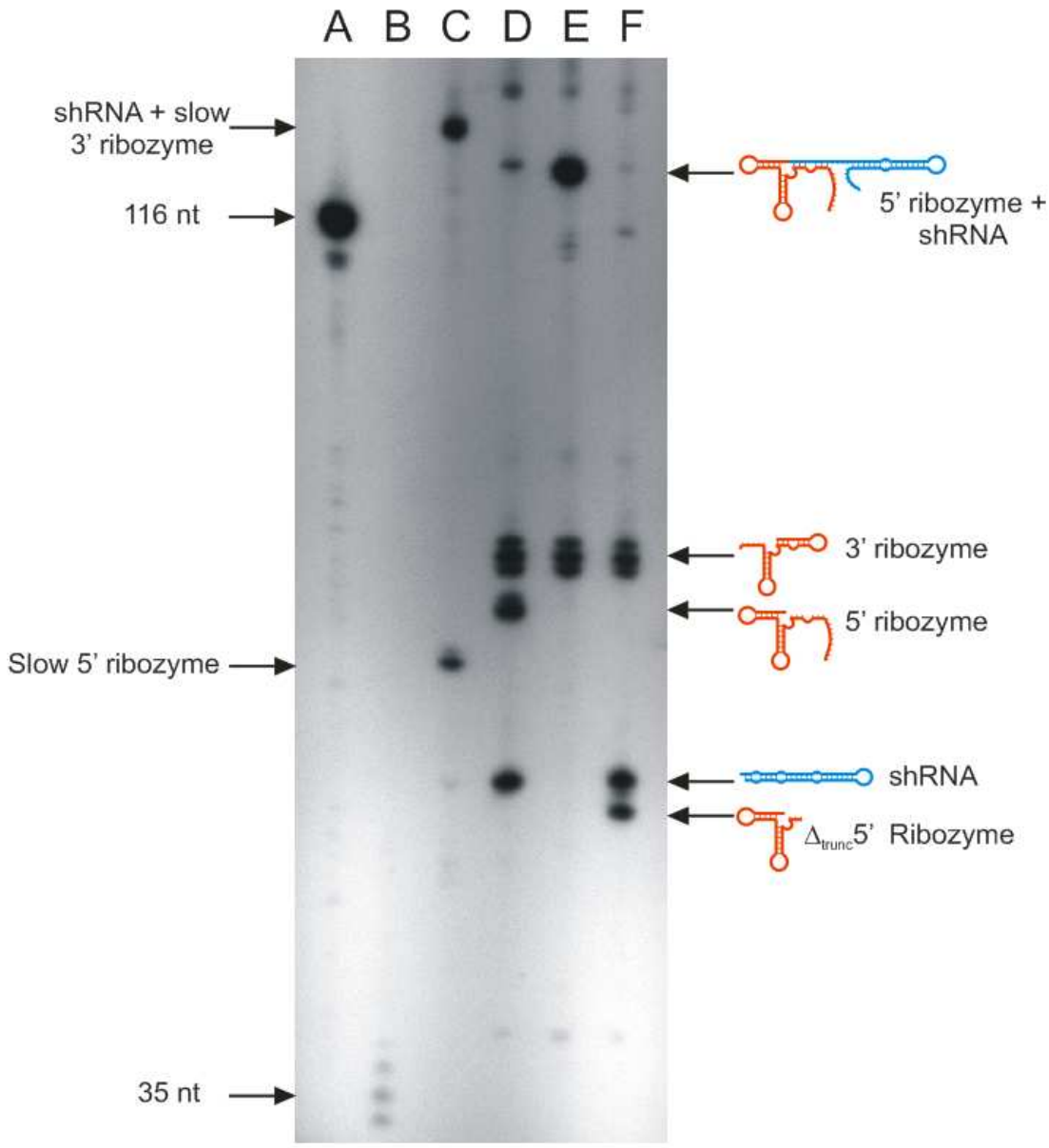
A B C D E F
shRNA + slow 3' ribozyme
116 nt
Slow 5' ribozyme
35 nt
5' ribozyme + shRNA
3' ribozyme
5' ribozyme
shRNA
Δtrunc5' Ribozyme

Figure 3. 3: An autoradiograph of *in vitro* transcription products subjected to electrophoresis in a 10% denaturing polyacrylamide gel.

Lanes A-B contain size markers, of 116 and 35 nt respectively. Lane C contains the RyPS system containing the minimal/slow ribozymes. On the left of the diagram, the two products produced by the minimal system are indicated. Lane D contains the functional faster RyPS, and lanes E-F contain faster ribozymes modified such that they are either non- or less functional. Lane E contains the 5' ribozyme knockout clone whereby the 5' ribozyme does not cleave, and F a truncated version of the 5' ribozyme, essentially functioning as a minimal ribozyme. On the right of the diagram, the knockout 5' ribozyme + shRNA product is indicated, below that all the other products produced by RyPS. The lowest label is the truncated 5' ribozyme, which is seen below the shRNA. Even though truncated, the 5' ribozyme is still functional.

A second autoradiograph was produced using PCR product as template for the *in vitro* transcription, as opposed to a template generated by restriction digest as before. When using PCR product as template, the size of the 3' ribozyme decreases because no additional downstream sequences are present, previously generated by restriction digestion. The following experiment contained additional controls, in the form of a 3' ribozyme knockout (Δ3'Rz RyPS) and a 5' and 3' ribozyme knockout (Δ5'Δ3'Rz RyPS). These two controls would provide confirmation of the species seen on the previous autoradiograph. Additionally, by changing the forward primers used to generate the template, one could modify the 5' ribozyme to be a different size from the original species. This was done by including 5 additional non-interfering bases to the forward primer. This would result in a template that after *in vitro* transcription, produces 5' ribozyme that has 5 additional bases. Template sizes generated by PCR and restriction digest have been compared in Figure 3.4.

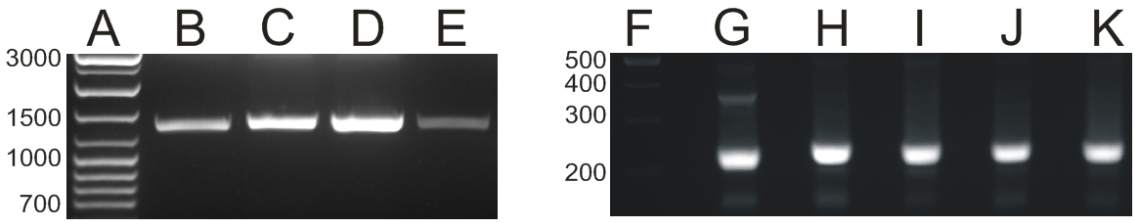

Figure 3. 4: Templates used for *in vitro* transcriptions.

In B-E the template comprises of the CMV promoter, an intron and extra nucleotides from the backbone, resulting in a fragment ~1350bp is size. This fragment is generated by a *Bgl*II/*Sma*I digest on the RyPS clones within pCI-neo. In G-K, the templates are generated by a PCR reaction and are far smaller than the previous template used. These fragments are approximately 210 bp is size. A) DNA size marker, B) slow/minimal RyPS template, C) RyPS template, D) Δ5'Rz RyPS template E) truncated 5'Rz RyPS template, F) DNA size marker, G) slow/minimal RyPS template, H) RyPS template, I) Δ5'Rz RyPS template, J) Δ3'Rz RyPS template and K) Δ5'Δ3'Rz RyPS template.

Table 2 and Figure 3.5 give a comparison of the products generated by RyPS after *in vitro* transcription using PCR product as template. The bracketed values indicate ribozyme sizes if the 5-base larger template was used to generate RNA.

Table 3. 2: Size predictions of the RyPS products produced by *cis*-cleavage after an *in vitro* transcription using PCR products as template

Product	5'Rz [+5] (nt)	3' Rz (nt)	shRNA (nt)	5'Rz-hairpin [+5] (nt)	Hairpin-3'Rz (nt)	RyPS [+5] (nt)
Fast System	75 [80]	73	69	144 [149]	142	217 [222]
Δ5'Rz Knockout	Absent	73	Absent	143 [148]	142	216 [221]
Δ3'Rz Knockout	75 [80]	Absent	Absent	144 [149]	141	216 [221]
Δ5'Δ3' Knockout	Absent	Absent	Absent	Absent	Absent	215 [220]

* Values denoted in [] were generated by PCR and are 5 nt larger than the original

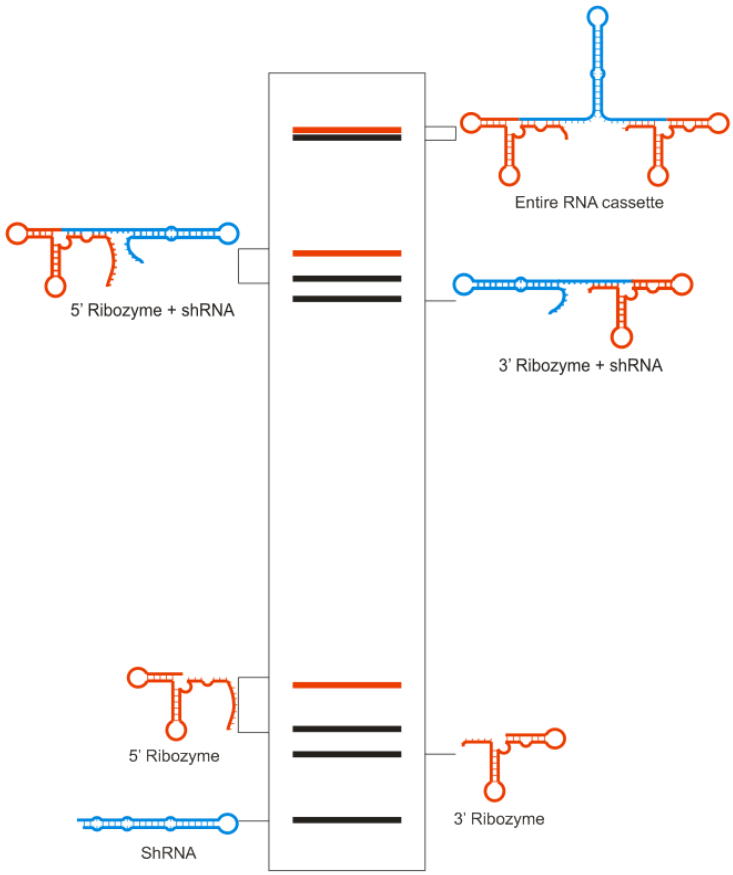

Figure 3. 5: Schematic representation of the RyPS products generated during *in vitro* transcription, separated by electrophoresis.

This figure serves to compare the differences between the 5' ribozyme when it is generated normally by PCR, and when it is generated to be 5 bases larger. This size difference is only seen where the 5' ribozyme is present, thus the 5' ribozyme, 5' ribozyme + shRNA and the entire RNA cassette are affected. Red bands represent the species with a 5 base larger 5' ribozyme, whereas black bands indicate normal fast RyPS species.

The 3’ ribozyme generated from the PCR template is significantly smaller than that generated from the restriction digest template. This is seen in Figure 3.6, where the 3’ ribozyme appears a few positions above the shRNA. In Figure 3.6, lanes A-D, various species of functional and knockout ribozymes are used. Lane B contains the 5’ ribozyme knockout, and should only produce a 3’ ribozyme and a 5’ ribozyme-shRNA conjugate after cleavage. Lane C contains the 3’ ribozyme knockout, and would conversely contain a released 5’ ribozyme and 3’-ribozyme-shRNA conjugate. Simply by comparing lanes A-C one is able to establish the species of each of the bands present by their disappearance and reappearance in each of the respective knockouts. The Δ5’ Rz RyPS and Δ3’Rz RyPS do not produce a shRNA fragment, thus the only fragment unique to the RyPS lane (Figure 3.6 lane A) is the lowest band, which should represent the shRNA species. By a similar process of elimination, and comparing lanes B and C in Figure 3.6, one is able to establish that the band above the shRNA is the 3’ ribozyme, and the band above that is the 5’ ribozyme. The 5’ ribozyme identity was confirmed further by comparing it to the species in lanes E-G, whereby the 5’ ribozyme species are 5 bases bigger, which correlate in size to the original ribozymes. These data provide convincing evidence as to the positioning and release of the species of RNA generated by RyPS.

Within the catalytic core, there are 4 nucleotides involved in allowing for the co-axial alignment of stems I and II causing the formation of the tertiary structure. These nucleotides (5’-$C_3U_4G_5A_6$-3’) were thought to be of a highly conserved nature, and any of their removal or alteration results in cleavage abrogation. However in an

attempt to generate the 5' and 3' ribozyme knockout mutants, the substitution reaction 5'-$C_3U_4G_5A_6$-3'→ 5'-$C_3C_4G_5A_6$-3'still resulted in cleavage in an *in vitro* environment (data not shown). Understandably cytosine and uracil are similar in structure which possibly allows for the ribozyme to fold into the tertiary conformation. Furthermore, Martick and Scott showed that substitution mutations of key nucleotides involved in the acid-base reactions within the core still allowed for cleavage to occur, albeit less. These types of changes within the ribozyme catalytic core were previously shown to prevent ribozyme cleavage, within the minimal system. The minimal hammerhead ribozyme was most likely dependent on higher concentrations of magnesium, but was also far more sensitive to changes within the catalytic core, as they might lead to greater instability of the tertiary structure. It was found that deletion of the uracil base prevented any cleavage activity, and is assumed that this would occur if any of the bases within the 5'-$C_3U_4G_5A_6$-3' motif were removed, since their role is that of a pivotal and core stabilizing nature, allowing for the extreme distortion of the naturally occurring double helix of stem I (Martick and Scott 2006).

On several occasions an RNA ladder was used. However this produced poor quality bands, which was not owing to the quality of RNA used, rather the size of the gel (41cm) which seemed to cause some of the bands to smudge.

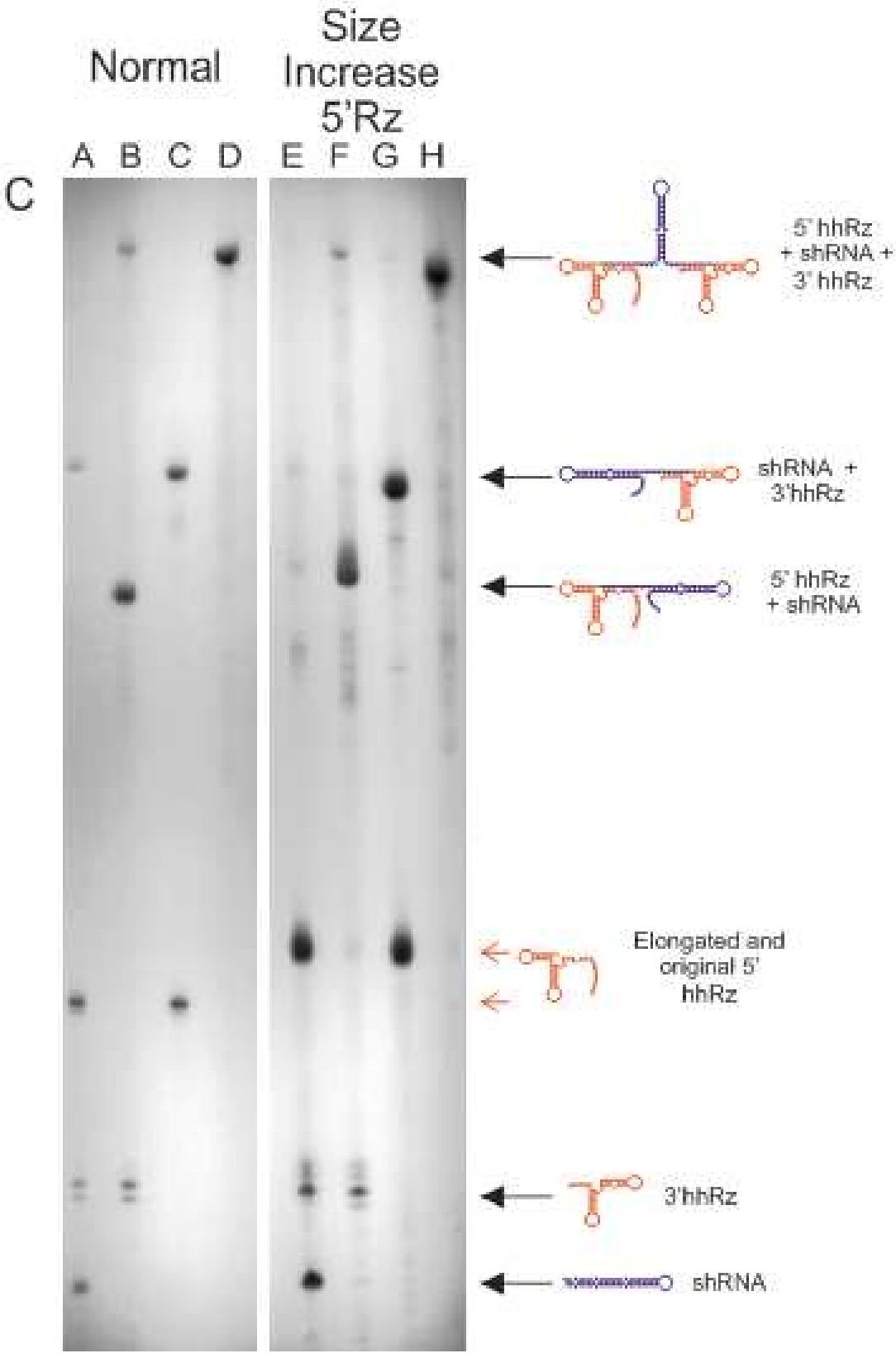
C
Normal
Size Increase 5'Rz
A B C D E F G H
5' hhRz + shRNA + 3' hhRz
shRNA + 3'hhRz
5' hhRz + shRNA
Elongated and original 5' hhRz
3'hhRz
shRNA

Figure 3. 6: An autoradiograph of the RyPS *in vitro* transcription products, using PCR generated templates.

Lanes A and E both contained the same fast functional RyPS template, however, lane E had a primer that increased the size of the 5' ribozyme template, the transcription product visibly larger in comparison. Lanes B and F contained the Δ5' ribozyme knockout clone as template, and a slight increase in the Δ5' ribozyme + shRNA species in lane F can be seen. Lanes C and G contained a Δ3' ribozyme knockout clone, again a size increase witnessed by the 5' ribozyme. Lastly Lanes D and H contained the Δ5'Δ3' ribozyme knockout as a template. From this result one can clearly deduce the species presented in the autoradiograph, denoted on the right side.

The greatest concern from the data is that the predicted sizes of the RNA species do not correlate to those seen on the autoradiograph. The 5’ ribozyme and 3’ ribozyme are predicted to be 2-3 bases apart however on the autoradiograph it would appear to be more. The shRNA is predicted to be 4 bases smaller than the 3’ ribozyme and 6 smaller than the 5’ ribozyme, which again appears to be different from the autoradiograph data. Owing to the nature of the system, no leeway can be given to the shRNA size or structure. The shRNA is an exact Dicer substrate and any alterations or modifications will results in the failure of its recognition, and no silencing will occur. Potentially the shRNA is the correct size, and the other fragments (5’ and 3’ ribozymes) are larger than anticipated.

Northern blot analysis of RNA generated by in vitro transcriptions

The RyPS has shown to have functional ribozymes in an *in vitro* environment, resulting in the release of 3 individual species. However as indicated by *in vitro* transcription, RyPS cleaves into 3 distinct species with sizes that vary to the intended values. Even though no measurement of size was done, the large variance in sizes of the cleavage products seen with *in vitro* transcription experiments led to the conclusion that even though the ribozymes had a high level of activity, their target site may differ from the intended site. Should RyPS release the shRNA as a differently sized species, no RNAi will be induced within the cellular environment.

Ultimately the best explanation of RyPS activity would be derived from the analysis of the products generated within a cellular environment, as that would include the various other agents involved in ribozyme cleavage within that environment, such as pH, metal ion concentration and innate RNAs and proteins. However since the initial *in vitro* transcription data indicated that RyPS was malfunctioning, analysis was initially performed on RNA generated in this manner. Isolation and identification of the individual RNA species generated by RyPS, within a size defining environment would give possible insight into which RNA species are not behaving according to the expected model. Northern blotting allows for the exact identification of RNA species, as they can be separated and defined by individual nucleotides. Furthermore, probing with a complementary radio-actively labelled oligonucleotide provides specific and sensitive detection of the target.

A northern blot was performed on the RyPS products generated by *in vitro* transcription, probing for each individual component. Each of the various knockout clones were included, which would further substantiate any data obtained from the northern blot.

The RNA was stained with ethidium bromide and viewed under UV trans-illumination after electrophoresis through a polyacrylamide gel. This step was included to validate RNA quality and consistency of RNA concentration. The data produced shows all RNA species present, and the various RyPS products are clearly visible. Various DNA oligonucleotides were end-labelled to serve as general size controls. Even though DNA and RNA have different electrophoretic mobility, they can still be compared to give a general indication of sizes present. Figure 3.7 shows an ethidium bromide stain of the acrylamide gel containing the *in vitro* transcription RyPS products.

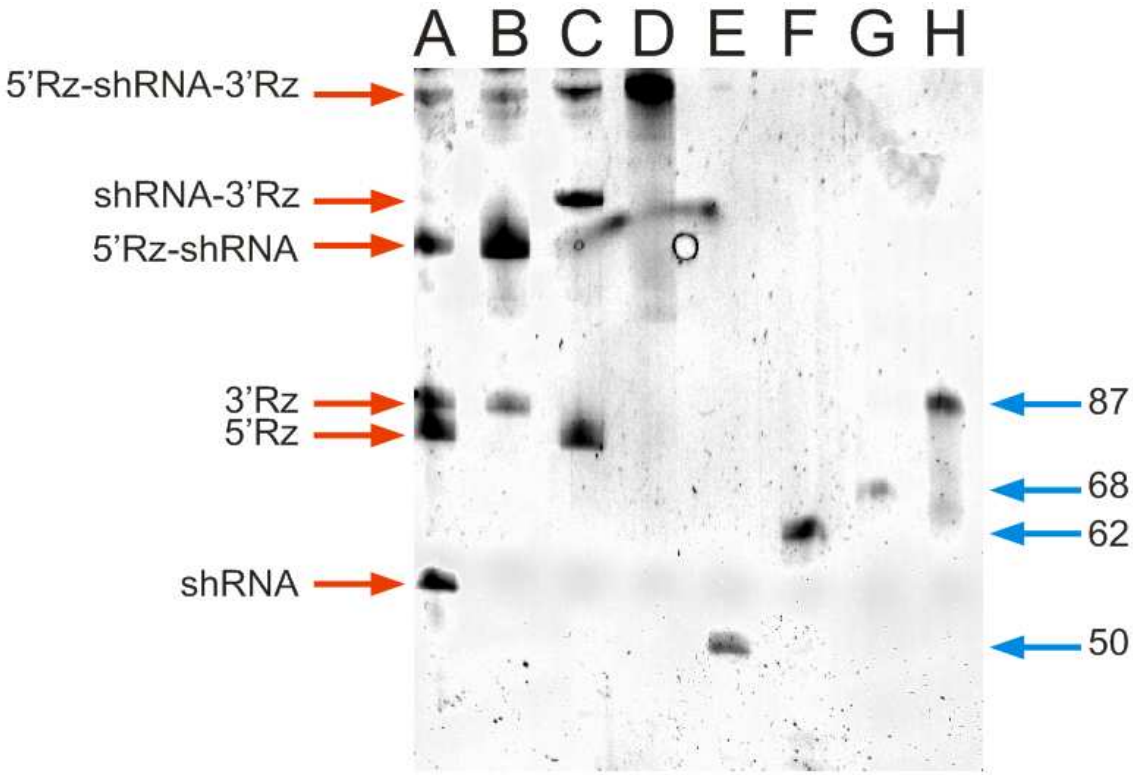
A B C D E F G H
5'Rz-shRNA-3'Rz
shRNA-3'Rz
5'Rz-shRNA
3'Rz
5'Rz
shRNA
87
68
62
50

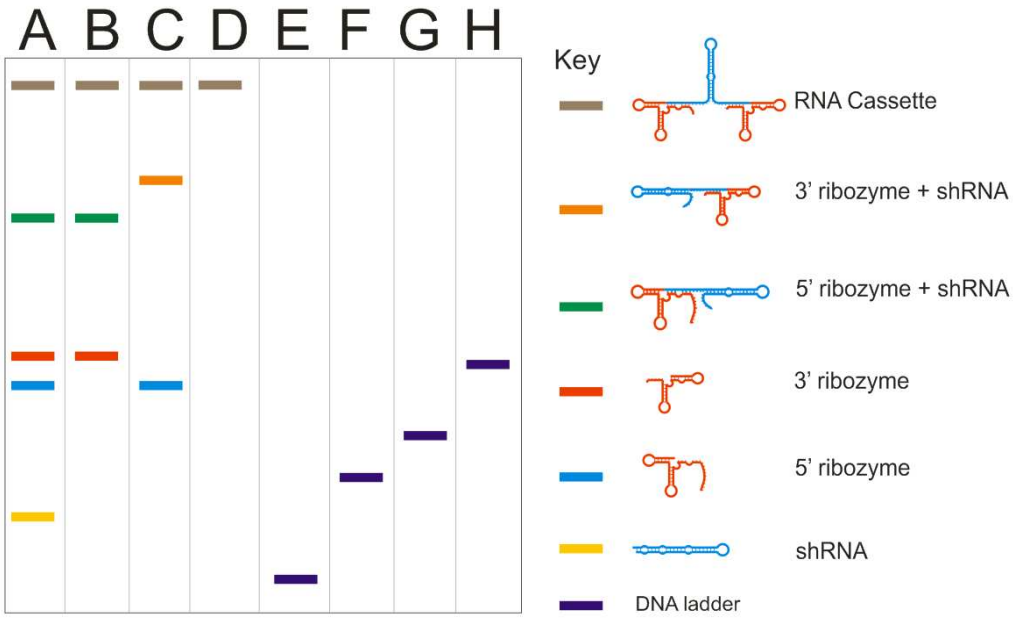
A B C D E F G H
Key
RNA Cassette
3' ribozyme + shRNA
5' ribozyme + shRNA
3' ribozyme
5' ribozyme
shRNA
DNA ladder

Figure 3. 7: An ethidium bromide stain of RNA generated by *in vitro* transcription prior to transfer onto a nitrocellulose membrane.

All RyPS knockout clones are included in lanes A-D. Lane A contains the functional RyPS, whereby each individual component of the RyPS is released. It was noted that the activity of the 5' ribozyme is less than expected, due the presence of 5' ribozyme-shRNA. The 5' ribozyme knockout clone in lane B, released only the 3' ribozyme while the 5' ribozyme and shRNA remained uncleaved. Similarly, lane C contains the 3' ribozyme knockout, in which the 5' ribozyme is released, and the 3' ribozyme does not cleave to release the shRNA. Lane D has both ribozymes knocked out, thus no cleavage product is released. RNA species are defined according to comparison of the RyPS and respective knockout clones, resulting in the identification of each species present by elimination. Lanes E-H are DNA sizes controls, indicated by the blue arrows on the right. Below the ethidium bromide stain of the *in vitro* transcription is a schematic illustration of the various species present in the above diagram, providing easier recognition.

Interestingly, the positioning of the shRNA is far lower than anticipated. According to what was expected from cleavage, the shRNA generated was meant to be 69 bases in size. In Figure 3.7, the shRNA species lies between 50-62 DNA bases, which suggests that the shRNA is somewhat smaller than the intended size. Furthermore similarly sized DNA will generally migrate further than its RNA counterpart, owing to the lack of the 2' oxygen. Taking this into consideration, the shRNA is far smaller than expected, and is assumed to be in the regions of 50-55 bases. If proven true, this product is unfit to generate knockdown of its homologous target.

Northern blot analysis confirmed what was deduced from the *in vitro* transcriptions and ethidium bromide stained RNA in Figure 3.7. In the analysis it was shown that the shRNA was far smaller that the intended sizes. Furthermore the 3' ribozyme is also smaller than intended, suggesting that the ribozymes are cutting at multiple sites. The RNA generated by *in vitro* transcriptions was probed individually for each RyPS species, shRNA, 5' ribozyme and 3' ribozyme, depicted in Figure 3.8.

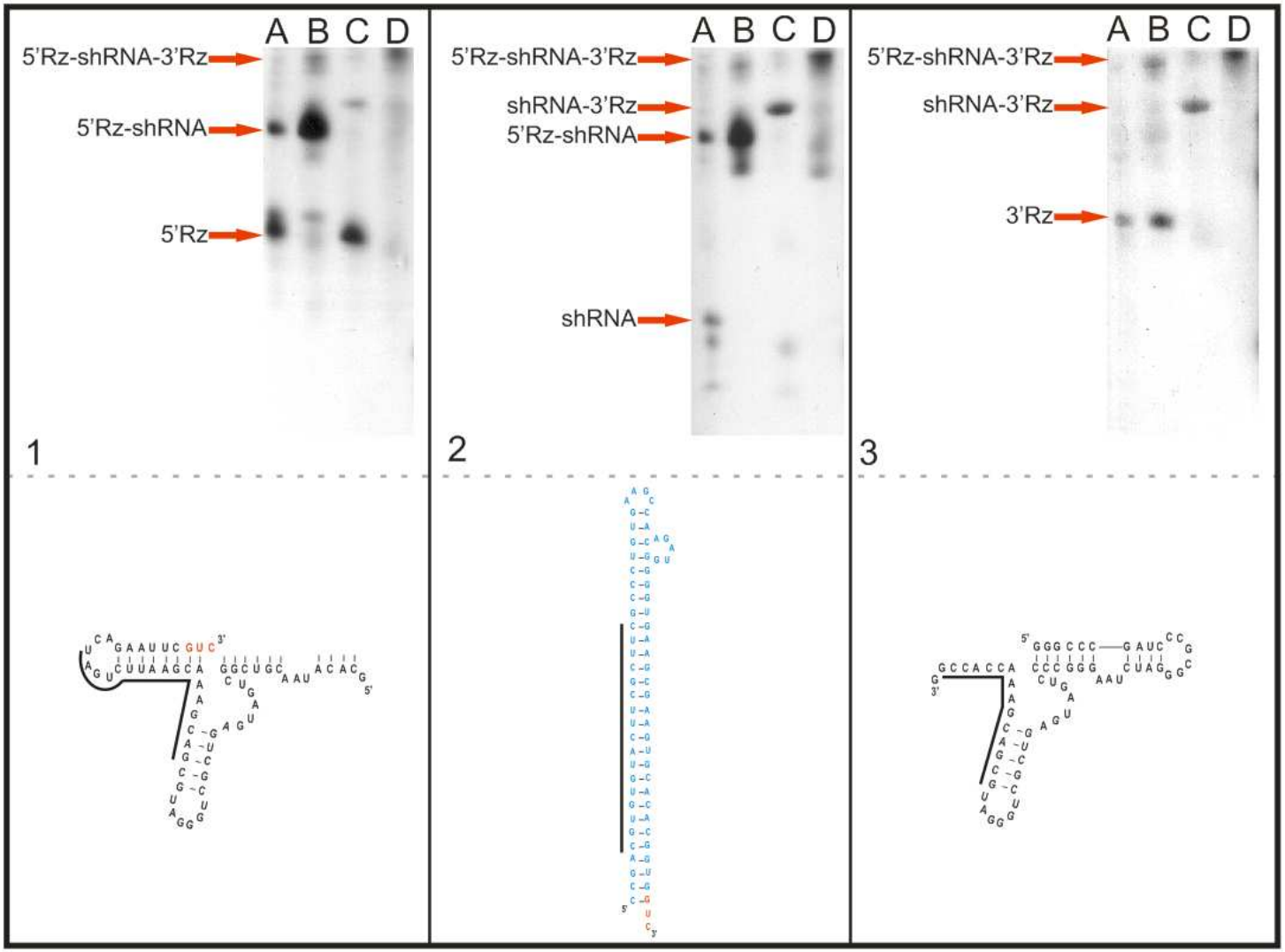
A B C D
5'Rz-shRNA-3'Rz
5'Rz-shRNA
5'Rz
1
A B C D
5'Rz-shRNA-3'Rz
shRNA-3'Rz
5'Rz-shRNA
shRNA
2
A B C D
5'Rz-shRNA-3'Rz
shRNA-3'Rz
3'Rz
3

Figure 3. 8: Comparison of the three northern blots for the 5' and 3' ribozymes and the shRNA of RyPS.

Lanes A-D are functional RyPS, 5'ribozyme knockout RyPS, 3' ribozyme knockout RyPS and 5'3' ribozyme knockouts, respectively. Data set 1 was probed for 5' ribozyme and is clearly visible in each of the respective lanes. The 5' ribozyme element is present in both the single 5' ribozyme as well as the uncleaved 5'Rz-shRNA conjugate. Some cross-reactively occurred with the 3' ribozyme, which is slightly visible in lanes A and B, and is owing to the potential overlap of the 5'probe with the 3' ribozyme owing to ribozyme similarity. Data set 2 was probed for shRNA, present in its processed form as well as any uncleaved products in lanes A-D. The shRNA was confirmed to be positioned between 50-62 DNA bases, according to the DNA oligonucleotide ladder, seen with ethidium bromide staining. Lastly, data set 3 probed for 3' ribozyme, appearing just above the 5' ribozyme position. Below each blot is a diagrammatic representation of the primer binding sites on each of the ribozymes and shRNA. Below each blot is a representation of the region in which each of the primers bound their respective target. Part of panel 1 is the 5' ribozyme, panel 2 the shRNA and panel 3, the 3' ribozyme.

As expected, the species identified by the northern blot analysis confirmed those produced by the ethidium bromide stain when comparing the various knockout clones. This confirms that the shRNA generated is by no means what is intended, thus is assumed to be unable in producing target knockdown. It would appear that the 5' ribozyme cleaves at the cleavage triplet as expected. However the 3' ribozyme seems smaller than the predicted size of 88 bases, seen positioned just above the 5' ribozyme in Figure 3.8. This would indicate that the 3' ribozyme processing is aberrant, and that the target cleavage sites are not being cut.

If this is so, it may be useful to determine where the ribozymes are cutting within RyPS as this will aid future and corrective design.

Cellular Assessment and HBV knockdown

Ultimately, the best measure to determine whether RyPS was functional was to place it in an environment where it is expected to induce knockdown of target. The cellular environment contains many elements that cannot be accounted for in the *in vitro* environment. Other RNA and proteins species play a role in the formation of secondary and tertiary structures. Divalent metal ion concentration is different to that of the *in vitro* environment, and is often at far lower concentrations within the cell, too low for the minimal/slow hammerhead ribozymes to function. Magnesium is required for the stability and formation of both secondary and tertiary structures of the ribozymes, previously also thought to be responsible for the cleavage activity. Ideally however, the faster hammerhead ribozymes constructed will be less dependent than the minimal species on the presence of magnesium ions for structure stabilization, as this is facilitated by the extra-core elements, such as the bulge on stem I.

To assess cleavage functionality knockdown assays were performed, having the shRNA target a reporter system. Knockdown was assessed using a dual luciferase reporter system. This reporter system utilizes Firefly luciferase and *Renilla* luciferase which are both encoded on one plasmid (psiCheck2.2). A multiple cloning site (MCS) is encoded just downstream of the *Renilla* luciferase gene, before the poly-adenylation signal. A target sequence from X ORF of HBV was cloned into the MCS, and its targeting by a shRNA would result in the knockdown of *Renilla* luciferase. Firefly luciferase is generated off a different expression system (Herpes simplex virus

promoter) and is unaffected by the shRNA and serves as an internal background control, allowing for uniformity when comparing multiple samples. Figure 3.9 diagrammatically describes the dual luciferase reporter system.

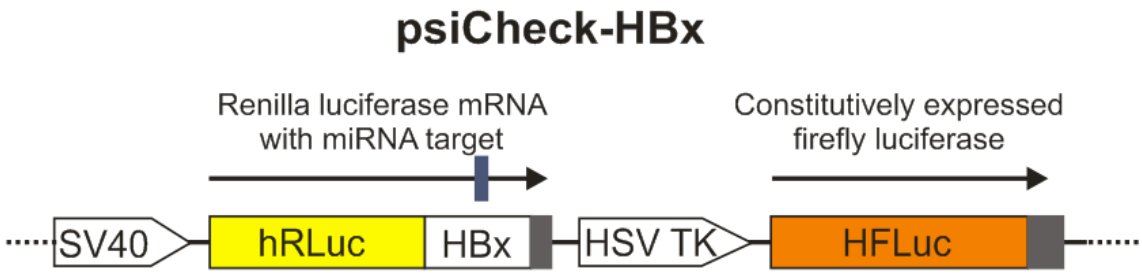

Figure 3. 9: A schematic representation of the region within psiCheck2.2-HBx containing the luciferase genes, *Renilla* luciferase (hRLuc) and Firefly luciferase (HFLuc).

Downstream of hRLuc is a region of the HBx gene, which contains the sites recognized by the shRNA released from RyPS (target noted as the blue stripe). Both luciferases are generated off different promoter systems.

Pol III promoters are generally used to produce small RNAs. Therapeutically these promoters have an advantage of being ubiquitously expressed in all cell types and not producing a 5' cap or 3' polyadenylation tail, which is ideal for generating hairpin molecules such as shRNAs. However, these promoters also have therapeutically undesirable properties. A well characterized and commonly used Pol III promoter is U6, which induces a high level of expression of its downstream gene, and can be expressed from any cell type.

Tissue culture studies provided data of the knockdown effect RyPS had on the luciferase-linked target. Human embryonic kidneys cells (Hek293) were transfected with the reporter system, with potential therapeutic RyPS template and controls, such as GFP. Various controls were included in the luciferase assay, such as a control hairpin.

The shRNA generated by RyPS has also been cloned into a U6 expression system, whereby the shRNA is generated by a U6 promoter. This construct has been previously used, and is known to have a very significant knockdown effect on its target (Carmona et al. 2006). The U6-shRNA served as a comparative control, ideally the gold standard which the RyPS knockdown was compared to. Thus should shRNA release from RyPS be successful, knockdown would be comparable to the U6-driven shRNA. All the results are normalized to a positive control which contains only the luciferase reporter system and no therapeutic (shRNA) molecules. A control hairpin expressed from U6 is also used, targeting the LacZ gene, to control for specific activity caused by either the U6 promoter or a shRNA. All the RyPS constructs are tested, including the minimal/slow RyPS, previously shown to have little to no activity within the cellular environment. It was anticipated that none of the knockout controls will be able to induce knockdown. Figure 3.10 compares the relative normalized knockdown of all the RyPS clones to the U6-driven shRNA. The data from the luciferase knockdown studies indicated that all of the RyPS species were unsuccessful in inducing knockdown of their target.

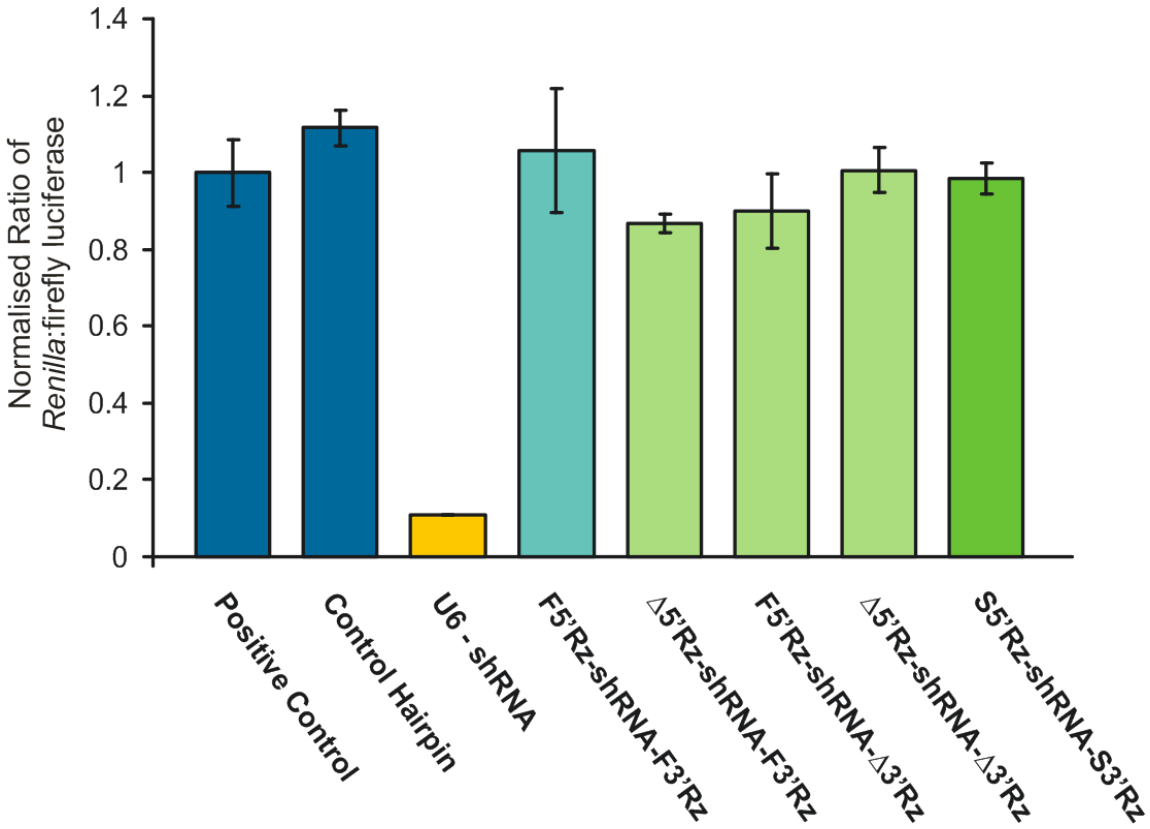

Figure 3. 10: Normalised ratio of *Renilla*:Firefly luciferase assay, using the dual luciferase reporter system.

Firefly luciferase provides a stable background luminescence as a control, while knockdown of *Renilla* luciferase can be directly compared to it. The positive control contained no forms of exogenous RNAi molecules, while the control hairpin contained a shRNA driven by the U6 promoter targeted against LacZ. This will cause no knockdown, as no innate sequences within the cell are similar. U6-shRNA produces a shRNA similar to that of RyPS, however, is generated of a U6 promoter. The various prefixes denote the following: F – fast ribozyme, S – slow/minimal ribozyme and Δ – knockout mutant of that ribozyme, causing it to be non-functional. The shRNA is functional against its target, as noted by U6-shRNA, causing up to 88% knockdown. No knockdown occurs with the RyPS clone indicating that the fast system is not functioning as intended.

The shRNA generated by the U6 promoter system induced 88% knockdown against the targeted HBV sequence. This suggests that the shRNA is functional, and can induce knockdown of its target effectively (Carmona et al. 2006). The slow/minimal RyPS has no functioning within a cellular environment as shown previously, and is confirmed by the lack of knockdown seen. This lack of knockdown was expected to occur with the all the knockout controls, owing to the inability to generate an exact Dicer substrate. The potential shRNA released by RyPS relies on the nuclear export protein exportin-5, to be transported into the cytoplasm. This interaction is facilitated by the interaction of the two nucleotide 3' overhang of the shRNA. This is absent from both knockout controls, Δ5'Rz RyPS and Δ3'Rz RyPS, as both have a ribozyme attached at 5' or 3' end, respectively. RyPS is generated by a Pol II promoter, and it is plausible that the 5' cap present on the mRNA strand containing RyPS allows for export of that particular strand into the cytoplasm. Thus the shRNA portion of Δ5'Rz RyPS and Δ5'Δ3'Rz RyPS may be exported into the cytoplasm, however being the incorrect substrate would not result in any knockdown. The fast RyPS did not produce a significant form of knockdown of its target. It is suspected that the RyPS fails to function within a cellular environment, or fails to cleavage into the correct products.

Additional testing of RyPS was done against HBV using pCH-3091, a greater than genome length copy, which has the capability for the generation of live HBV virus (Nassal 1992). Similar controls and samples were tested as before in the dual luciferase assay. An ELISA against the surface antigen of HBV (HBsAg) was performed, using the supernatant from transfected cells. This assay was used to confirm the results obtained from the luciferase assay. The basis of this experiment relies on the direct targeting on viral mRNA and knockdown efficacy is measured by a decrease in viral products/particles. Even though the efficacy of this assay is measured by monitoring surface antigen knockdown, it is also a reflection of the effects of the shRNA against other HBV proteins such as the polymerase.

The ELISA is a less sensitive assay compared to the luciferase assay, mainly owing to the lack of an internal control. Thus the results obtained from the ELISA were neither as sensitive nor accurate, however did give a clear indication of the similarity of the results obtained from the luciferase assay. Similarly, very poor knockdown was generated by all the RyPS clones shown in Figure 3.11.

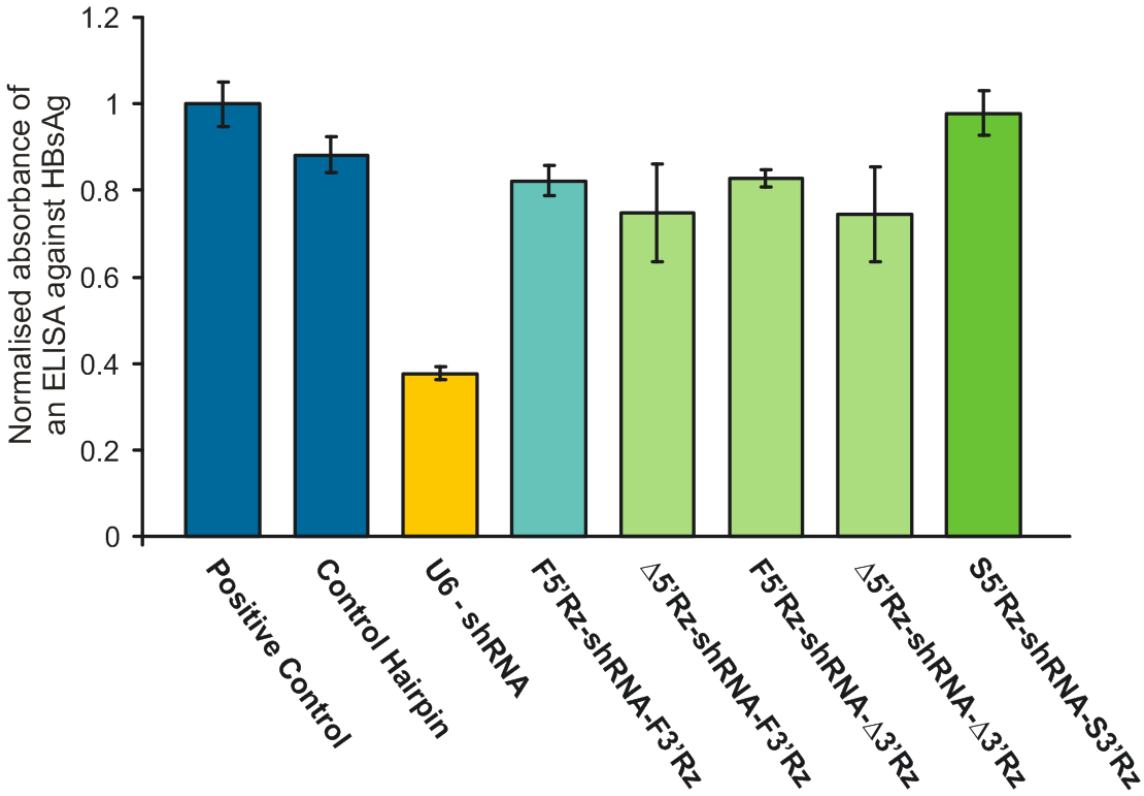

Figure 3. 11: A normalized ELISA against HBsAg of RyPS against live HBV.

Huh7 cells were transfected with a replication competent HBV plasmid (pCH3091). Similar to the luciferase assay, knockdown of HBsAg was assessed to validate RyPS efficacy. The positive control contained no forms of exogenous RNAi molecules, while the negative control contained a shRNA driven by the U6 promoter targeted against LacZ. U6 RyPS hairpin produces a shRNA similar to that of RyPS, however, is generated of a U6 promoter. The various prefixes denote the following: S – slow/minimal ribozyme, F – fast ribozyme and Δ – knockout mutant of that ribozyme. This data reinforces the lack of activity by the RyPS clone.

The data obtained from the HBsAg ELISA share similarities with the previous dual luciferase assay, confirming that the knockdown activity from RyPS does not occur. The shRNA produced against HBV has a 38% knockdown efficiency. This increased value may be owing to multiple factors, including transfection efficiency or the cells being swamped with live virus. Most importantly it is noted that the RyPS clones produce similar knockdown to the positive control, thus no form of significant knockdown did occur.

The lack of fast RyPS activity could be attributed to several factors, one of the more relevant being cleavage activity. It is not known whether RyPS is functional within a cellular environment. The original designers of the fast ribozyme within RyPS (Saksmerprome et al. 2004) created a chimaeric structure which would be able to increase the ribozymes activity *in vitro*. It was not tested within a cellular environment, however is assumed to function owing to the tertiary structure stability created by the extra-core elements. A complication in determining the reason for lack of RyPS activity is that it is not known if the ribozymes are cleaving in their intended sites. If the ribozymes cleave in a site other than the intended, the shRNA released cannot induce knockdown of its target, and may explain the lack of knockdown seen thus far. Combining this information, together with that of the *in vitro* cleavage data, it would appear that the incorrectly sized products are being released.

An important factor that required testing was RyPS activity within a cellular environment. This was required for several reasons, as the ribozyme was not a naturally occurring species and was a chimaeric structure. The required tertiary conformation for cleavage may not be met under cellular concentrations of divalent

magnesium ions. Another factor that may be preventing cleavage is that the ribozymes were locked within a system with strong secondary structures, particularly the shRNA which may affect their functioning. Cellular factors within the cell may affect folding, induce compartmentalization or degradation. All these factors may play a role in the lack of knockdown by RyPS. Testing the cleavage capabilities of RyPS within a cellular environment provided clarity whether the ribozymes were able to function. The RyPS was cloned within the dual luciferase system, and by monitoring knockdown, assessment was made on the activity of each the ribozymes in RyPS.

Assessment of intracellular ribozyme activity

To confirm that the ribozymes found in RyPS are functional within a cellular environment, the entire RyPS system was cloned into the MCS of psiCheck2.2, immediately downstream of the *Renilla* luciferase gene. Any ribozyme activity would result in the cleavage of the *Renilla* mRNA, leading to the loss of translational functioning. This would cause a decrease in *Renilla* fluorescence and can be compared to a non-cleaved control, Δ5'Δ3'Rz RyPS, which kept the mRNA intact. This system is described in Figure 2.6, illustrating the basic experimental procedure.

Cleavage of the mRNA strand by a ribozyme will cause the transcript to be prone to degradation by intracellular RNases. Thus any knockdown observed can be accounted for by ribozyme cleavage. Hek293 cells were transfected with each species of *Renilla* luciferase-RyPS, and knockdown of *Renilla* was assessed after 48 hours. In Figure 3.12, the non-cleaving knockout, 5'ΔFRz – shRNA – 3'ΔFRz (Δ5'Δ3'Rz RyPS) was used as the normalizing non-cleaving control, as it is known that no cleavage will occur with that variant, even within *in vitro* environments which are most conducive to ribozyme cleavage. The data indicated that the minimal/slow RyPS behaves in a manner similar to Δ5'Δ3'Rz RyPS, unable to function within a cellular environment. These data, together with the data from the dual luciferase and ELISA indicate that the minimal RyPS has no cellular functioning.

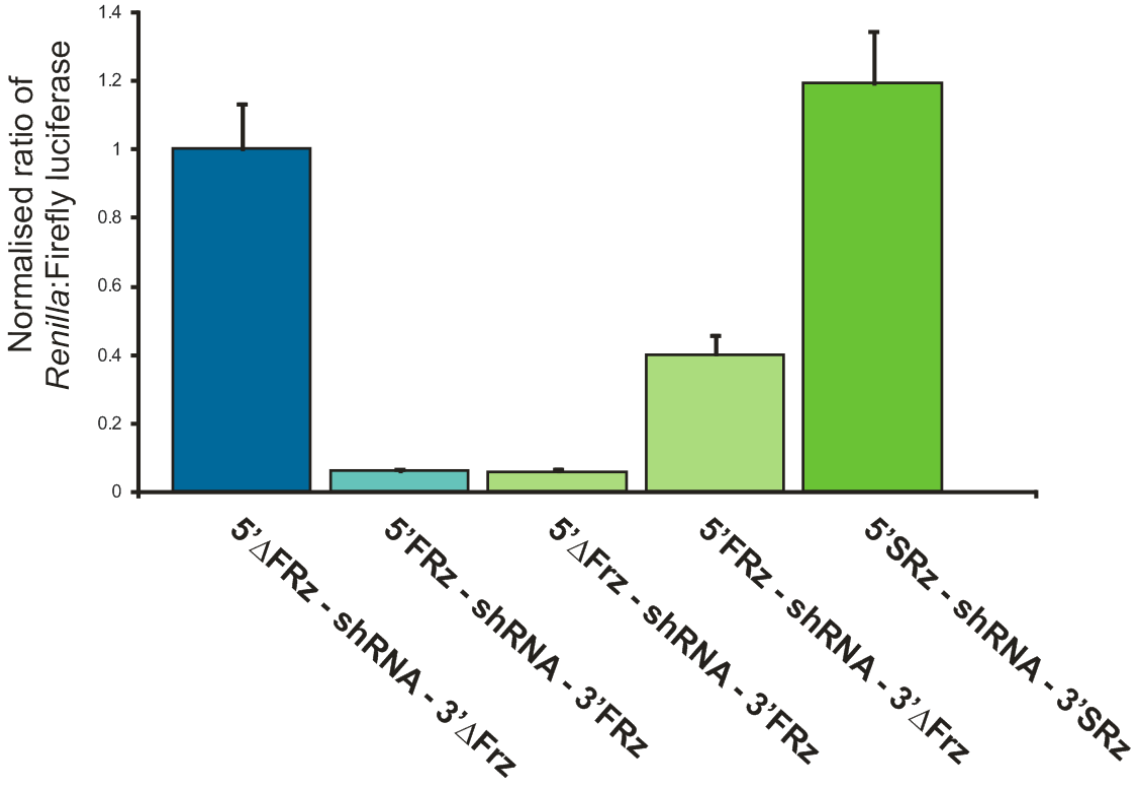

Figure 3. 12: A normalized ratio of *Renilla*:Firefly dual luciferase assay, in detection of RyPS ribozyme intracellular activity.

Cleavage activity of any of the ribozymes would result in *Renilla* luciferase mRNA degradation and less fluorescence, as compared to the internal Firefly luciferase control. The clone containing 5'ΔFRz – shRNA – 3'ΔFRz (Δ5'Δ3'Rz RyPS) was used as the normalizing control, since it is known that it is completely non-functional. This was followed by a functional RyPS (5'FRz – shRNA – 3'FRz), then the Δ5'Rz RyPS (5'ΔFRz – shRNA – 3'FRz) both causing greater than 90% knockdown. The Δ3'Rz RyPS (5'FRz – shRNA – 3'ΔFRz) is seen to cause 60% reduction in *Renilla* luciferase. The far right column contained the minimal RyPS system (5'SRz – shRNA – 3'SRz), and results in no knockdown of *Renilla*.

The data from Figure 3.12 indicate that all the fast ribozymes function. RyPS and Δ5' ribozyme RyPS share similar knockdown values, indicating that the knockdown generated was owing to the activity of the 3' ribozyme. When cleavage was solely dependent on the 5' ribozyme (Δ3'Rz RyPS), 60% was achieved indicating that the 5' ribozyme is less effective at cleavage compared to the 3' ribozyme. The decreased amount of cleavage from the 5' ribozyme cannot account for a complete lack of knockdown in the ELISA and luciferase RyPS-RNAi based studies. At 60% functionality some form of knockdown should still be seen, which raises two concerns. Initially why is RyPS incapable of causing knockdown of its target, and secondly why the 5' ribozyme has less functionality than its 3' counterpart, as both ribozymes are essentially structurally similar. The data collected thus far indicates that RyPS is a catalytically active molecule, however the *in vitro* transcriptions indicated ribozyme cleavage does not occur as anticipated, and is most likely cleaving in regions other than the designated cleavage triplets.

The predicted secondary structure generated from a nucleotide modelling engine available online, gave some indication why the 5' ribozyme only produced 60% activity in the RyPS-luciferase experiments.

Predictive modelling of RyPS secondary structure

Predictive modelling is useful in determining general conformations taken by molecules in a set environment. With this information possible monomer-monomer interactions can be analyzed, as well as any topological information generated. Typically a nucleotide folding program provides information on the possible base pairing combinations, as well as the most stable structural forms that are likely to occur. mFold (http://frontend.bioinfo.rpi.edu/applications/mfold/cgi-bin/rna-form1.cgi) is a web-based RNA folding program, whereby input of a particular RNA sequence allows for the prediction of its multiple secondary structures, arranged in accordance to the overall molecule stability, noted by ΔG (Gibbs 1876). The RNA sequence of RyPS was analyzed and the most favourable structure to form was comparatively similar to that of the intended structure, depicted in Figure 3.13. Within the RyPS structure, the component forming the shRNA has taken preference to form over that of the ribozymes because of the strong innate hairpin secondary structure. It appears that the 3' ribozyme is structurally unaffected, as stem III remains intact, and extra-core elements within stems I and II remain unaffected. The data in Figure 3.12 correlated to the activity of the 3' ribozyme as the predictive modelling suggested. However, modelling also predicted that the 5' ribozyme structure was affected by the secondary structure of the shRNA, and this led to stem I on the 5' ribozyme not forming the 5'-UAA-3' bulge required for enhanced cleavage activity. Not all activity ribozyme was lost, suggesting that the 5' ribozyme had a form of stabilized tertiary structure, albeit weaker and was not as effective in

maintaining a tertiary structure required for cleavage. The two proposed secondary structures are schematically drawn in Figure 3.13., both comparing the differences caused by the shRNA of the intended structure and the predicted structure.

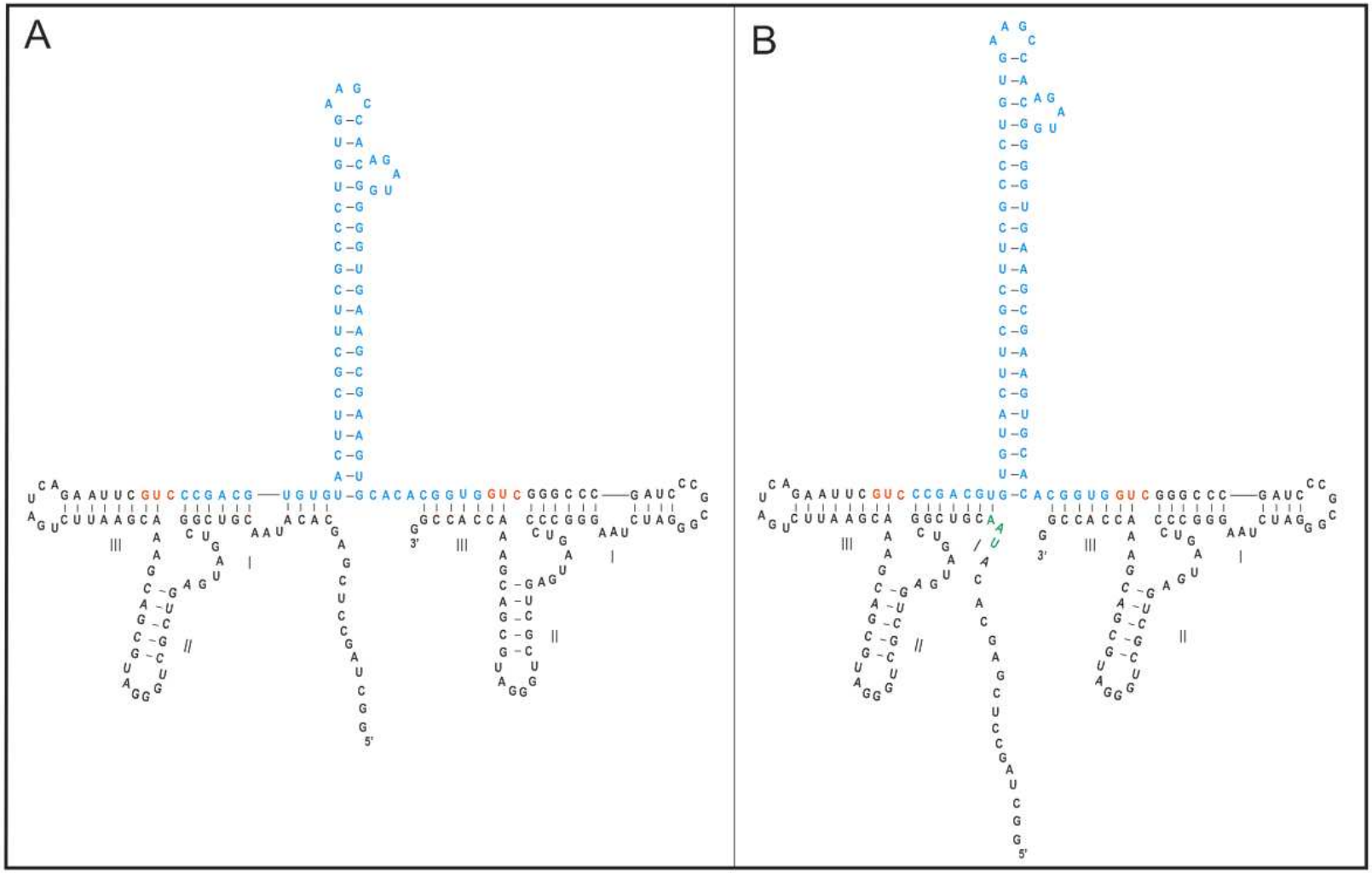
A
B

Figure 3. 13: Intended and predicted structures of RyPS.

The original ideal structure for RyPS is shown by **A**, however when analysed with RNA folding software, it was found that **B** had a preference of forming. A mis-formed region in B is highlighted in green (UAA), which is known to increase the cleavage efficiency of the ribozyme. The blue region contains the nucleotides that form the shRNA, the black nucleotides indicate the flanking ribozymes (5' ribozyme on the left, 3' ribozyme on the right), and the red nucleotides indicate the cleavage triplets (GUC) on each of the ribozymes.

The stabilization of the hairpin disrupted one of the most crucial elements required by the 5' ribozyme for its enhanced functioning. This could most likely account for the 60% cleavage efficiency when Δ3' ribozyme RyPS was cloned into psiCheck2.2 (Figure 3.12). This disruption is not completely inhibitory of cleavage, and the 5' ribozyme still maintains cleavage activity, albeit less. This is thought to occur as a result of the dynamic nature of RNA which is by no means a static structure, and is structurally dynamic. At any one instant the favourable cleavage conformation may occur, which will allow for the activity of the 5' ribozyme. Furthermore, the three nucleotides responsible for the bulge may still provide a basis for tertiary structure stabilisation however, a less stable system forms.

Data taken from the previous experiments indicated that RyPS had cleavage activity within an *in vitro* and cellular environment. However, as indicated by the *in vitro* transcriptions data RyPS behaved in an unexpected manner, generating products incapable of performing their intended function. The following set of data gave a clear indication of the species produced during *in vitro* transcriptions, which suggested that the unintended malformation of the 5' ribozyme had little effect on the products produced from ribozyme cleavage.

Topography of the template as well as the product may have an influence on the functioning of T7 polymerase which is responsible for RNA generation in all the *in vitro* transcription reactions. Small loops and sequence motifs are known to influence polymerases, such as additional start and stops sites, or binding motifs, however, this is an unlikely cause to the truncations of the RyPS products. When

tested in cell culture, human polymerases are also unable to transcribe a product capable of inducing target knockdown, suggesting that a similar product is being formed either using a T7 bacterial promoter or the mammalian CMV promoter.

Determination of RyPS cleavage sites: Primer extension reactions

It was established that the shRNA produced was not what was intended and was far smaller than expected. There are only two factors which could play a role in the generation of the shRNA. The first was the 5' ribozyme, which according to size correlations appeared to be correctly sized. The second was the 3' ribozyme, and from size comparisons appeared to be smaller than the predicted size. These data indicate that one of the ribozymes (or both) is responsible for generating products unfit for inducing the RNAi response. Establishing the site of cleavage would confirm that aberrant cleavage has taken place and would provide some explanation to mechanism of the RyPS cleavage and perhaps explain the mis-cleavage results obtained. Primer extension reactions can provide accurate information as to where a target oligonucleotide starts. To clarify the exact site of cleavage, a concurrent sequencing reaction was performed, in which sequencing information directly correlated to the primer extension data owing to the common start primer used.

A primer extension reaction was performed on non radioactive RNA generated by *in vitro* transcription. Radio isotope-labelled DNA primers were designed to bind downstream of the 5' and 3' ribozyme cleavage sites, and when

subjected to reverse transcription the primer would be extended until the polymerase falls off the RNA template. A sequencing reaction was performed using the same primers, on a DNA template (plasmid origin). Thus for every base added in the sequencing reaction, it is matched by the reverse transcription reaction. Therefore, at the point where the reverse transcriptase falls off the template RNA, these data would correlate to the base at which cleavage occurred on the sequencing control. Figure 2.10 explains the overall methodology used to determine the cleavage sites of RyPS.

The 5' ribozyme cleavage site was analyzed by having the probe bind to the shRNA. This would have extended to the start of the shRNA molecule, and would indicate the end of the 5' ribozyme (and hence the cleavage site). Figure 3.14 depicts that the primer extension data showed that the 5' ribozyme was able to successfully form a structure capable of cleaving at the desired cleavage triplet. Thus it is assumed that the 5' ribozyme in any of the *in vitro* data sets is the correct size (75 bases). This occurs despite the bulge on stem I not forming correctly, suggesting that the 5' ribozyme retains some form of correct cleavage activity.

Analysis of the cleavage data of the 3' ribozyme showed that cleavage did not occur at the desired triplet, and did so at another site downstream of the proposed cleavage triplet illustrated in Figure 3.14. The exact site of cleavage cannot be confirmed, however is estimated to occur just before the UAA bulge motif of stem I. For this to occur, the 3' ribozyme would have to fold into a structure capable of fully supporting the highly conserved cleavage pocket, as well as provide some form of stability required during cleavage. Predictive RNA folding has shown that it is

unlikely for any form of structure to be produced in order to allow for cleavage as proposed by the primer extension data.

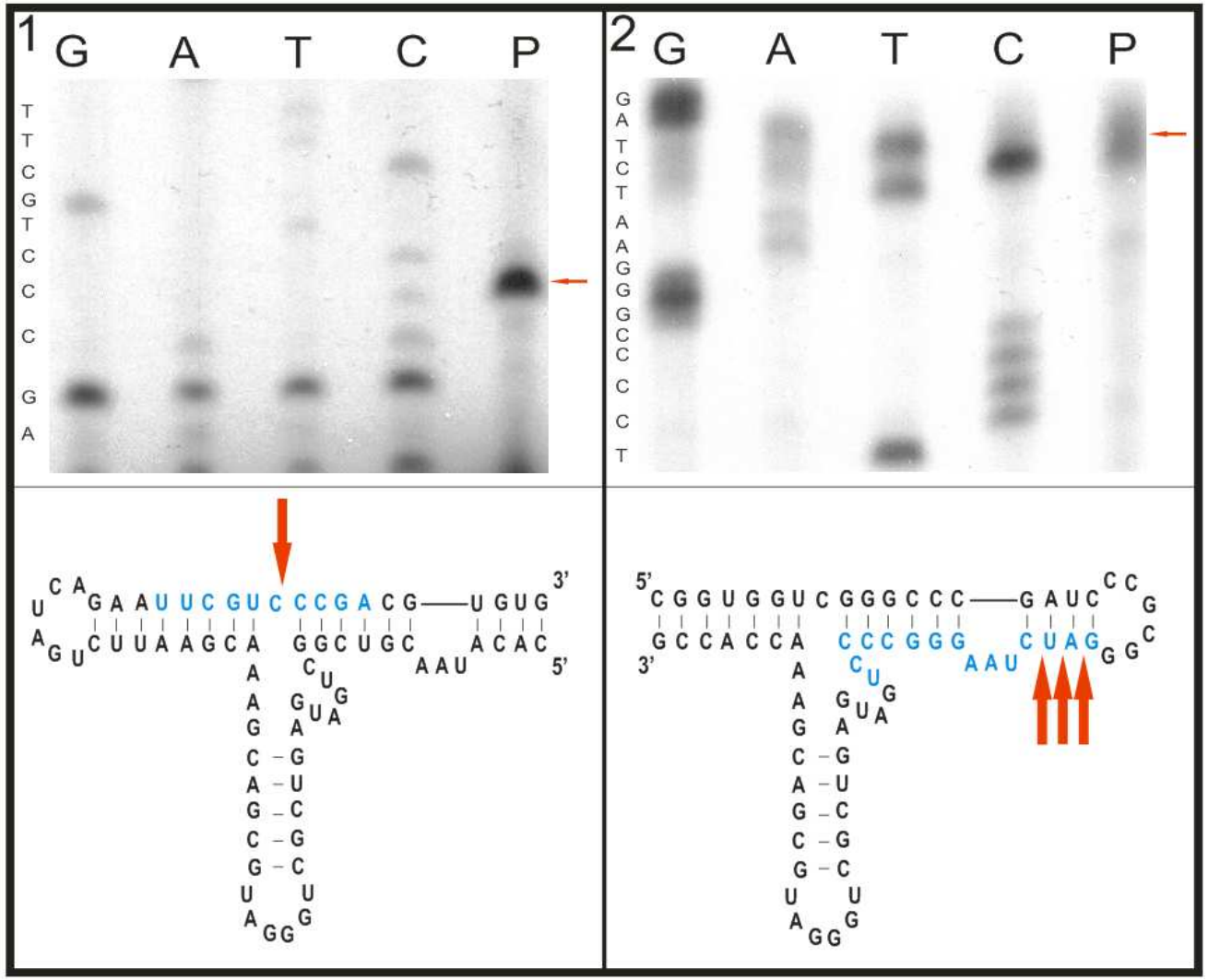
1
G
A
T
C
P
TTCGTCCCCGA
2
G
A
T
C
P
GATCTAAGGGGCCCCCT
5'
3'
3'
5'

Figure 3. 14: Primer extension reactions together with sequencing data indicate the region of cleavage caused by each of the ribozymes.

Lanes G, A, T and C provide sequencing data of the regions around the 5’ and 3’ ribozyme cleavage triplet. In panel 1, Lane P contains the primer extension product, and its termination correlates to after the GTC cleavage triplet of the 5’ ribozyme. In Panel 2, the primer extension reaction (Lane P) accompanied with sequencing data indicate the region of cleavage within stem I of the 3’ ribozyme, downstream of the predicted ribozyme cleavage site, indicative of aberrant cleavage. Below each respective panel is a mapped site of both the 5’ and 3 ribozymes. The 5’ ribozyme is mapped to cleave after the GUC cleavage triplet. The 3’ ribozyme is mapped to cleave within stem I, near the 5’-UAA-3’ bulge.

It would appear that the 5’ ribozyme cleaves in the predicted region, releasing the shRNA at the correct point. The 3’ ribozyme however does not cleave at the correct site, and would produce a hairpin larger than expected. This does not correlate with the data previously shown in the northern blots, thus it is thought that the 3’ ribozyme cleaves in multiple regions of the RyPS. The event of additional processing may be the most likely cause of the smaller RyPS products. It is assumed that the 5’ ribozyme is unaffected by potential additional processing, confirmed by both the primer extension reactions and northern blots and it is seen that the 5’ ribozyme is of the predicted size. However it is found that the shRNA generated is far smaller than what is required and expected, and cannot possibly function as an RNAi molecule. The dilemma occurs because the 3’ ribozyme, if processing further up stream into the shRNA, should be far larger than it appears on the northern blot. The 3’ ribozyme appears smaller than its expected size (88 bases), and is a similar size to the 5’ ribozyme (approximately 78 bases). This would indicate that a form of additional processing is occurring by the ribozymes, or that the polymerase is prematurely releasing from the DNA template, hence the additional bands seen around the 3’ ribozymes after *in vitro* transcriptions (results Figure 3.3 and 3.6). It is unclear whether the components of RyPS would have a propensity bind to each other, as secondary structure analysis shows little extra interaction between the ribozymes and short hairpin. Searching for potential binding sites with complementary sequence alignment tools has yielded no results either. It is postulated however, that it only requires a cleavage triplet NUH (possibly even NHH) and enough stable binding in stems I and III to allow for tertiary structure stability, and cleavage could occur. This

event may occur on the shRNA, allowing the antisense strand to be cleaved, which is unlikely, and the stability of the shRNA would not allow for partial binding by any of the ribozymes.

Ultimately it is unknown which ribozyme causes the additional cleavage of the shRNA, however further investigation may shed some light on the matter. Using the primer extension reaction, and using a series of primers that tile upstream from the 3' ribozyme, one should be able to determine whether the 3' ribozyme be truncated in any manner. It is thought that the 5' ribozyme is not responsible for the decreased size of the 3' ribozyme, because when it is knocked-out in control clones, a similar 3' ribozyme product forms in comparison to the functional RyPS (Figure 3.6), thus factors other than the 5' ribozyme are responsible for its truncation. It is not known which ribozyme is involved in the truncation of the shRNA.

The cleavage triplet in hammerhead ribozymes which allows for the greatest rate of cleavage has been defined as NUH, which is present in multiple forms around the stem I bulge, and could provide a putative cleavage site. Some groups have broadened this definition to NHH, which greatly increases the potential cleavage sites around the bulge on stem one of the 3' ribozyme. However cleavage at that point is very unlikely to occur, owing to the fact that the ribozyme structure is too unstable to utilize any of the nucleotides around the bulge as a cleavage site. Should cleavage occur as predicted by the primer extensions, the RyPS products would have the following sizes: 5' ribozyme - 75 nucleotides, shRNA - 87 (69 + 18) nucleotides and

3’ ribozyme - 70 (88 – 18) nucleotides. This is known not to be true, as the northern blot studies have proven otherwise (first demonstrated by the ethidium bromide stain of RyPS and the knockout clones prior to blotting). The cleavage site indicated by the primer extension is thought to be incorrect, as no other 3’ ribozyme products support this data in the northern blot analysis. The product produced during 3’ ribozyme primer extension is most likely an artefact of the reaction, or is the result of additional processing performed by either the 5’ ribozyme or 3’ ribozyme.

One concern was the lack of adherence of the cleavage products to the predicted sizes. RNA ladders were tried with little success, often resulting in double and faint bands, unrelated to the condition of the RNA. Thus the analysis of the knockout mutants gave an indication of which products are present in the autoradiograph. In both autoradiograph figures, it is seen that the expected size of the hairpin (69), the 5’ribozyme (75) and 3’ ribozyme (88) were not observed, and that one of the products (or both potentially) are differently sized. There are myriad possibilities as to why the RyPS system does not function as expected, the most feasible being structure and additional processing. It is known that both the 5’ and 3’ ribozymes are functional within a cellular environment (up to 90%), as seen using RyPS downstream of *Renilla* luciferase in Figure 3.12 in the results section. RyPS ribozyme cleavage is highly active within the cellular environment, demonstrating that the faster ribozymes cleave within that environment. As expected the slow RyPS is unable to induce knockdown of *Renilla*, indicating that those minimal ribozymes do not function within the cellular environment.

Disruption of the bulge on stem I has its effect on ribozyme cleavage. This disruption was first noticed in secondary structure analysis using the internet based program m-fold. In this it was predicted that the shRNA within the structure takes preference in forming, causing a shorter stem I of the 5' ribozyme (Figure 3.13). This disrupts the bulge on stem I, which is responsible for the tertiary structure stabilization, and is assumed to be responsible for decreased cleavage. This was shown by the 3' ribozyme RyPS knockout, whereby cleavage of the *Renilla* luciferase mRNA was solely dependent on the 5' ribozyme, which had a mis-formed bulge on stem I. Furthermore is it assumed that it is a requirement for extra-core elements to be stable in structure, allowing for an increase in cleavage.

It is speculated that an additional cleavage reaction is taking place on the shRNA, as it is far smaller than the originally predicted size of 69 bases. Furthermore the 3' ribozyme is smaller than anticipated (< 88 bases) in the region of 8-10 bases. It is unknown what the causes are to these truncated products. One may suggest that additional cleavage is occurring, whereby the ribozymes are able to recognize additional elements other than the predicted cleavage site, and are able to form the tertiary structures required for cleavage to occur. Alternatively, the plasmid template may have become truncated during the cloning process. This is owing to the high frequency of secondary structure in the DNA and is known not to be found favourable in bacterial genomes, and is often excised, however this is unlikely as the knockout clones are able to generate similar products to the functional RyPS.

Ultimately, cleavage is sequence dependent, and a change of shRNA within the cassette will provide a different sequence and may prevent its truncation. Sequence complementarity between the ribozymes and certain sections of the shRNA will need to be avoided, to prevent any unintended cleavage occurring. One may also consider revising the hammerhead ribozymes used. The ribozymes used in RyPS are an adaptation of the peach latent mosaic viroid (PLMVd) hammerhead ribozyme, and a more naturally occurring ribozyme may provide a better predictable cleavage, since it has to function naturally without compromising viral replication. In addition to ribozyme exchange, disruption of the bulges on stem I should be avoided, caused by the secondary structure of the shRNA.

One potential means of overcoming the disruption of the bulge on stem I, is to make it independent of binding to the shRNA. This was done using ribozyme derived from satellite tobacco ringspot virus (sTRSV) by Nelson et al. 2005. They created a hammerhead ribozyme with a looped stem I, which is independent from other ribozyme elements. If incorporated into the RyPS system, a diagrammatic representation of the secondary structure is shown in Figure 3.15.

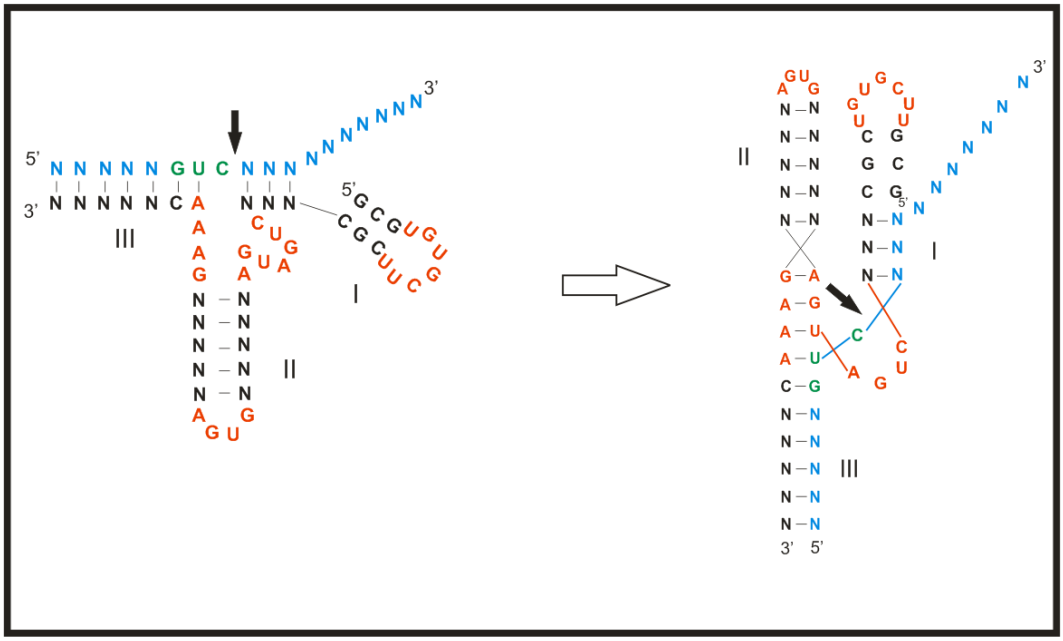

Figure 3. 15: A schematic representation of the possible adaptation to the currently used ribozymes in RyPS.

This new version avoids disruption of extra core elements, by the shRNA, allowing for the formation of the loop I loop II kissing interaction.

RyPS usage extends beyond HBV treatment to the treatment of other diseases including cancer, viruses and autosomal diseases. Another benefit of the system is synthetic RNA production, which would require the replicative properties of T7 polymerase, which is also far cheaper to produce than the current methods employed for this. However, the greatest benefit of RyPS is the tissue-specific inducible expression of a shRNA. Pol II promoters will allow for the systemic delivery of RyPS, however will only be effective in targeted tissues. The level of expression of RyPS can be controlled and regulated, as it is unnecessary to mass produce RNAi therapeutic molecules intracellularly, and as shown by some groups has led to cell

death. Furthermore, RyPS offers the potential to be expressed from a single Pol II promoter as a concatemer of RyPS sequences, all containing various shRNA molecules, decreasing the chance for escape mutants developing. Ultimately RyPS requires further thorough analysis of potential intra- and inter-binding activity, typically in the form of various hammerhead ribozyme species, shRNA species and combinations of both. Understanding that as little cross reactivity must occur between individual RyPS components will help lessen the occurrence of unintended cleavage products. If this can be accomplished, RyPS stands great potential to be developed into a therapeutic molecule for use in countries that can no longer depend on expensive unstable drugs.

Appendices

Appendix 1

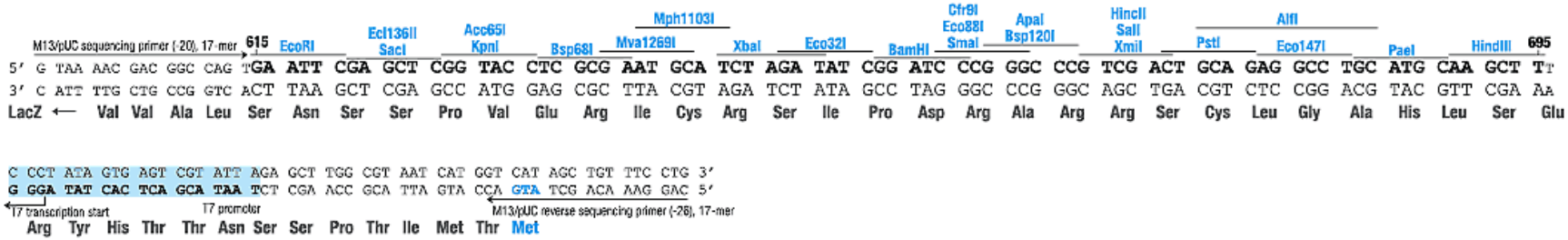

Figure A1: The multiple cloning site (MCS) is shown, flanked by the M13F/R sites. Restriction sites are unique within the MCS and are cut by enzymes shown in blue. DNA fragment insertion occurs at the *Eco32I* site during T/A cloning. This figure is taken from the user notes on pTZ57R.

Appendix 2

6x Agarose DNA Loading Dye

0.03% (w/v) Xylene cyanol FF

0.015% (w/v) Orange G

60% Glycerol

60 mM EDTA

Boric Acid Buffer for electrophoresis

10 mM Sodium hydroxide

pH to 8.5 with boric acid

Ethidium bromide stock (100 x)

100 mg EtBr dissolved in 10 ml distilled water, stored at room temperature.

LB broth and plates supplemented with ampicillin

10 g Bacto-Tryptone

5 g Bacto-Yeast Extract

5 g Sodium Chloride

1 ml 1000x ampicillin stock

Up to 1 L distilled water

To make agar plates, add 12 g agar

Ampicillin stock (1000x)

50% (w/v) Ampicillin

50% (v/v) distilled water

50% (v/v) ethanol

IPTG and X-Gal stocks

200 mg IPTG per 1ml distilled water

20 mg X-Gal per1ml dimethyl formamide

10x TBE buffer (pH 8)

0.685 M Tris-HCl

0.8895 M Boric Acid

0.02 M EDTA

Denaturing polyacrylamide gel (10%)

8 M Urea

0.5% (w/v) Bis-acrylamide

9.5% (w/v) Acrylamide

1x TBE

0.05% (v/v) TEMED

0.5% (v/v) Ammonium persulphate stock

Ammonium persulphate (APS) stock

100 mg APS in 1 ml distilled water

Phosphate-buffered saline

0.21 g KH_2PO_4

9 g NaCl

0.726 g $Na_2HPO_4.7H_2O$

Made up to 1 L and autoclaved

RNase free water

1 ml DEPC in 1 L of water

Incubate overnight at 37°C and autoclave the following day.

Appendix 3

It should be noted that any reactions involving the use/generation of RNA should be done as RNase free as possible. The environment one generally works in contains a variety of species of RNases, particularly those shed by humans. RNases are generally difficult to get rid of, and special precautions need to be taken to ensure the best quality RNA is produced. Gloves should be worn at all times, ensuring that they are sprayed with 70% ethanol intermittently, as well as an RNase degrading soap (such as RNase-Away). Instruments such as glass wear and spatulas should be washed with 1% SDS solution and rinsed with DEPC treated water, covered in foil and a standard autoclave procedure performed. All surfaces should be cleaned with an RNase degrading substance (1% SDS solution can be used). It is advisable to wear a face mask, to prevent aerosols entering the reaction environment. Any components to a reaction should be RNase free, including the water used and any chemical added. It is suggested to use chemicals separated from general lab use. Any large volumes of water that need to be used (such as water used for buffers) should be treated with DEPC first.

References

Akashi H, Matsumoto S, Taira K (2005) Gene discovery by ribozyme and siRNA libraries. Nat Rev Mol Cell Biol 6(5): 413-422.

Aravin AA, Naurnova NM, Tulin AV, Vagin VV, Rozovsky YM et al. (2001) Double-stranded RNA-mediated silencing of genomic tandem repeats and transposable elements in the D. melanogaster germline. Current Biology 11(13): 1017-1027.

Barichievy S, Saayman S, von Eije KE, Morris KV, Arbuthnot P et al. (2007) The Inhibitory Efficacy of RNA POL III-Expressed Long Hairpin RNAs Targeted to Untranslated Regions of the HIV-1 5' Long Terminal Repeat. Oligonucleotides 17(4): 419-432.

Bartel DP (2004) MicroRNAs: Genomics, Biogenesis, Mechanism, and Function. Cell 116: 281-297.

Basyuk E, Suavet F, Doglio A, Bordonne R, Bertrand E (2003) Human let-7 stem-loop precursors harbor features of RNase III cleavage products. Nucl Acids Res 31(22): 6593-6597.

Blount KF, Uhlenbeck OC (2005) The Structure Function Dilemma of the Hammerhead Ribozyme. Annu Rev Biophys Biomol Struct 34: 415-440.

Bohnsack MT, Czaplinski K, Gorlich D (2004) Exportin 5 is a RanGTP-dependent dsRNA-binding protein that mediates nuclear export of pre-miRNAs. RNA 10(2): 185-191.

Bratty J, Chartrand P, Ferbeyre G, Cedergren R (1993) The hammerhead RNA domain, a model ribozyme. Biochimica et Biophysica Acta 1216: 345-359.

Brody E, Abelson J (1985) The "spliceosome": yeast pre-messenger RNA associates with a 40S complex in a splicing-dependent reaction. Science 228(4702): 963-967.

Buzayan JM, Hampel A, Bruening G (1986) Nucleotide sequence and newly formed phosphodiester bond of spontaneously ligated satellite tobacco ringspot virus RNA. Nucl Acids Res 14(24): 9729-9743.

Cai X, Hagedorn CH, Cullen BR (2004) Human microRNAs are processed from capped, polyadenylated transcripts that can also function as mRNAs. RNA 10(12): 1957-1966.

Canny MD, Jucker FM, Pardi A (2007) Efficient Ligation of the Schistosoma Hammerhead Ribozyme. Biochemistry 46(12): 3826-3834.

Carmona S, Ely A, Crowther C, Moolla N, Salazar FH et al. (2006) Effective Inhibition of HBV Replication in Vivo by Anti-HBx Short Hairpin RNAs. Mol Ther 13(2): 411-421.

Clouet-D'Orval B, Uhlenbeck OC (1996) Kinetic characterization of two I/II format hammerhead ribozymes. RNA 2(5): 483-491.

Dange V, Van Atta RB, Hecht SM (1990) A Mn2(+)-dependent ribozyme. Science 248(4955): 585-588.

Daros JA, Flores R (1995) Identification of a Retroviroid-Like Element from Plants. Proceedings of the National Academy of Sciences 92(15): 6856-6860.

De la PenÄ M, Gago S, Flores R (2003) Peripheral regions of natural hammerhead ribozymes greatly increase their self-cleavage activity. The EMBO Journal 22(20): 5561-5570.

Denli AM, Tops BBJ, Plasterk RHA, Ketting RF, Hannon GJ (2004) Processing of primary microRNAs by the Microprocessor complex. Nature 432(7014): 231-235.

Dykxhoorn DM, Lieberman J (2006) Knocking down Diseases with siRNAs. Cell 126: 231-235.

Epstein LM, Gall JG (1987) Self-cleaving transcripts of satellite DNA from the newt. Cell 48(3): 535-543.

Faehnle CR, Joshua-Tor L (2007) Argonautes confront new small RNAs. Curr Opin Chem Biol 11(5): 569-577.

Fagard M, Boutet S, Morel J-B, Bellini C, Vaucheret H (2000) AGO1, QDE-2, and RDE-1 are related proteins required for post-transcriptional gene silencing in plants, quelling in fungi, and RNA interference in animals. Proceedings of the National Academy of Sciences 97(21): 11650-11654.

Ferbeyre G, Smith JM, Cedergren R (1998) Schistosome Satellite DNA Encodes Active Hammerhead Ribozymes. Mol Cell Biol 18(7): 3880-3888.

Fire A, Albertson D, Harrison SW, Moerman DG (1991) Production of antisense RNA leads to effective and specific inhibition of gene expression in C. elegans muscle. Development 113(2): 503-514.

Fire A, Xu S, Montgomery MK, Kostas SA, Driver SE et al. (1998) Potent and specific genetic interference by double-stranded RNA in Caenorhabditis elegans. Nature 391(6669): 806-811.

Forster AC, Symons RH (1987) Self-cleavage of virusoid RNA is performed by the proposed 55-nucleotide active site. Cell 50(1): 9-16.

Gibbs JW (1876) On the Equilibrium of Heterogeneous Substances. Trans Connect Acad 3: 108-248.

Gitlin L, Karelsky S, Andino R (2002) Short interfering RNA confers intracellular antiviral immunity in human cells. Nature 418(6896): 430-434.

Gregory RI, Yan K-p, Amuthan G, Chendrimada T, Doratotaj B et al. (2004) The Microprocessor complex mediates the genesis of microRNAs. Nature 432(7014): 235-240.

Grimm D, Streetz KL, Jopling CL, Storm TA, Pandey K et al. (2006) Fatality in mice due to oversaturation of cellular microRNA/short hairpin RNA pathways. Nature 441: 537-541.

Grishok A, Tabara H, Mello CC (2000) Genetic Requirements for Inheritance of RNAi in C. elegans. Science 287(5462): 2494-2497.

Grishok A, Pasquinelli AE, Conte AE, Li N, Parrish S et al. (2001) Genes and Mechanisms Related to RNA Interference Regulate Expression of the Small Temporal RNAs that Control C. elegans Developmental Timing. Cell 106: 23-24.

Guerrier-Takada C, Gardiner K, Marsh T, Pace N, Altman S (1983) The RNA moiety of ribonuclease P is the catalytic subunit of the enzyme. Cell 35: 849-857.

Han J, Burke JM (2005) Model for General Acid-Base Catalysis by the Hammerhead Ribozyme: pH-Activity Relationships of G8 and G12 Variants at the Putative Active Site. Biochemistry 44: 7864-7870.

Han J, Lee Y, Yeom K, Nam J, Heo I et al. (2006) Molecular Basis for the Recognition of Primary microRNAs by the Drosha-DGCR8 Complex. Cell 125: 887-901.

Haseloff J, Gerlach WL (1989) Sequences required for self-catalysed cleavage of the satellite RNA of tobacco ringspot virus. Gene 82(1): 43-52.

Hertel KJ, Herschlag D, Uhlenbeck OC (1994) A kinetic and thermodynamic framework for the hammerhead ribozyme reaction. Biochemistry 33(11): 3374-3385.

Hertel KJ, Pardi A, Uhlenbeck OC, Koizumi M, Ohtsuka E et al. (1992) Numbering system for the hammerhead. Nucl Acids Res 20(12): 3252-.

Hutchins CJ, Rathjen PD, Forster AC, Symons RH (1986) Self-cleavage of plus and minus RNA transcripts of avocado sunblotch viroid. Nucl Acids Res 14(9): 3627-3640.

Hutvagner G, McLachlan J, Pasquinelli AE, Balint E, Tuschl T et al. (2001) A Cellular Function for the RNA-Interference Enzyme Dicer in the Maturation of the let-7 Small Temporal RNA. Science 293(5531): 834-838.

Izant JG, Weintraub H (1984) Inhibition of thymidine kinase gene expression by antisense RNA: a molecular approach to genetic analysis. Cell 36: 1007-1015.

Jackson AL, Bartz SR, Schelter J, Kobayashi SV, Burchard J et al. (2003) Expression profiling reveals off-target gene regulation by RNAi. Nat Biotech 21(6): 635-637.

Jeffries AC, Symons RH (1989) A catalytic 13-mer ribozyme. Nucl Acids Res 17(4): 1371-1377.

Judge AD, Sood V, Shaw JR, Fang D, McClintock K et al. (2005) Sequence-dependent stimulation of the mammalian innate immune response by synthetic siRNA. Nat Biotech 23(4): 457-462.

Karpala AJ, Doran TJ, Bean AGD (2005) Immune responses to dsRNA: Implications for gene silencing technologies. Immunol Cell Biol 83(3): 211-216.

Khvorova A, Reynolds A, Jayasena SD (2003a) Functional siRNAs and miRNAs Exhibit Strand Bias. Cell 115: 209-216.

Khvorova A, Lescoute A, Westhof E, Jayasena S (2003b) Sequence elements outside the hammerhead ribozyme catalytic core enable intracellular activity. Nature Structural Biology 10: 708-712.

Kisseleva N, Khvorova A, Westhof E, Schiemann O (2005) Binding of manganese(II) to a tertiary stabilized hammerhead ribozyme as studied by electron paramagnetic resonance spectroscopy. RNA 11(1): 1-6.

Kok KH, Ng M-HJ, Ching Y-P, Jin D-Y (2007) Human TRBP and PACT Directly Interact with Each Other and Associate with Dicer to Facilitate the Production of Small Interfering RNA. J Biol Chem 282(24): 17649-17657.

Kruger K, Grabowski PJ, Zaug AJ, Sands J, Gottschling DE et al. (1982) Self-splicing RNA: Autoexcision and autocyclization of the ribosomal RNA intervening sequence of tetrahymena. Cell 31(1): 147-157.

Lambert D, Heckman JE, Burke JM (2006) Three Conserved Guanosines Approach the Reaction Site in Native and Minimal Hammerhead Ribozymes†. Biochemistry 45: 7140-7147.

Lee L, Jeon K, Lee J, Kim S, Kim VN (2002) MicroRNA maturation: stepwise processing and subcellular localization. EMBO J 21(17): 4663-4670.

Lee Y, Hur I, Park S, Kim Y-K, Suh MR et al. (2006) The role of PACT in the RNA silencing pathway. EMBO J 25(3): 522-532.

Lee Y, Ahn C, Han J, Choi H, Kim J et al. (2003) The nuclear RNase III Drosha initiates microRNA processing. Nature 425(6956): 415-419.

Li M, Li H, Rossi JJ (2006) RNAi in Combination with a Ribozyme and TAR Decoy for Treatment of HIV Infection in Hematopoietic Cell Gene Therapy. Ann NY Acad Sci 1082(1): 172-179.

Lian S, Fritzler MJ, Katz J, Hamazaki T, Terada N et al. (2007) Small Interfering RNA-mediated Silencing Induces Target-dependent Assembly of GW/P Bodies. Mol Biol Cell 18(9): 3375-3387.

Liu J, Valencia-Sanchez MA, Hannon GJ, Parker R (2005a) MicroRNA-dependent localization of targeted mRNAs to mammalian P-bodies. Nat Cell Biol 7(7): 719-723.

Liu J, Rivas FV, Wohlschlegel J, Yates JR, Parker R et al. (2005b) A role for the P-body component, GW182, in microRNA function. Nat Cell Biol 7(12): 1261-1266.

Liu J, Carmell MA, Rivas FV, Marsden CG, Thomson JM et al. (2004) Argonaute2 Is the Catalytic Engine of Mammalian RNAi. Science 305(5689): 1437-1441.

Lott WB, Pontius BW, von Hippel PH (1998) A two-metal ion mechanism operates in the hammerhead ribozyme-mediated cleavage of an RNA substrate. Proceedings of the National Academy of Sciences 95(2): 542-547.

MacRae IJ, Ma E, Zhou M, Robinson CV, Doudna JA (2008) In vitro reconstitution of the human RISC-loading complex. Proceedings of the National Academy of Sciences 105(2): 512-517.

MacRae IJ, Zhou K, Li F, Repic A, Brooks AN et al. (2006) Structural Basis for Double-Stranded RNA Processing by Dicer. Science 311(5758): 195-198.

Marques JT, Devosse T, Wang D, Zamanian-Daryoush M, Serbinowski P et al. (2006) A structural basis for discriminating between self and nonself double-stranded RNAs in mammalian cells. Nature Biotechnology 24(5): 559-565.

Martick M, Scott WG (2006) Tertiary Contacts Distant from the Active Site Prime a Ribozyme for Catalysis. Cell(126): 1-12.

Mello CC, Conte Jr D (2004) Revealing the world of RNA interference. Nature Genetics 431: 338-342.

Nassal M (1992) The arginine-rich domain of the hepatitis B virus core protein is required for pregenome encapsidation and productive viral positive-strand DNA synthesis but not for virus assembly. J Virol 66(7): 4107-4116.

Nelson JA, Shepotinovskaya I, Uhlenbeck OC (2005) Hammerheads Derived from sTRSV Show Enhanced Cleavage and Ligation Rate

Constants. Biochemistry 44: 14577-14585.

Patzel V, Rutz S, Dietrich I, Koberle C, Scheffold A et al. (2005) Design of siRNAs producing unstructured guide-RNAs results in improved RNA interference efficiency. Nature Biotechnology 23: 1440-1444.

Prody GA, Bakos JT, Buzayan JM, Schneider IR, Bruening G (1986) Autolytic Processing of Dimeric Plant Virus Satellite RNA. Science 231(4745): 1577-1580.

Proud GC (1995) PKR: anew name and new roles. Trends in Biochemical Sciences 20(6): 241-246.

Przybilski R, Graf S, Lescoute A, Nellen W, Westhof E et al. (2005) Functional Hammerhead Ribozymes Naturally Encoded in the Genome of Arabidopsis thaliana. Plant Cell 17(7): 1877-1885.

Rojas AA, Vazquez-Tello A, Ferbeyre G, Venanzetti F, Bachmann L et al. (2000) Hammerhead-mediated processing of satellite pDo500 family transcripts from Dolichopoda cave crickets. Nucl Acids Res 28(20): 4037-4043.

Romano N, Macino G (1992) Quelling: transient inactivation of gene expression in Neurospora crassa by transformation with homologous sequences. Mol Microbiol 6: 3343-3353.

Ruby JG, Jan CH, Bartel DP (2007) Intronic microRNA precursors that bypass Drosha processing. Nature 448(7149): 83-86.

Saksmerprome V, Roychowdhury-Saha M, Jayasena S, Khvorova A, Burke DH (2004) Artificial tertiary motifs stabilize trans-cleaving hammerhead ribozymes under conditions of submillimolar divalent ions and high temperatures. RNA 10: 1916-1924.

Salehi-Ashtiani K, Szostak JW (2001) In vitro evolution suggests multiple origins for the hammerhead ribozyme. Nature 414(6859): 82-84.

Saville BJ, Collins RA (1990) A site-specific self-cleavage reaction performed by a novel RNA in neurospora mitochondria. Cell 61(4): 685-696.

Schwarz DS, Hutvagner G, Du T, Xu Z, Aronin N et al. (2003) Asymmetry in the Assembly of the RNAi Enzyme Complex. Cell 115: 199-208.

Sharp PA (1987) Splicing of messenger RNA precursors. Science 235(4790): 766-771.

Sledz CA, Holko M, de Veer MJ, Silverman RH, Williams BRG (2003) Activation of the interferon system by short-interfering RNAs. Nat Cell Biol 5(9): 834-839.

Soldan SS, Plassmeyer ML, Matukonis MK, Gonzalez-Scarano F (2005) La Crosse Virus Nonstructural Protein NSs Counteracts the Effects of Short Interfering RNA. J Virol 79(1): 234-244.

Song E, Lee S, Wang J, Ince N, Ouyang N et al. (2003) RNA interference targeting Fas protects mice from fulminant hepatitis. Nature Medicine 9(3): 347-351.

Symons RH (1997) Plant pathogenic RNAs and RNA catalysis. Nucl Acids Res 25(14): 2683-2689.

Tabara H, Grishok A, C. Mello C (1998) REVERSE GENETICS:RNAi in C. elegans: Soaking in the Genome Sequence. Science 282(5388): 430-431.

Takagi Y, Warashina M, Stec WJ, Yoshinari K, Taira K (2001) SURVEY AND SUMMARY: Recent advances in the elucidation of the mechanisms of action of ribozymes. Nucl Acids Res 29(9): 1815-1834.

Timmons L, Fire A (1998) Specific interference by ingested dsRNA. Nature 395(6705): 854-854.

Timmons L, Court DL, Fire A (2001) Ingestion of bacterially expressed dsRNAs can produce specific and potent genetic interference in Caenorhabditis elegans. Gene 263(1-2): 103-112.

Torres RA, Bruice TC (1998) Molecular dynamics study displays near in-line attack conformations in the hammerhead ribozyme self-cleavage reaction. Proceedings of the National Academy of Sciences 95(19): 11077-11082.

Uhlenbeck OC (2003) Less isn't always more. RNA 9(12): 1415-1417.

Weinberg MS, Ely A, Barichievy S, Crowther C, Mufamadi S et al. (2007) Specific Inhibition of HBV Replication In Vitro and In Vivo With Expressed Long Hairpin RNA. Mol Ther 15(3): 534-541.

Wilson JA, Richardson CD (2006) Future Promise of siRNA and Other Nucleic Acid Based Therapeutics for the Treatment of Chronic HCV. Infectious Disorders - Drug Targets(Formerly Current Drug Targets - Infectious Disorders) 6: 43-56.

Wu H-N, Lin Y-J, Lin F-P, Makino S, Chang M-F et al. (1989) Human Hepatitis delta Virus RNA Subfragments Contain an Autocleavage Activity. Proceedings of the National Academy of Sciences 86(6): 1831-1835.

Yeom K-H, Lee Y, Han J, Suh MR, Kim VN (2006) Characterization of DGCR8/Pasha, the essential cofactor for Drosha in primary miRNA processing. Nucl Acids Res 34(16): 4622-4629.

Yi R, Qin Y, Macara IG, Cullen BR (2003) Exportin-5 mediates the nuclear export of pre-microRNAs and short hairpin RNAs. Genes Dev 17(24): 3011-3016.

Zheng Z-M, Tang S, Tao M (2005) Development of Resistance to RNAi in Mammalian Cells. Ann NY Acad Sci 1058(1): 105-118.